Interaction of Alfalfa with Transient Water and Salt Transport in the Rootzone

Research Report No. 135

August 1994

U. S. SALINITY LABORATORY
AGRICULTURAL RESEARCH SERVICE
U. S. DEPARTMENT OF AGRICULTURE
RIVERSIDE, CALIFORNIA

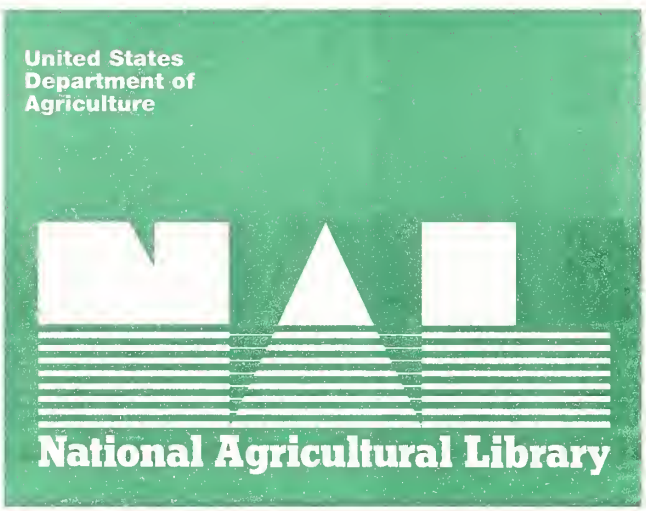
United States
Department of
Agriculture
National Agricultural Library

Interaction of Alfalfa with Transient Water and Salt Transport in the Rootzone

C. Dirksen, M. J. Huber, P. A. C. Raats, S. L. Rawlins
J. van Schilfgaarde, J. Shalhevet, and M. Th. van Genuchten

Research Report No. 135

August 1994

U. S. SALINITY LABORATORY
AGRICULTURAL RESEARCH SERVICE
U. S. DEPARTMENT OF AGRICULTURE
RIVERSIDE, CALIFORNIA

EXTENDED ABSTRACT

Crops grown in arid and semi-arid regions are subject to continuous and dynamic interactions between water uptake by plant roots, soil-water pressure and osmotic potential distributions, water and salt fluxes resulting from existing potential gradients, and irrigation scheduling. The objective of this study was to obtain detailed and accurate data for a variety of experimental conditions that can serve as a basis for developing and testing conceptual models of these complex interactive processes, and to gain more understanding of the dynamic behavior of living plants in general.

Alfalfa was grown in six laboratory soil columns for more than two years. A variety of pressure and osmotic soil water potential distributions were obtained by varying the osmotic head of the irrigation water between -2.4 and -22.0 m, the leaching fraction (L) between 0 and 0.5, and the irrigation interval between 1 and 12 days. Soil water content and potential distributions were measured with a two-dimensional gamma ray attenuation scanner, tensiometer-pressure transducer combinations, and salinity sensors, all automated with a data accumulation system. Other measurements included irrigation and drainage volumes and salinities, crop yields, illuminance, leaf water potentials, root length distributions, and soil hydraulic properties. Chapter 1 gives a general overview of the experiments, and a theoretical framework of the study as a whole. Chapter 2 describes the experimental conditions, apparatus and procedures, gives results of detailed samplings of the soil columns, and evaluates the accuracy of observed data. Salt and water transport, root water uptake distributions, and other plant factors are discussed in Chapters 3 through 5.

Chapter 3 reports results for the daily irrigation schedule. At L = 0.08, the plants concentrated the soil solution to a minimum h_o of about -75 m in 130 days. After this, the total salt content of this column as a whole continued to increase with time. The drainage water for L = 0.25 reached an approximately steady salinity after 50 days. Daily evapotranspiration, ET, during the 16-hour light periods varied from about 3.5 mm immediately after cutting the alfalfa, to as much as 11 and 20 mm for the full-grown canopies in the saline and non-saline columns, respectively. During periods of high ET,

hydraulic fluxes became small and often were reversed in the top of the columns at the end of the irrigation intervals. The divergence of the flux density during these periods was very small, so that the measured rates of change in the water content provided good approximations for the rates of root water uptake. One example for relatively wet conditions showed that the maximum correction for the divergence of the depth-integrated flux density was only 14% of the root water uptake. Water uptake during the initial salinization process occurred preferentially in the non-saline bottom parts of the columns, whereas the water content in the top part of the column containing the most saline irrigation increased appreciably. As the salinization progressed, water uptake became relatively shallower. Essentially all water uptake in the most saline columns took place in the top 0.30 m; water uptake distributions inferred from hydraulic data agreed well with those predicted from steady-state salinity distributions.

Chapter 4 concerns the more than seven months when four columns were irrigated at intervals of 4, 6, 8, and 12 days, respectively, with water having an osmotic head, h_o, of -12 m. A fifth column received tap water (h_o = -2.4 m) at 6 day intervals. Each column received the same total amount of water in uniform doses. The larger the application per irrigation, and hence the lower the irrigation efficiency, the deeper the salts leached during each irrigation, and the less saline the columns became. Salinity in the column with the 12-day interval (D-12) increased gradually with depth. The zone of maximum root water uptake initially shifted downward with time, but the soil became so dry near the end of the second 12-day irrigation interval of each growth period that evapotranspiration and yield were reduced drastically. In contrast, the column with the 4-day interval (B-4) never dried out, and evaporation remained relatively constant during the final irrigation intervals of each growth period. However, salinity increased rapidly with depth, and most root water uptake took place in the top part of the column. The average salinity of column B-4 was much larger than that of column D-12. Water and salt transport in column B-4 was in many respects similar to that under daily irrigation. The water uptake distributions under non-stress conditions corresponded reasonably well with the total potential distributions. A somewhat larger water uptake reduction with decreasing water content occurred under

limited stress conditions than could be accounted for by the pressure potential. This result may be due to increased soil resistance, or due to contact resistances at the soil-root interface. The total soil water potential under severe stress was nearly constant throughout the root zone in one column, but not in the others. Plants in most columns wilted rather quickly after suspending the irrigations and harvesting at the end of the regular irrigation intervals.

Chapter 5 deals with aspects specific to the alfalfa plants. Early salinization and high salinities of the irrigation water reduced yields more than late salinization and a high salinity in the bottom of the rootzone. Transpiration ratio's calculated for several growth periods, varied between 500 and 900 kg water per kg dry matter produced. Root development was sufficient for maximum water uptake to occur at those soil depths where the soil water potentials were most favorable. For the non-saline soil column, differences between total heads of soil water and leaf water were relatively constant above soil water contents of about 0.11 m^3 m^{-3}, but increased below that value. The maximum local rate of root water uptake, and an estimated maximum root conductivity for this same column, increased linearly with soil water content. Turgor pressure heads decreased at first slowly from about 45 m for non-saline conditions to about 35 m at an average soil water osmotic head of -43 m, and then rapidly to zero at -62 m. Differences between total leaf water heads in light and darkness were about 45 m. Total leaf water heads correlated well with the average osmotic head of each column individually, but not with the average pressure or osmotic heads of any third depth interval in the columns. Total leaf water heads for all saline columns together correlated well with both the uptake-weighted mean osmotic head and the total head at the time of measurement. This suggests that plants attempt to maximize the uptake-weighted mean head. While the uptake-weighted mean osmotic head was lower under 4-day than under 12-day irrigation, the shorter irrigation interval produced about 10% higher yields.

ACKNOWLEDGEMENTS

We wish to express our sincere appreciation for the help received from our colleagues at the U.S. Salinity Laboratory. Only in part has this found expression in co-authorship of this report. R. Austin automated the read-out of the salinity sensors, modified the gamma scanner, and was an indispensable trouble-shooter on many other occasions. J. D. Oster and J. D. Rhoades consulted on the salinity determinations of the soil samples, while J. D. Wood and D. A. Layfield carried out most of these measurements. D. A. Layfield also made plant analyses. G. J. Hoffman consulted on leaf water potential measurements and oxygen concentration measurements. S. D. Merrill set up the root length determinations. Much help was also received from students at the University of California, Riverside. The programming and data processing work was carried out successively by D. S. Johnson, K. C. Stevensen, Jr., K. H. Freyermuth, and P. N. Lowe. Cathy Elliot made many of the leaf water potential measurements, while C. Hall did most of the root length determinations. Finally, the figures were drawn by C. Curtis, and the photography was done by J. E. Higbee and R. D. LeMert.

TABLE OF CONTENTS

LIST OF FIGURES

LIST OF TABLES

LIST OF VARIABLES

C Solute concentration of soil water [M L^{-3}]

C_o Average concentration of irrigation water [M L^{-3}]

$C_{r,\,max}$ Maximum root conductivity [L T^{-1}]

h_g Gravimetric head [L]

h_h Hydraulic head [L]

h_o Osmotic head [L]

$\bar{h}_{os}$ Average osmotic head of soil water [L]

$\bar{h}_{ol}$ Leaf osmotic head [L]

$\tilde{h}_{os}$ Uptake-weighted mean osmotic head [L]

h_p Pressure head [L]

h_{pd} Imposed pressure head at drainage tubes [L]

h_{pl} Leaf pressure head [L]

h_t Total head [L]

h_{tl} Total leaf water head [L]

h_{ts} Total soil water head [L]

$\tilde{h}_{ts}$ Uptake-weighted mean total head [L]

I Irrigation interval [T]

K Hydraulic conductivity [L T^{-1}]

L Leaching fraction [-]

L_r Root length density [L L^{-3}]

q Volumetric fluid flux density [L T^{-1}]

$\bar{q}_i$ Daily amount of irrigation [L]

$\bar{q}_d$ Daily amount of drainage [L]

q_o Imposed irrigation flux density at soil surface [L T^{-1}]

R Plant flux resistance [L^{-1} T]

t Time [T]

z Soil depth [L]

θ Volumetric water content [$L^3 L^{-3}$]

θ_s Average volumetric soil water content [$L^3 L^{-3}$]

θ_{sat} Saturated volumetric soil water content [$L^3 L^{-3}$]

λ Root water uptake rate [T^{-1}]

λ_{max} Maximum root water uptake rate [T^{-1}]

1. INTRODUCTION

Irrigation agriculture in arid and semi-arid regions is vulnerable to salinity problems. Plants normally take up only a small fraction of the minerals dissolved in irrigation waters; the remainder accumulates in the soil unless it is leached out. If not by natural rainfall, leaching needs to be accomplished by applying excess irrigation. When water is scarce, as little excess water as possible should be used, even though this will lead to increased salinities in the lower parts of the rootzone. Water percolating through the soil profile often dissolves salts that already were present in the soil, thus increasing the absolute salt load of the irrigation return flow. Decreasing the quantity of leaching water can cause salt concentrations in the bottom of the root zone to reach such high values that some salts precipitate, resulting in a decrease of the absolute salt load in the return flow. In areas where only irrigation water of relatively high salinity is available, it is important to know how crop yields respond to salinity. Most salt tolerance studies have been carried out with uniform salt distributions, either using salt solutions or involving soils irrigated at relatively high leaching fractions. A much more complex problem is how plants interact and adjust to soil water contents and soil water salinities that vary in both space and time.

Irrigated crops in arid and semi-arid regions are subject to continuous and dynamic interactions between water uptake patterns and prevailing pressure and osmotic potential distributions. These interactions are complicated further by water and salt fluxes resulting from established water potential gradients, and by irrigation scheduling. Crop yields depend strongly on root water uptake, with possibly different effects at different growth stages. Also, osmotic stress on roots may result in drastic reductions in the synthesis of growth regulators (cytokinins), which in turn may cause reductions in growth (*Itai and Vaadia*, 1971). Given these complex interactions, it is not surprising that there are contradictory reports in the literature on how to integrate soil salinity to obtain that parameter which best correlates with plant yield. One group (e.g., *Shalhevet and Bernstein*, 1968; *Bower et al.*, 1969; *Ingvalson et al.*, 1976) suggests that crop response should be related primarily to the mean soil salinity, and hence that yield is affected strongly by the higher salinities in the bottom of the root zone. Another group (e.g., *Wadleigh et al.*, 1947; *Lunin and Gallatin*,

1965; *Bingham and Garber*, 1970, *Bernstein and Francois*, 1973) assumes that yields are related better to the upper rootzone salinity and/or the irrigation water salinity, and that yields are less affected by deep rootzone salinities. A corollary to the latter position is that yields are determined by some kind of weighted mean salinity, of which the uptake-weighted mean salinity (*Raats*, 1974; *Hoffman and van Genuchten*, 1983) intuitively would appear to be most attractive.

The objective of this study was to obtain detailed and accurate data that could serve as a basis for developing and testing conceptual-mathematical models of these complex interactive processes, and to gain more understanding of the dynamic behavior of living plants. The experimental data were obtained with alfalfa, grown in densely instrumented laboratory soil columns and harvested at approximately 24-day intervals for more than two years. A variety of pressure and osmotic potential distributions in the rootzone were established by varying the quantity and salinity of the irrigation water, as well as the irrigation frequency. The study had two major phases. During the first major phase, six columns were irrigated daily either with different irrigation water salinities and/or at different leaching fractions. One column was sampled destructively at the end of this phase. During the second major phase, four columns received the same total amount of water of the same salinity, but at intervals ranging from 4 to 12 days. One column (A) received only tap water throughout the study. Each of the two major phases was followed by a period with a less rigorous experimental plan to introduce new experimental conditions, and to conduct special studies with individual columns. Experimental details, a general evaluation of the accuracy of the data, and some data not specific to a particular phase are reported in Chapter 2. The water and salt transport processes during each of the major phases are discussed in Chapters 3 and 4, respectively. Plant factors such as leaf water potentials and hydraulic resistances, in conjunction with variously weighted mean salinities, are treated in Chapter 5.

Table 1.1 lists the time sequence of treatments and experimental conditions for the two-year period. This table is meant to serve as a quick reference to the experiments discussed in this report. All dates will be given as Julian days, preceded by a digit indicating the particular year. For instance, Julian day 148 of 1975 will be indicated as J5148.

Table 1.1. Time sequence of treatments for the six soil columns.

Column:	A	B	C	D	E	F
Julian Date						
5120	Seeding of alfalfa.					
5134	Thinning to 44 x 10^{-4} m^2 per plant.					
5141	Start of light periods between 5:00 - 21:00.					
5148	Start of daily irrigations at target leaching fractions (L) and osmotic heads (h_o, m):					
	L 0.25 h_o -2.4	L 0.45 h_o -22.0	L 0.18 h_o -13.2	L 0.14 h_o -2.4	L 0.08 h_o -13.2	L 0.14 h_o -2.4
	All drainage tubes at pressure head h_{pd} = -4.0 m					
5174	Harvest I.					
5197	Installation of 8 drip lines per column.					
5207	Harvest II.					
5219	All h_{pd} = -3.0 m.					
5227	Harvest III.					
5252	Harvest IV.					
5272	Harvest V.					
5273	Quick salinization of columns D and F. Afterwards:					
				0.18 -13.2		0.08 -13.2
5297				h_{pd} = -6.0		h_{pd} = -6.0
5282	h_{pd} = -6.0					
5288				h_{pd} = -2.5		h_{pd} = -2.5
5297	Harvest VI.					
5299	All h_{pd} = -2.0 m.					
5301				h_{pd} = -1.5		
5304	Lights on 4:00 to 20:00.					
5308	Salinity sensors and tensiometers 17 mm into column.					
5310	All h_{pd} = -3.0 m.					
5321	Harvest VII.					
5322	All h_{pd} = -2.0 m.					
5325	Removed dead plant from column A.					
5346	Harvest VIII.					
5350	All h_{pd} = -1.5 m.					
5365				h_{pd} = -3.5		
6014	Harvest IX					destructive sampling

Table 1.1 (Continued)

Column:	A	B	C	D	E	F

Julian Date

6016 All h_{pd} = -1.5 m.
6036 Harvest X.
6065 Harvest XI.
6070 Start of non-daily irrigations; average irrigation of 14.3 mm per day with h_o = -12.0 m (column A at h_o = -2.4 m) at interval I (days):

I = 3	I = 3	I = 7	I = 2	I = 5

6093 Harvest XII.

6102	I = 3

6121 Harvest XIII.
6123 Average irrigation of 12.9 mm per day.
6126 New 2.44 long lights.
6131 Lights on between 19:00 and 11:00.
6135 Start of fertilization.
6149 Harvest XIV.

6156	I = 6	I = 4	I = 8	I = 12	I = 6

6167 Installation of 1.20 m long lights across center.
6173 Harvest XV. Start of 24-day irrigation cycle. Average irrigation of 14.3 mm per day.
6181 Lights on between 20:00 - 8:00.
6279 Lights on between 8:00 - 10:00.
6317 Columns E under plastic cover until J6329.
7023 Scheduled harvest and irrigations postponed 4 days.
7028 Harvest XXIV. Column A shifted to sub-irrigations (see *Dirksen and Raats*, 1985). Column C returned to daily irrigation until J 7100.
7125 Column C was dried out until plants wilted; canopy removed; irrigation of 114.3 mm water with h_o = -20 m.
7136 h_{pd} = -2.5 m on column C.
71516 h_{pd} = -6.0 m on column C.
7129 Additional irrigation of 114.3 mm on column C using water with h_o = -2.8 m for hydraulic conductivity determination.
7175 Cores removed from column C for flux-controlled sorptivity measurements; destructive sampling of columns B, D and E. Column A placed on nailboard.

1.1. *Theoretical Framework*

Water potentials throughout this report are expressed in terms of amount of energy per unit weight of solution. The unit most frequently used for this purpose is the meter of head. Theoretically, this unit can be used only when the density of the solution in question is constant (*Koorevaar et al.*, 1983). Solution densities in this study varied as a result of concentration gradients. We will still use the head unit for water potential by tacitly assuming that the unit refers to meters of water with a density of 1000 kg m^{-3}.

The total head h_t consists of three components:

$$h_t = h_p + h_o + h_g \tag{1.1}$$

where the subscripts p, o, and g refer to pressure, osmotic, and gravitational components, respectively. The gravitational head h_g is the height above an arbitrarily chosen reference level. The osmotic head h_o includes only the contribution of solutes in the bulk solution, not those in diffuse double layers. The osmotic head only affects water flow across semi-permeable membranes such as is the case during root water uptake. Measured electrical conductivities (EC) in this study were converted to osmotic heads (h_o) according to h_o (m) = -40 EC (S m^{-1}).

The driving force for movement of the soil solution is the gradient of the hydraulic head. Contrary to standard usage but consistent with the present notation, the hydraulic head will be written here as

$$h_h = h_p + h_g \tag{1.2}$$

The flux density of water q (m^3 m^{-2} s^{-1} or m s^{-1}) in unsaturated soil is described by Darcy's law which in the case of one-dimensional vertical flow reduces to

$$q = -K(\theta)\frac{\partial h_h}{\partial z} = -K(\theta)\left(\frac{\partial h_p}{\partial z} - 1\right) \tag{1.3}$$

where $K(\theta)$ is the hydraulic conductivity (m^3 m^{-3} s^{-1} or m s^{-1}) as a function of the volume fraction of water, θ (m^3 m^{-3}), commonly referred to as the volumetric water content. Also,

z is depth (m); consequently, $h_g = -z$, and hence $h_h = h_p - z$.

The flow of water is further subject to the principle of conservation of mass which, for one-dimensional vertical flow with concurrent water uptake by plant roots, is given by

$$\frac{\partial \theta}{\partial t} = -\frac{\partial q}{\partial z} + \lambda \tag{1.4}$$

where $\lambda = \lambda(z,t)$ is the (negative) source strength, in absolute value equal to the local rate of root water uptake ($m^3\ m^{-3}\ s^{-1}$). The root water uptake rate, $\lambda(z,t)$, depends on such variables as the osmotic and pressure head distribution, the root characteristics, and the evaporative demand. The term $\partial q/\partial z$ is the divergence of the flux density. Because alfalfa covered the soil well throughout the study, direct evaporation from the soil surface is likely negligible. This makes the integral of λ over the entire root zone equivalent to the actual evapotranspiration rate, *ET*. A main objective of this study was to investigate the dependence of λ on non-uniform osmotic and pressure head distributions in the soil. One approach to derive values for λ is to apply Eq. (1.4) to measured water content and water flux density (or hydraulic head and hydraulic conductivity) distributions.

Integrating Eq. (1.4) between times t_1 and t_2 and depths z_1 and z_2, and dividing by the time and depth intervals $(t_2 - t_1)$ and $(z_2 - z_1)$, gives

$$\frac{\int_{t_1}^{t_2}\int_{z_1}^{z_2}\frac{\partial \theta}{\partial t}\,dz\,dt}{(t_2-t_1)(z_2-z_1)} = -\frac{\int_{t_1}^{t_2}\int_{z_1}^{z_2}\frac{\partial q}{\partial z}\,dz\,dt}{(t_2-t_1)(z_2-z_1)} + \frac{\int_{t_1}^{t_2}\int_{z_1}^{z_2}\lambda\,dz\,dt}{(t_2-t_1)(z_2-z_1)} \tag{1.5}$$

If the time and depth intervals are chosen such that λ can be assumed constant, then

$$\lambda = \frac{\int_{z_1}^{z_2}\theta(t_2)\,dz - \int_{z_1}^{z_2}\theta(t_1)\,dz}{(t_2-t_1)(z_2-z_1)} + \frac{\int_{t_1}^{t_2}q(z_2)\,dt - \int_{t_1}^{t_2}q(z_1)\,dt}{(t_2-t_1)(z_2-z_1)} \tag{1.6}$$

The first term on the right-hand side represents the rate of change of the water content (RCWC) and the second term represents the divergence of the water flux density (DF).

During steady-state flow, the λ-distribution can also be derived from the slope of the dilution profile (*Raats*, 1974):

$$\lambda = q_o C_o \frac{d(1/C)}{dz} \tag{1.7}$$

where C is the concentration of the soil solution at depth z, and q_o and C_o are the average flux density and concentration of the irrigation water at the surface. This equation needs corrections because irrigation water usually is applied intermittently rather than at a steady rate. In that case q_o must be averaged over one or more irrigation cycles. Also, plants transpire only during daylight hours, usually at non-uniform rates. Equation (1.7) defines an equivalent, constant water uptake rate that results in the same total extraction over 24 hours as the actual space- and time-dependent root water uptake distribution. Actual rates over smaller time periods can be many times larger than this equivalent rate.

2. EXPERIMENTAL

2.1. *Physical Model and Accessories*

The laboratory experiments were carried out using the soil water flow model with two-dimensional automatic gamma ray attenuation scanner described by *Dirksen and Huber* (1978). The physical model was divided into eight columns, each with dimensions 0.394 x 0.178 x 1.07 m high (the width of column F was only 0.349 m). Only six of these columns (A through F) were used, each with its own irrigation and drainage system. The front walls of the columns consisted of 9.5-mm thick glass plates through which soil packings, wetting fronts, and root distributions could be observed (Fig. 2.1a). Normally, the glass walls were covered with black cloth to keep the roots in the dark. The back walls were made of 9.5-mm thick aluminum plates through which tensiometers, salinity sensors, irrigation tubes, and oxygen probes were inserted (Fig. 2.1b).

The columns were packed with Pachappa very fine sandy loam (52.4% sand, 39.5% silt and 8.1% clay) taken from the top 0.3 m of soil at the U. S. Salinity Laboratory site. Before packing, 20% P_2O_5 superphosphate was mixed with the soil at a rate of 5.2 gram P per kg of soil. The soil was dropped through a chute with a perforated plate about 1.0 m above the top of the model. Whereas this method initially appeared to give satisfactory packings, air currents often caused some particle separation and non-horizontal layering. To minimize this problem, the walls were tapped with a mallet, both during packing and after the soil column was filled and weighted down with lead blocks. Some variations in bulk density still remained and showed up especially after wetting and drying. The columns were saturated with water and drained twice to settle the soil pack and to determine the soil hydraulic conductivities with the instantaneous profile method (*Watson*, 1966).

Soil water contents were measured non-destructively with the two-dimensional gamma ray attenuation scanner. This apparatus could scan automatically any number of columns at any preset time interval. Gamma counts normally were made in three vertical scans per column at the following depths: every 10 mm between 0.01 and 0.10 m depth, every 25 mm between 0.10 and 0.30 m depth, and every 50 mm between 0.30 and 1.05 m depth.

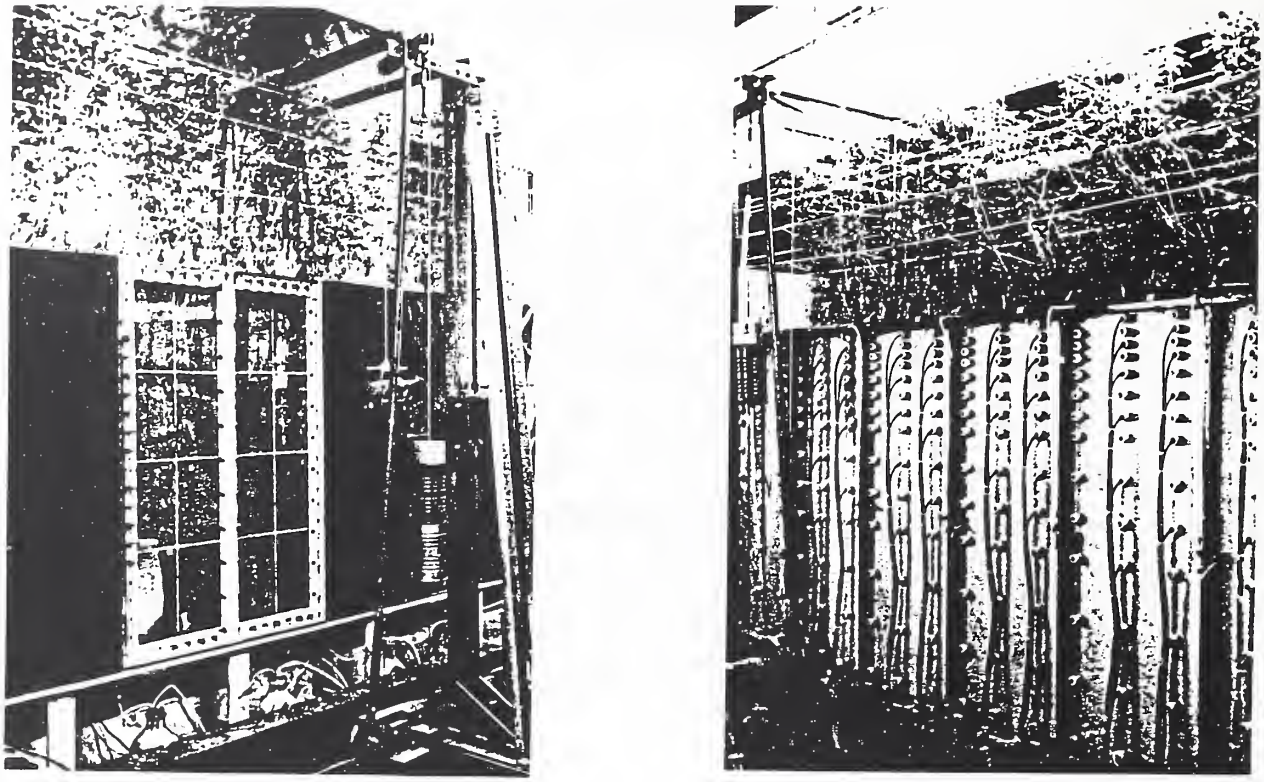

Fig. 2.1. Soil water flow model with automatic two-dimensional gamma ray, tensiometer and salinity sensor scanning devices, equipped for plant growth

Reported water contents for each depth are all averages of the three scans. Except for column E, bulk densities of the columns were determined with gamma scans while they were still dry. Column E was already wetted before final alignment of the gamma source and detector. Its bulk density distribution and the corresponding dry counts were estimated based on the water contents of the other columns at the end of the drainage period prior to seeding. Gravimetric sampling at the end of the study indicated that this estimate needed little adjustment. The soil surface was reworked to about 50 mm before seeding. This and the large root crowns prevented accurate absolute water content measurements near the surface. Water content changes over periods of one or more days could be measured accurately.

Irrigation water salinities were obtained by adding equal molar (charge basis) quantities of NaCl and $CaCl_2$ to the irrigation water. Because alfalfa fixes nitrogen, and because phosphate was added to the soil, no additional fertilizers were applied to the columns for a year. Starting on Julian day 135 of 1976 (J6135), small amounts of K, Mg, NH_4, and Ca nitrates and phosphates were added to the irrigation water. The desired amounts of irrigation water were measured into containers which were then pumped empty. At first, water was supplied through three ceramic tubes positioned lengthwise on the surface of each column, but this proved unsatisfactory. The air entry value of the ceramic tubes was too high for the positive displacement pump to overcome when the water supply ran out. The high pressures eventually stripped the pump gears. On J5197, the ceramic tubes were replaced by eight open-ended fine plastic spaghetti tubes per column, evenly distributed over the soil surface. On J6125, the number of tubes was increased to 14 per column. Occasionally irrigation water was applied directly to the soil surface. Before the soil columns were packed, three ceramic tubes (5.5 mm OD) were installed parallel to the glass front at 0.55 m depth in each column (see Fig. 5.4). These tubes were used for sub-irrigation during special treatments.

Each column had two parallel ceramic tubes (13 mm OD) at the bottom for drainage. Drainage water was collected in partially-evacuated glass bottles and its volume and osmotic head (h_o) usually were measured daily. The negative pressure heads imposed on the drainage tubes (h_{pd}) are listed in Table 1.1. They were regulated in each bottle separately with light-emitting diodes and phototransistors on mercury manometers (*Austin and Rawlins*, 1977).

2.2. *Experimental Studies*

Both the daily irrigations and the salinity treatments were started on J5148. Throughout the study, column A received only tap water with osmotic head h_o= - 2.4 m. Its target leaching fraction (L) was 0.25. Column B received irrigation water of h_o = -22.0 m with target L = 0.5. Columns C and E were irrigated with water of h_o = -13.2 m with

target L's of 0.18 and 0.08, respectively. Columns D and F received tap water until J5273 when they were quickly salinized to resemble columns C and E, respectively. Thereafter. they were irrigated identically to columns C and E until J6014. Column F was sampled on J 6014, while daily irrigation was continued on the other columns.

On J 6070 we began to irrigate columns A through E at intervals of 3, 3, 7, 2 and 5 days, respectively. Beginning on J6102, column A was irrigated at 2-day intervals because of infiltration problems encountered with the use of tap water. The irrigation intervals were changed on J6156 to 6, 4, 8, 12, and 16 days, respectively, and this schedule was continued until J7023. During both periods of non-daily irrigation, all columns received the same total amount of water at a an average rate of 14.3 mm per day, except for a 10% reduction between J6123 and J6174. They also received water of the same salinity of h_o = -12.0 m (except for column A). The period between J6014 and J6156 was an adjustment period during which the irrigation frequency was modified twice, the lights were changed, and fertilizer was added to the irrigation water. Only incidentally will we make use of the data from this period. The two major phases are the daily irrigation phase from J5148 to J6014, and the non-daily irrigation phase from J6174 to J7028. They both cover nine growth periods: I through IX, and XVI through XXIV, respectively. These two major phases are discussed separately in Chapters 3 and 4, respectively.

After the non-daily irrigation phase, a number of special studies were initiated on individual columns. Column A was sub-irrigated, at first through the ceramic tubes half-way down the column and later from the bottom. The top of this column was allowed to dry out to see if the roots would leak water into the dry soil. The effect of O_2 and CO_2 concentrations on this leakage was also studied. The results are reported in a separate paper (*Dirksen and Raats*, 1985). Column C was returned to daily irrigation to obtain better tensiometric data than those obtained during the first major phase. Some of these data are used in Chapter 3.

2.3. *Soil Water Salinity and Potential Measurements*

The salinity of the soil solution was measured in-situ with salinity sensors (Model

5100, Soilmoisture Equipment Company, Santa Barbara, CA[1]) pushed against the soil with a spring. At first they were installed flush with the back wall. To alleviate edge effects, they were inserted later about 17 mm into the soil (on J5308). This modification improved the consistency of the measurements appreciably. The 100 salinity sensors were read automatically in about 40 minutes. Measuring positions in each column were located in three vertical rows at depths of 0.02, 0.05, 0.08, 0.11, 0.15, 0.20, 0.25, 0.30, 0.40, 0.50, 0.60, 0.75, 0.90 and 1.05 m. One row was located near the center of the face of each column, and the two others at about one-third from the edge and near the edge of the face (Fig. 2.1b).

The same measuring positions were used also for the tensiometers. The self-made tensiometers had the same outside dimensions as the salinity sensors and were also held against the soil with a spring. Initially, the salinity sensors and tensiometers were alternated along each of the two most central rows. Because the salinity exhibited appreciable spatial variability, starting on J6143 the two central rows were used for salinity sensors and the edge row for the tensiometers (Fig. 2.1b). All 144 tensiometers initially were measured with one servo-pressure sensor (Model 314D, Sundstrand Data Control, Inc., Redmond, WA) through a series of hydraulic switches. The switching could be done automatically in a number of different sequences and at any desired time interval. After some time, the hydraulic switches became unsatisfactory because of leakage between ports. Solenoid valves proved totally unsatisfactory for hydraulic switching owing to heating problems. Therefore, from J6335 on, only eight tensiometers were used at any time, each one semi-permanently connected to its own pressure sensor. The pressure sensors were moved from column to column as needed.

The salinity sensor and tensiometer data, as well as the counts of the gamma scanner, were all recorded on punched paper tape. The tapes were read with an optical tape reader and the data stored, first on magnetic tape cassettes and later on floppy discs. Processing and analysis of the data was done with a programmable calculator and plotter.

---

[1]The mention of commercial equipment by name is for the convenience of the reader and does not imply endorsement of that product by the U.S. Department of Agriculture.

2.4. *Destructive Sampling*

At the end of growth period IX, on J6014, column F was sampled in detail. Horizontal cores of 25 mm diameter were taken along 5 vertical rows. The bottom of the cores were at depths 0.05, 0.075, 0.10, 0.125, 0.15, 0.20, 0.25, 0.30, 0.40, 0.50, 0.60, 0.75, 0.90, and 1.025 m. The cores themselves were divided into three to six parts. Water contents and osmotic heads were determined for each part, the osmotic head via the electrical conductivity (EC) of extracts of 1:1 soil-water mixtures. The bulk density was determined for the core as a whole. Below the cores, starting at 0.15 m depth, about 10-mm thick layers of soil were collected from across the entire column. Osmotic heads of these layers were determined via EC's of 1:1, 1:0.5, and 1:0.25 soil-water extracts, and via chloride concentrations from 1:1 soil water extracts. A measure of anion exclusion was obtained by titration with $Mg(NO_3)_2$.

The four narrow soil columns that remained between the five rows of cores in column F were cut according to the depth intervals of the cores given above; they were also divided in half between the front and back walls. These soil samples were kept refrigerated in closed jars filled with a preservative liquid until the soil could be washed away and root lengths determined by the line-intercept technique of *Newman* (1966). Root lengths were expressed on a volumetric basis using the weight of the original soil samples and the bulk densities of the cores.

The remaining columns were sampled at the end of the study in a variety of ways. Column A was taken from the model on a nailboard. The soil was washed away and the root system photographed. No root length or weight measurements were taken on this column. Columns B, D, and E were sampled in essentially the same way as column F before. However, the washed-out root samples were simply centrifuged and weighed rather than used for determining root lengths with the more time-consuming line-intercept technique. Irrigation on column C was stopped on J7100 and the column was allowed to dry until the alfalfa wilted. After the plants were removed, the hydraulic conductivity was determined using the instantaneous profile method during drainage without evaporation. On J7175, 0.10-m diameter cores were taken at 0.15-m depth intervals to determine the

hydraulic diffusivity and conductivity functions with the flux-controlled sorptivity method (*Dirksen*, 1979). Small undisturbed soil samples from all columns were taken to determine the soil water retention function with a pressure membrane apparatus. Also, an undisturbed core, 100 mm in diameter and 10 mm in height, from one of the columns was placed on a ceramic plate and taken stepwise thought two wetting and drying cycles. For each equilibrium of the tensiometer pressure, the water content was measured by gamma ray attenuation. Soil water retention functions were composed also from simultaneous soil water content and pressure head measurements during the experiments themselves.

2.5. *Plant Factors*

Alfalfa (Medicago sativa L) was seeded on J5120 at a density of nine seeds per location and 16 locations per column, evenly distributed over the 0.0700 m^2 surface area. Two weeks later, the stand was thinned to one plant per location. The surface area of the outside column F was only 0.0621 m^2, leading to only 14 plants for this column. Both stands amounted to about 230 plants per m^2. The first harvest was obtained on J5174. Thereafter, alfalfa normally was harvested at intervals between 24 and 28 days, with a few exceptions ranging from 20 to 33 days. There were 29 growth periods and harvests in total. They are denoted by roman numerals I through XXIX. At each harvest, green and dry weights were determined and percentages dry matter calculated. Plant analyses made on some of the cuttings all showed normal mineral content. There were at times problems with aphids and other insects, situations which required regular spraying with insecticides. On one occasion the alfalfa was harvested after only 20 growth days because of a particularly serious infestation, especially in the non-saline column A. Generally, the alfalfa looked healthy and grew rapidly to a height of about 0.60 m in 24 days. The alfalfa was cut about 0.12 m above the soil surface to enhance quick regrowth. The canopy was confined by twine to prevent it from being damaged by the gamma scanner. The cross-sectional area of the canopy near the top was up to about 2.5 times that at the soil surface. Because the canopy was exposed to light also from the sides, the rates of evapotranspiration per unit soil surface area were much higher than those normally encountered in the field: up to 20 mm per day with 16

hours of light.

At first, total and osmotic leaf water potentials were measured on excised discs with thermocouple-psychrometers. Because these measurements exhibited large standard deviations, we switched later to a pressure chamber and measured only total potentials of the top clusters of leaves. These data were much more consistent. At one time, the measuring positions of the tensiometers in the wettest column were used to install oxygen concentration probes during daily irrigation. The oxygen concentrations were about 12%, well above that generally considered adequate for proper root functioning. Thus, aeration was no longer considered a matter of concern. Further details of the plant measurements are given in Chapter 5.

2.6. *Environmental Conditions*

Two banks of twelve 2.44-m (8 ft) long fluorescent lights, about 0.52 m wide, were suspended end-to-end over the columns at a height of about 0.90 m above the soil surface. They extended about 0.65 beyond the outside columns, and were mounted in boxes with thin tedlar sheets at about 0.80 m above the soil surface to keep the heat of the lamps away from the plants. The boxes also allowed the temperature of the lights to be controlled within reasonable limits by forced ventilation. The fluorescent lights (Vita-Lite, Duro-Test Corp., North Bergen, NJ) are designed specifically for plant growth and do not require additional incandescent lights. We followed at first the manufacturer's recommendation and operated the lights at about 41 C, but the illuminance (luminous flux density, lumen/m^2 or lux) at this temperature decreased drastically with time. On J6126, a new bank of lights was installed and operated at around 25 C. This made some improvement, but the illuminance still decreased more rapidly than was desirable for the experiments. Illuminance values were measured with an illumination meter (Weston, Model 603, Newark, NJ), irregularly at first, but more regularly after the illuminance problems became apparent. Figure 2.2 shows typical illuminance values versus height above the soil surface near the beginning, middle and end of each light set. To compensate for the low illuminance at the junction of the two light banks above column B, shorter lights were suspended across and below the 2.44 m

lights. While this was done at first poorly with 0.61-m long lights (curve J6125 B), the 1.22-m long lights of higher intensity used later were found to be adequate (curve J7137 B). The illuminance in the canopy was increased also by hanging reflecting shades from the edge of the lights to a point below the soil surface. Figure 2.3 shows the decrease in illuminance with time observed with the second set of lights. The plotted values are averages of the illuminance values at 0.15, 0.31, 0.46 and 0.62 m above the soil surface. The relative values were about the same during the first set of lights. Column B generally received the lowest illuminance of all columns. Column F received essentially the same illuminance as column E. From the start of the experiments until J6181, the lights were on for a period of 16 hours per day, thereafter only for 12 hours per day.

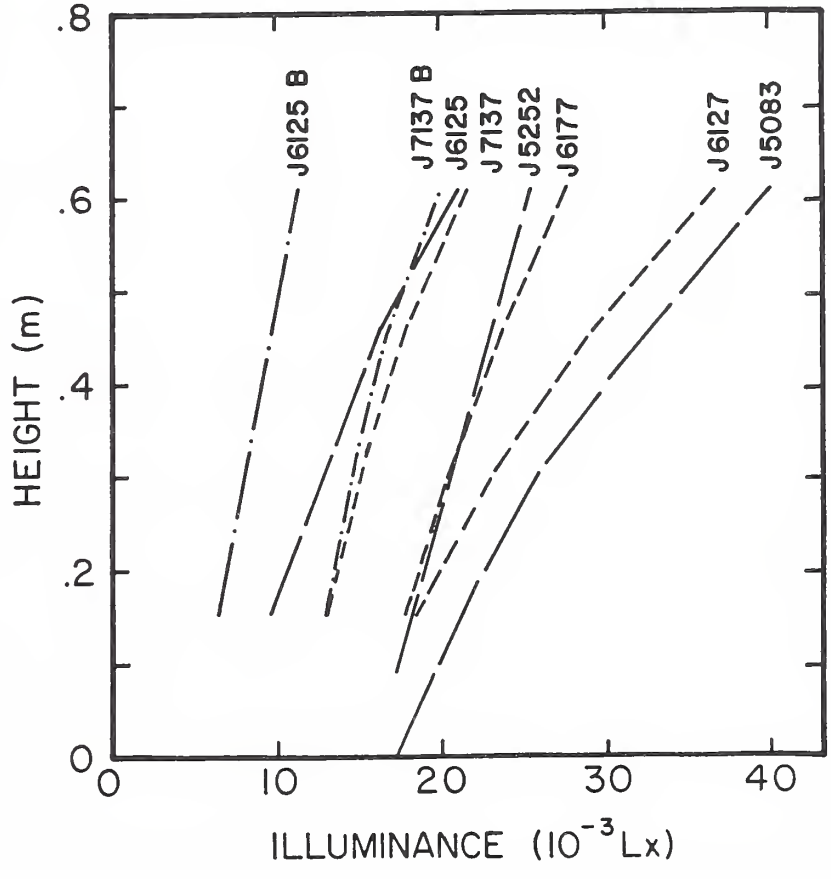

Fig. 2.2. Illuminance versus height above the soil surface at different times during operation of two different sets of lights. Curves J6125 B and J7137 B were obtained at the junction of the two light banks.

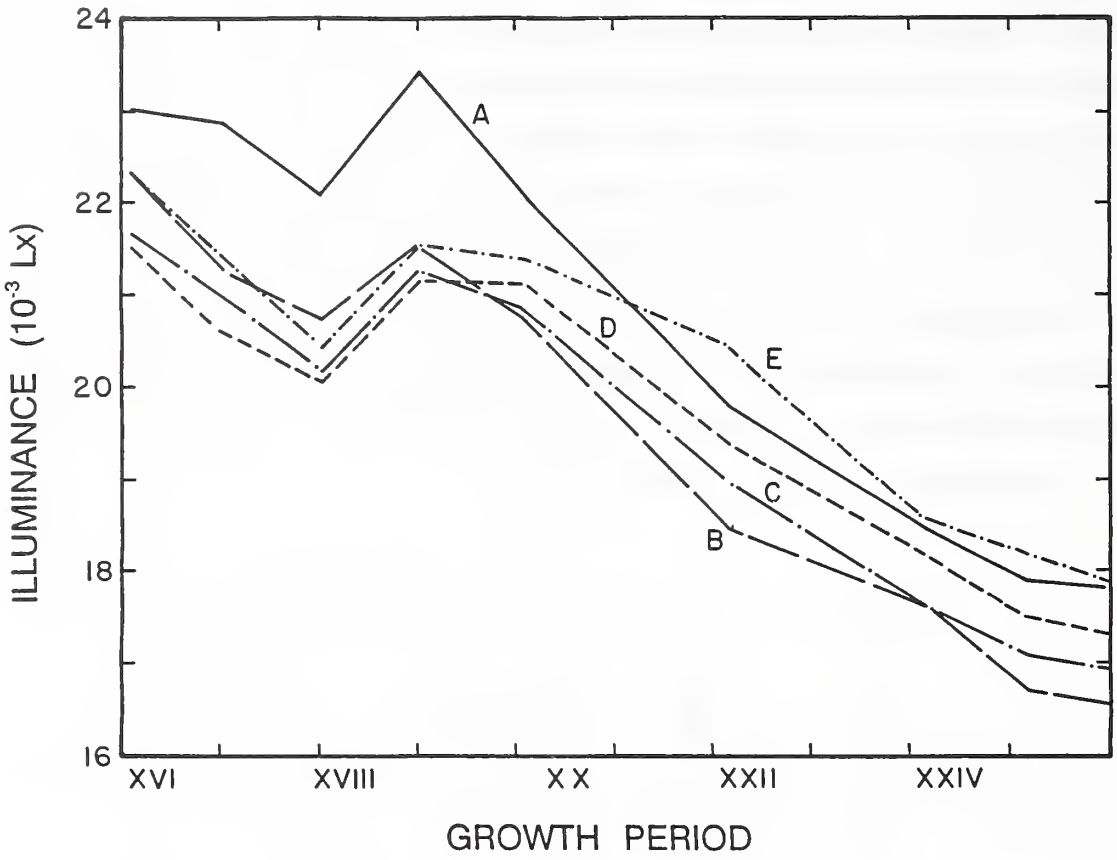

Fig. 2.3. Average of illuminances at four heights above the soil surfaces of five columns during operation of the second set of lights.

To prevent reductions in evapotranspiration, air was blown from outside the shades into the canopy through a perforated tube. The room was air-conditioned and its temperature and relative humidity monitored with a thermo-hydrograph. The temperature in the summer generally varied between 25 and 26 C during the night and between 24 and 25 C during the day. The relative humidity was highest during the day and occasionally reached 80 percent, while at night it was usually around 45 percent. In the winter the relative humidity was nearly equal during day and night, usually around 50 percent, whereas the temperature fluctuated somewhat more: between 25 C during the day and 22 C during the night.

2.7. *Experimental Results*

2.7.1. *Bulk Densities and Water Contents*

Figure 2.4 shows bulk densities obtained with the gamma scanner immediately after packing and before any wetting (data were not available for column E). Except for column B, the average bulk density was about 1540 kg m^{-3}; column B was slightly denser. Figure 2.5 shows the average bulk densities determined gravimetrically from cores taken at the end of the study. They agree fairly well with those in Figure 2.4. Column E was packed somewhat differently and had relatively low bulk densities at intermediate depths. Visually, the columns appeared to be more non-uniform than these data indicate.

Figure 2.6 compares for four columns the average of gravimetrically determined water contents of cores (solid lines) with adjusted water contents that were determined with the gamma apparatus immediately before sampling (broken lines). They all agree very well except near the soil surface. The adjustments of the gamma water contents in Figure 2.6 were: -0.05 m^3 m^{-3} to -0.025 changing linearly from top to bottom for column B, -0.05 m^3 m^{-3} for column E, and -0.0375 m^3 m^{-3} for columns D and F. Hence, three of the four columns needed the same average adjustment of 0.038 m^3 m^{-3}. Column E needed a slightly larger adjustment; this was not surprising since the water contents of this column initially were based on estimated gamma reference counts, as discussed earlier. The adjustments for the other columns were not entirely unexpected because the absolute water contents were based on gamma reference counts through newly packed dry soil columns. Subsequent wetting and drying cycles and the developing roots all tended to increase the soil packing and thus, in effect, change the reference counts. Based on the results in Figure 2.6, all reference counts were changed such that the gamma water contents of columns A, B, C, D, and F were reduced uniformly by 0.04 m^3 m^3, and those of column E by 0.05 m^3 m^{-3}.

In spite of these adjustments, the absolute values of the water contents were still not very accurate near the surface. During and shortly after irrigations, water contents generally increased from the surface down to about 0.20 m, while one would expect them to be more or less uniform (e.g., see Figs. 2.10 and 4.4). This effect became somewhat more

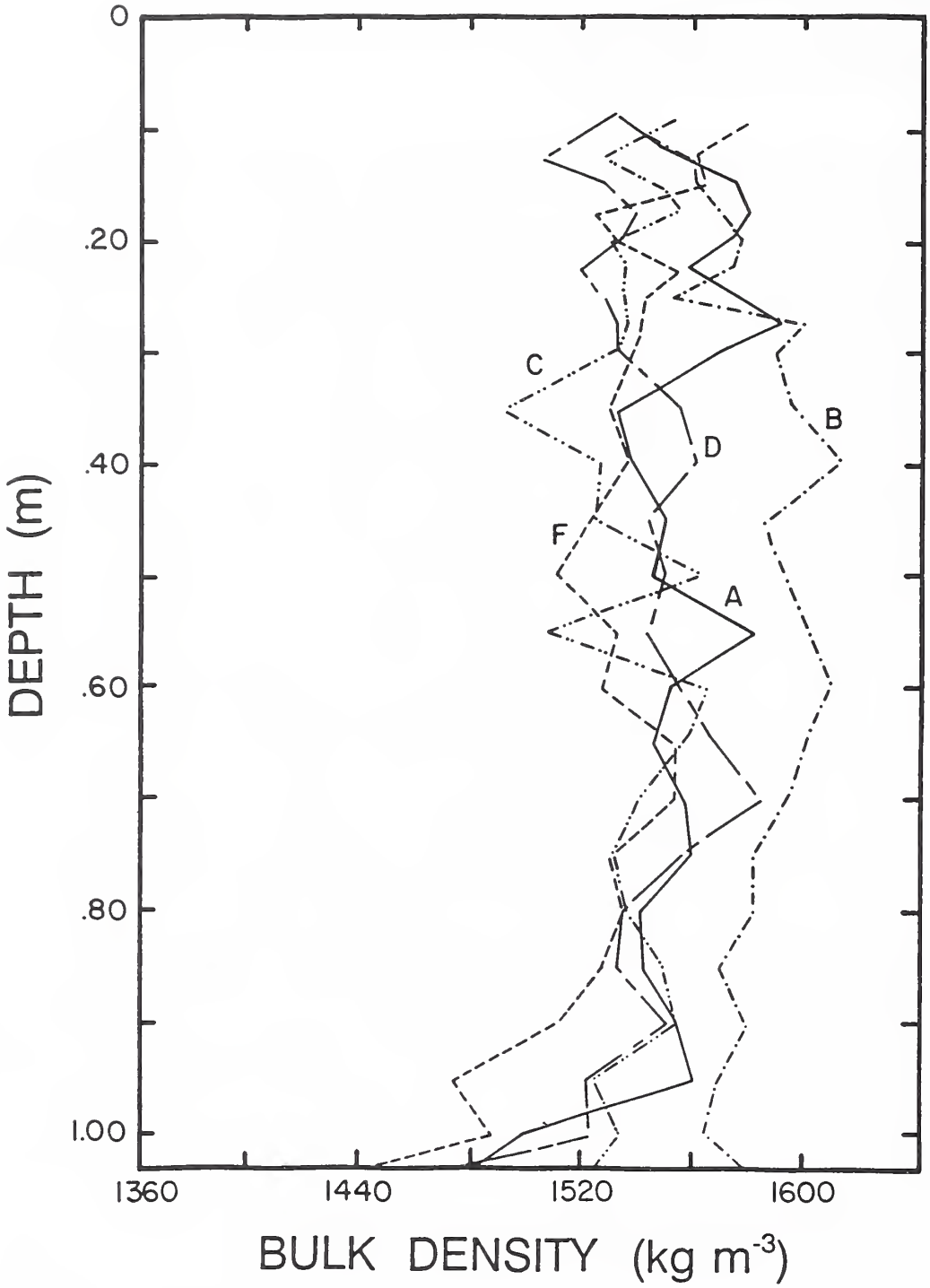

Fig. 2.4. Bulk density distributions in five columns before wetting as derived from gamma ray measurements

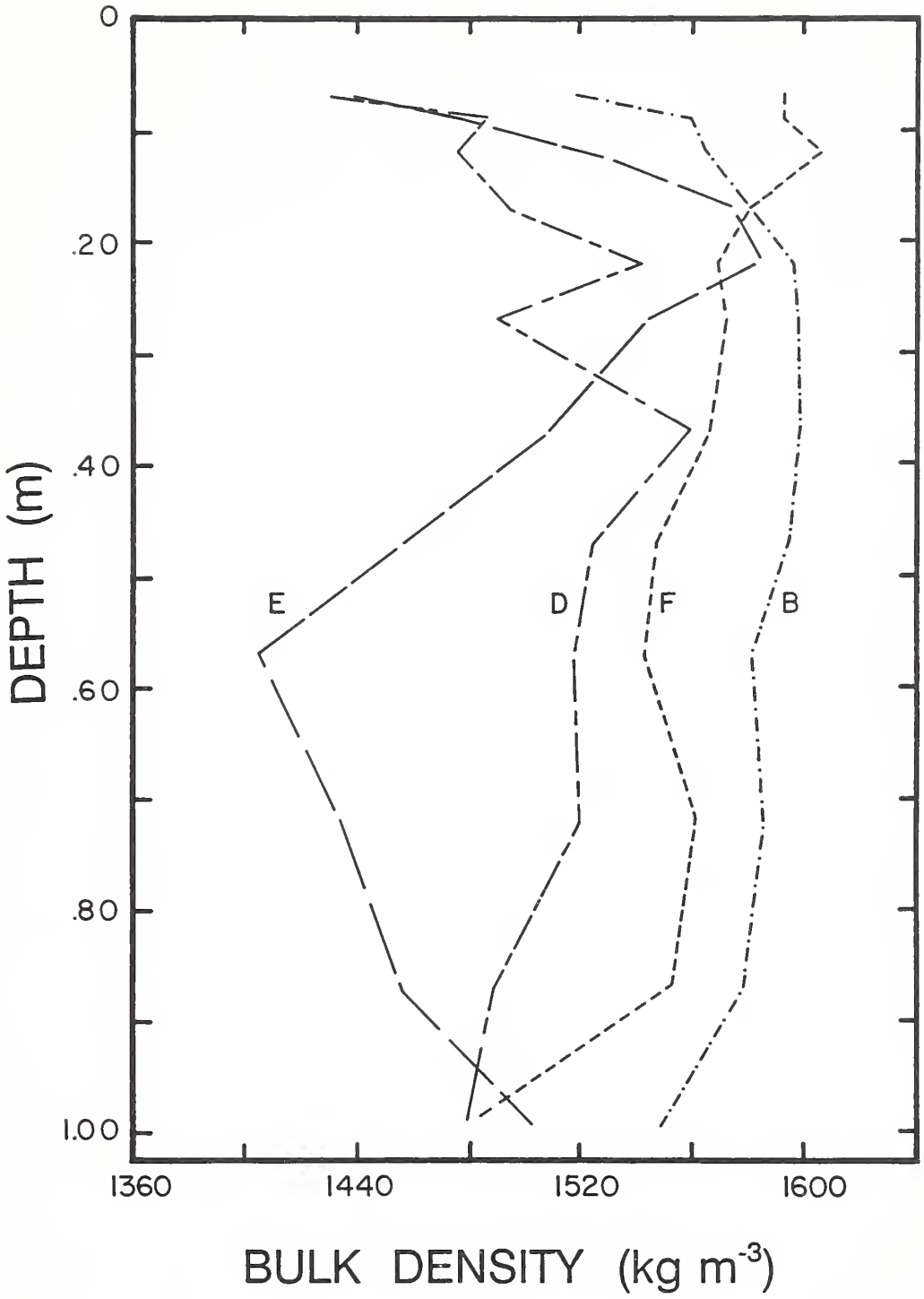

Fig. 2.5. Bulk density distributions in five columns as derived gravimetrically from core samples of four columns

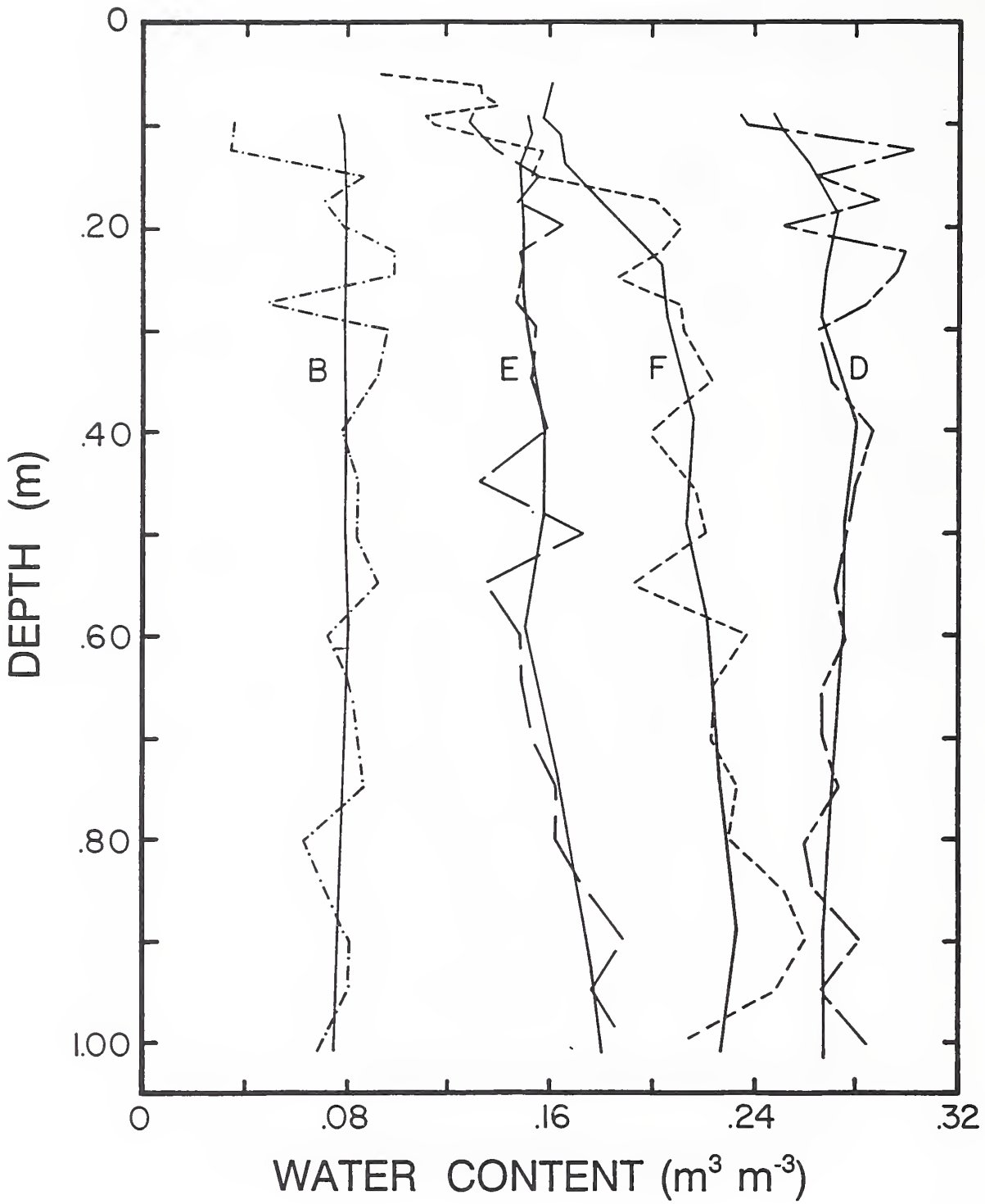

Fig. 2.6. Comparison of water contents obtained gravimetrically (solid lines) and with gamma ray measurements (broken lines)

pronounced with time. The relatively low water contents near the soil surface may have been a result of the volume occupied by roots, since this volume is not available for water storage during infiltration (Fig. 5.4 shows that the root volume in column A was substantial near the soil surface at the end of the experiments). Soil swelling also may have been a factor: a looser soil pack will attenuate fewer gamma ray photons, and this will be interpreted as a lower water content. The problem has not been resolved satisfactorily. Absolute water contents near the surface usually varied so much between the closely spaced measuring points that they could not be shown graphically with adequate resolution. However, changes in water contents relative to those measured just prior to irrigation were usually very regular and could be shown readily. An example of this is shown in Figure 3.15.

There were other abrupt differences in the soil water contents. For example, Figures 3.11 and 3.12 show relatively low water contents at depth z = 0.55 m on J5249 that did not exist before that day. These lower water contents, which persisted during the subsequent wetting period, were most likely due to the formation of cracks during the extreme drying period between days J5244 and J5249. Similarly, the relatively wet spot at z = 0.70 m on day J5215 disappeared between J5244 and J5249. We believe that these and similar large variations in other water content distributions were real. When water content profiles of more columns are given in one figure, such as in Figures 4.10, and 4.11, the variations are smoothed for greater clarity. Otherwise they are left as is. Measurements of changes in water content over short periods of time were not affected by roots or any other long-term disturbances. The accuracy of individual water contents was normally within $\pm$ 0.002 $m^3\ m^{-3}$. However, a small error in reference counts corresponding to a systematic error of only 0.001 $m^3\ m^{-3}$ in individual water contents, amounts to a difference of 1 mm of water for the whole column. This was often equivalent to one hour of evapotranspiration.

2.7.2. *Soil Hydraulic Properties*

Figure 2.7 shows the wetting and drying soil water retention curves. The curves are composed of data from the different sources discussed in section 2.4 on destructive sampling. There were some variations within the data of individual columns, but no consistent

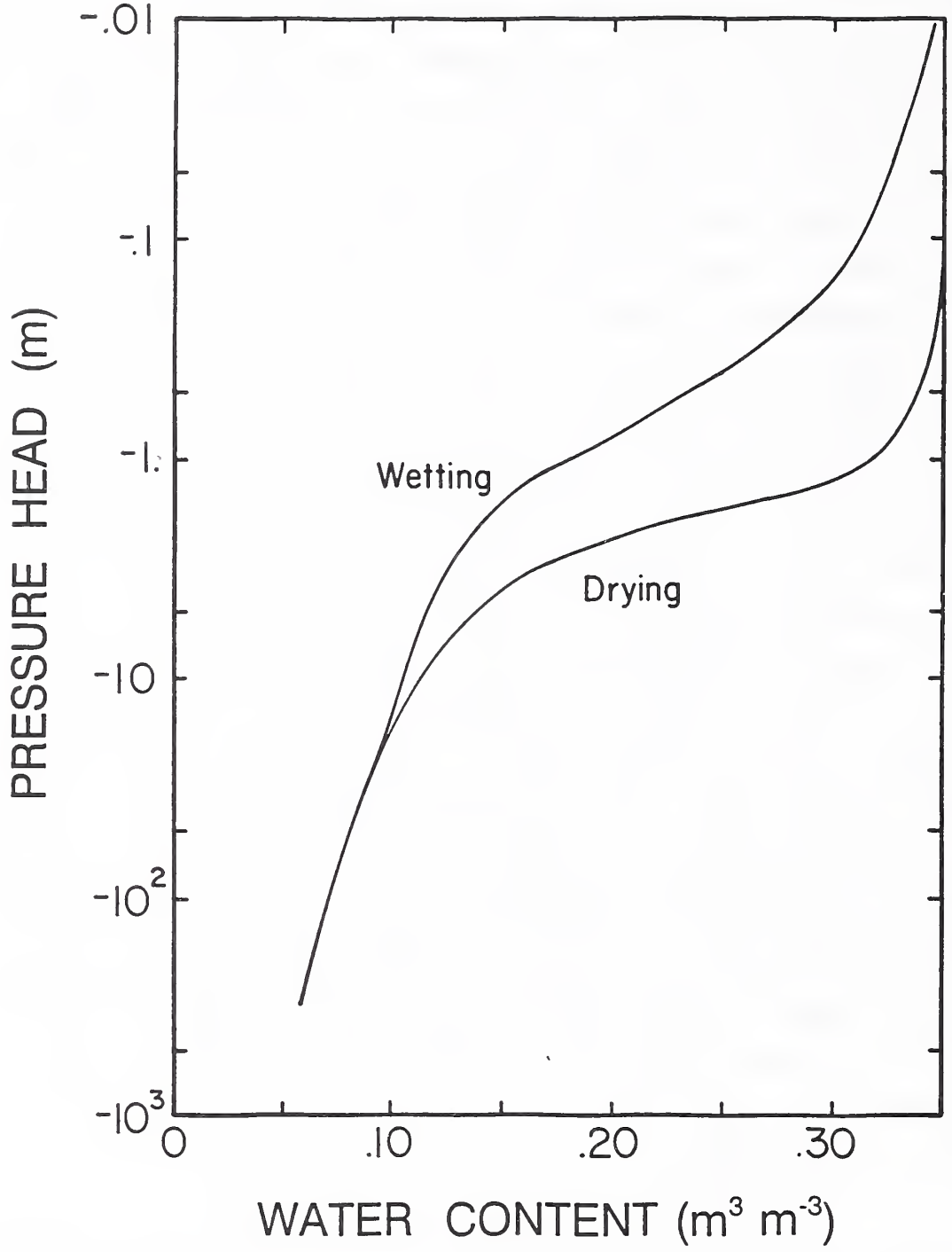

Fig. 2.7. Soil water retention curve of the Pachappa soil used in this study.

differences among the columns. The water retention curves should represent the retention behavior of all columns reasonably well.

Figure 2.8 shows for seven columns the hydraulic conductivity, K, as a function of water content, θ, determined during drainage before the columns were seeded with alfalfa. Since only tap water was used up to that time, hydraulic conductivities later probably changed somewhat because of the effects of severe soil drying, higher irrigation water salinities, soil particle settling, and compaction by plant roots. Figure 2.8 also shows the hydraulic conductivity derived from simultaneous flux-controlled sorptivity and tensiometer pressure measurements (*Dirksen*, 1979) on cores from column C obtained on J7175. Compared to the drainage-derived curve for column C, the sorptivity-derived hydraulic conductivities were slightly smaller at low water contents and higher at high water contents. It took several weeks to obtain the drainage data and they only gave results for water contents above 0.20 m^3 m^{-3}, whereas the sorptivity method gave results down to less than 0.10 m^3 m^{-3} in about half a day. The entire sorptivity curve is shown in Figure 2.9; this figure also includes estimates of the hydraulic conductivity obtained during draining of column C prior to sampling, but after the alfalfa plants were removed. The agreement is good at the intermediate water contents where one expects the data to be the most accurate. At higher water contents, the gradients are small, the fluxes large, and water contents change fast. At lower water contents, fluxes become very small and accurate determination becomes more difficult. Except for the values at the lower and higher water contents, the straight line through the drainage data indicates an exponential relationship for $K(\theta)$. This line deviates from the sorptivity data at the lower water contents. However, the K-value for the lowest water content corresponds closely with the sorptivity curve. Only the sorptivity curve was used in subsequent analyses.

The wetting of column C, prior to the drainage referred to in connection with Figure 2.9, was carried out on J7125 and J7129 by means of two ponding stages of 114.3 mm water each. Figure 2.10 shows water content distributions during the second stage of wetting and drying. The second wetting started at 11:00 on J7129 and was finished at about 16:30. Figure 2.11 shows hydraulic heads h_h for 8 depths on J7129, and part of J7130. Note that $h_h = 0$ for saturation at the soil surface.

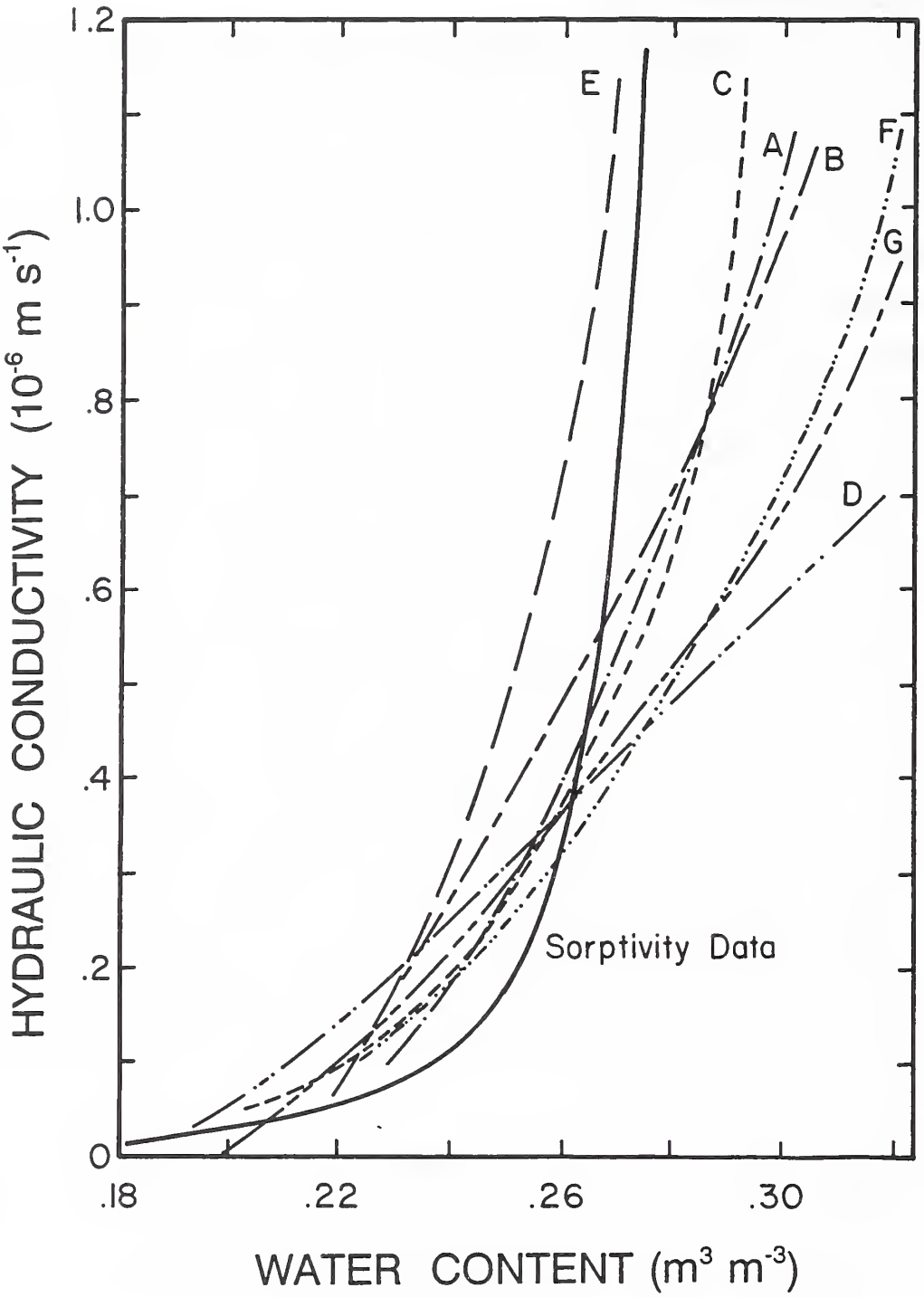

Fig. 2.8. Soil hydraulic conductivity functions for the seven soil columns. The solid line was derived from flux-controlled sorptivity measurements on cores from column C

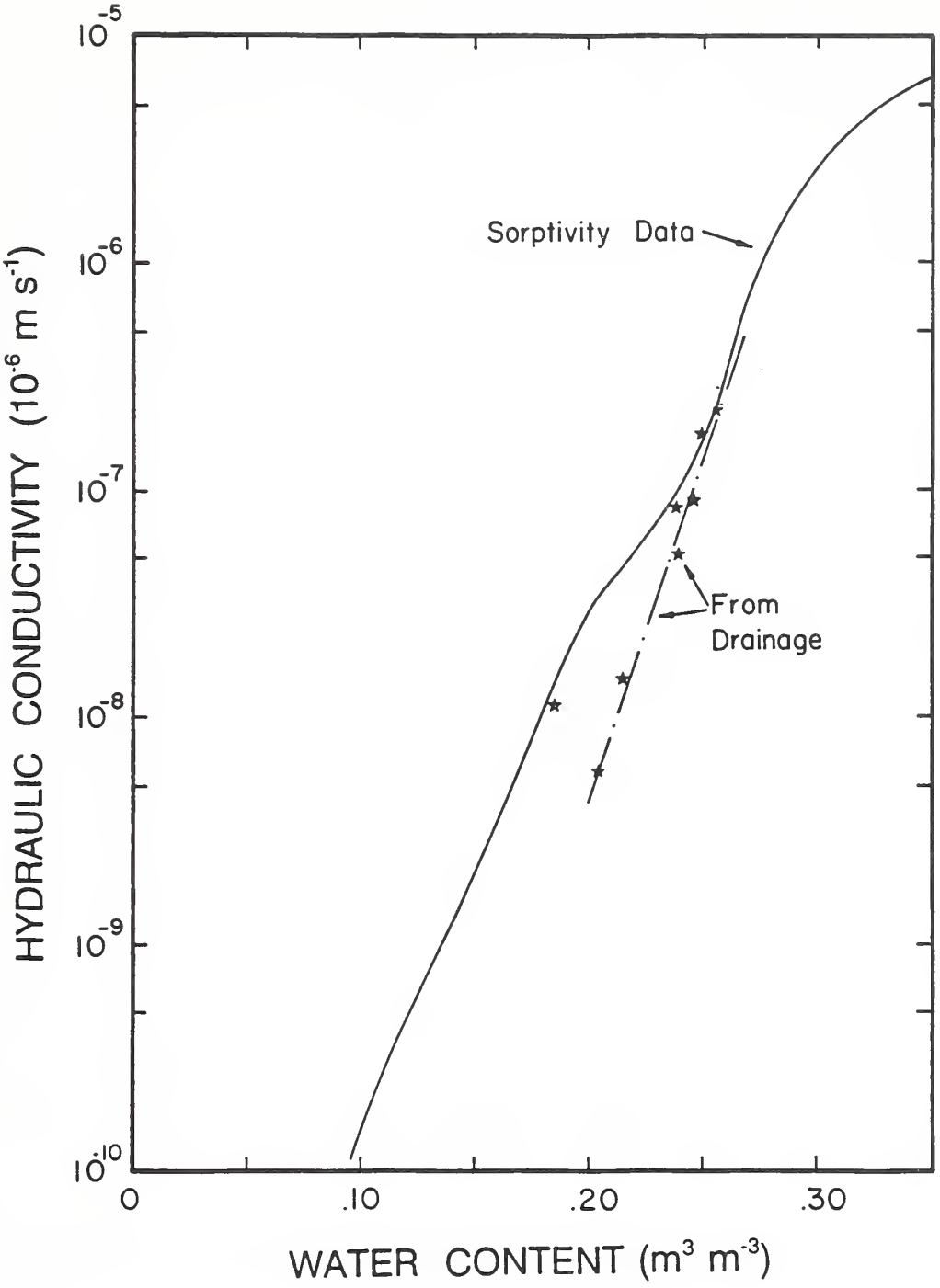

Fig. 2.9. Soil hydraulic conductivity function of column C as obtained from the sorptivity data (solid line) and drainage data using the instantaneous profile method. The dashed-dotted line was fitted through the drainage data.

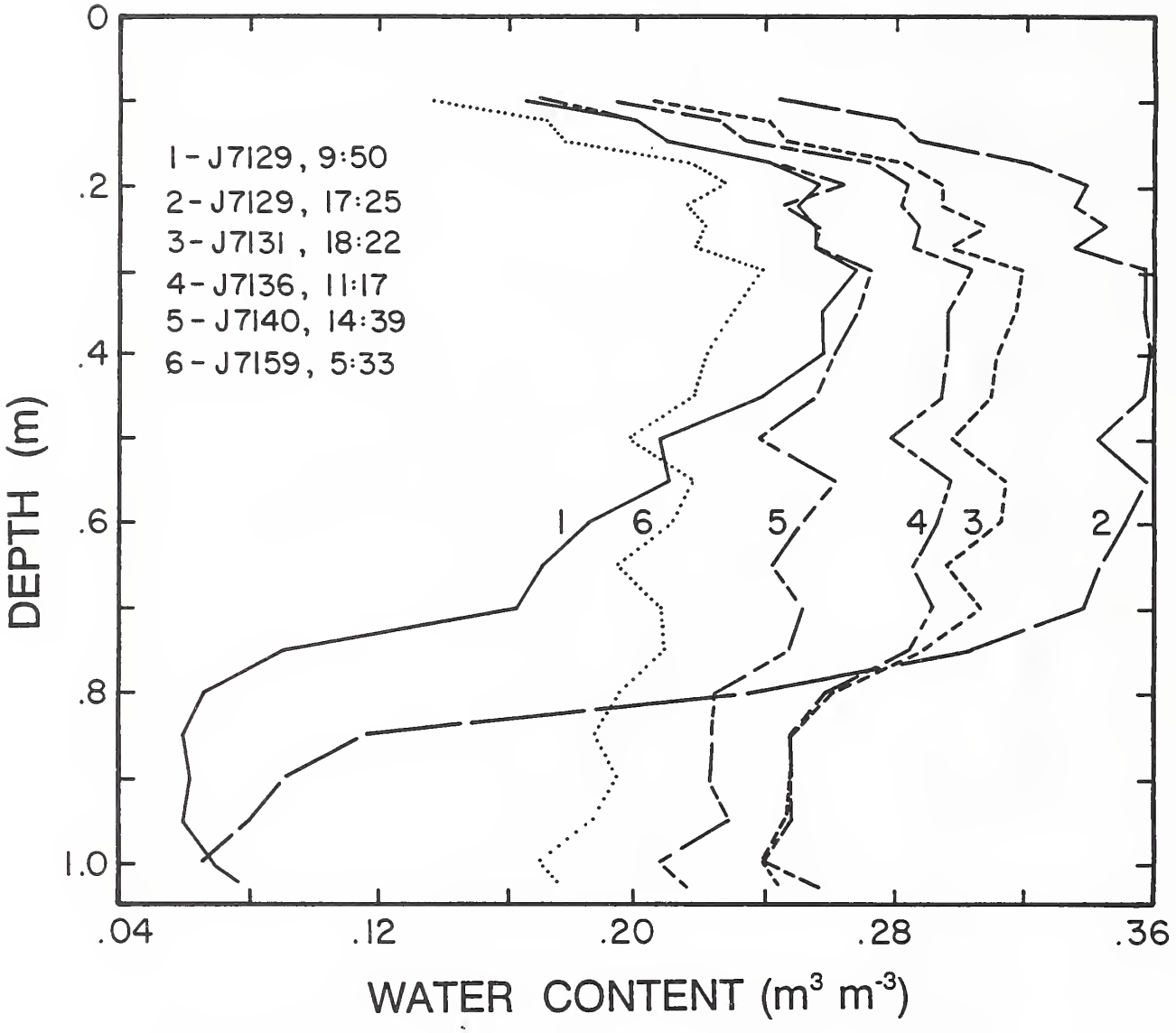

Fig. 2.10. Water content distributions in column C during wetting on J7129 and the ensuing drainage period.

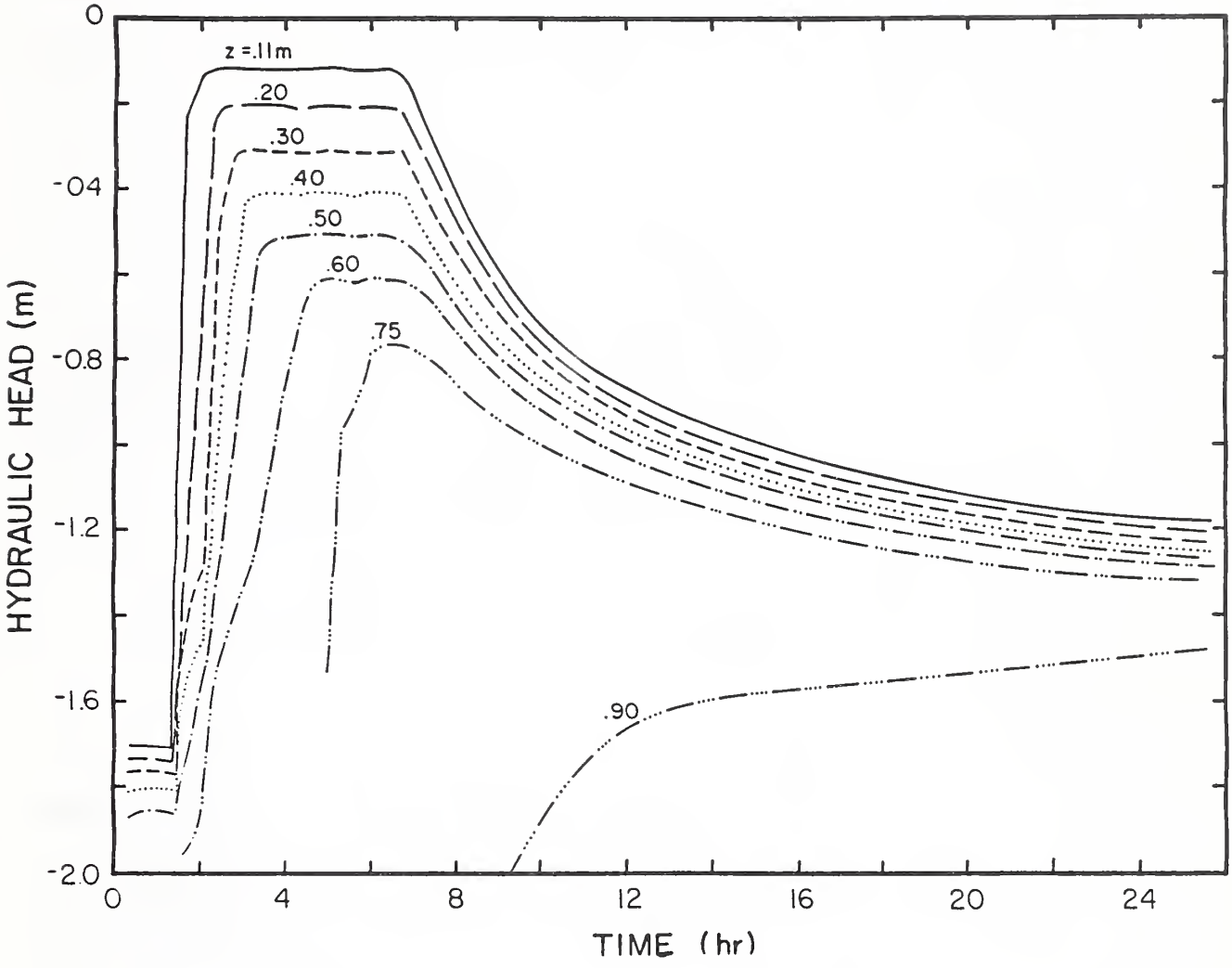

Fig. 2.11. Hydraulic heads at various depths, z, in column C during wetting and drainage on J7129.

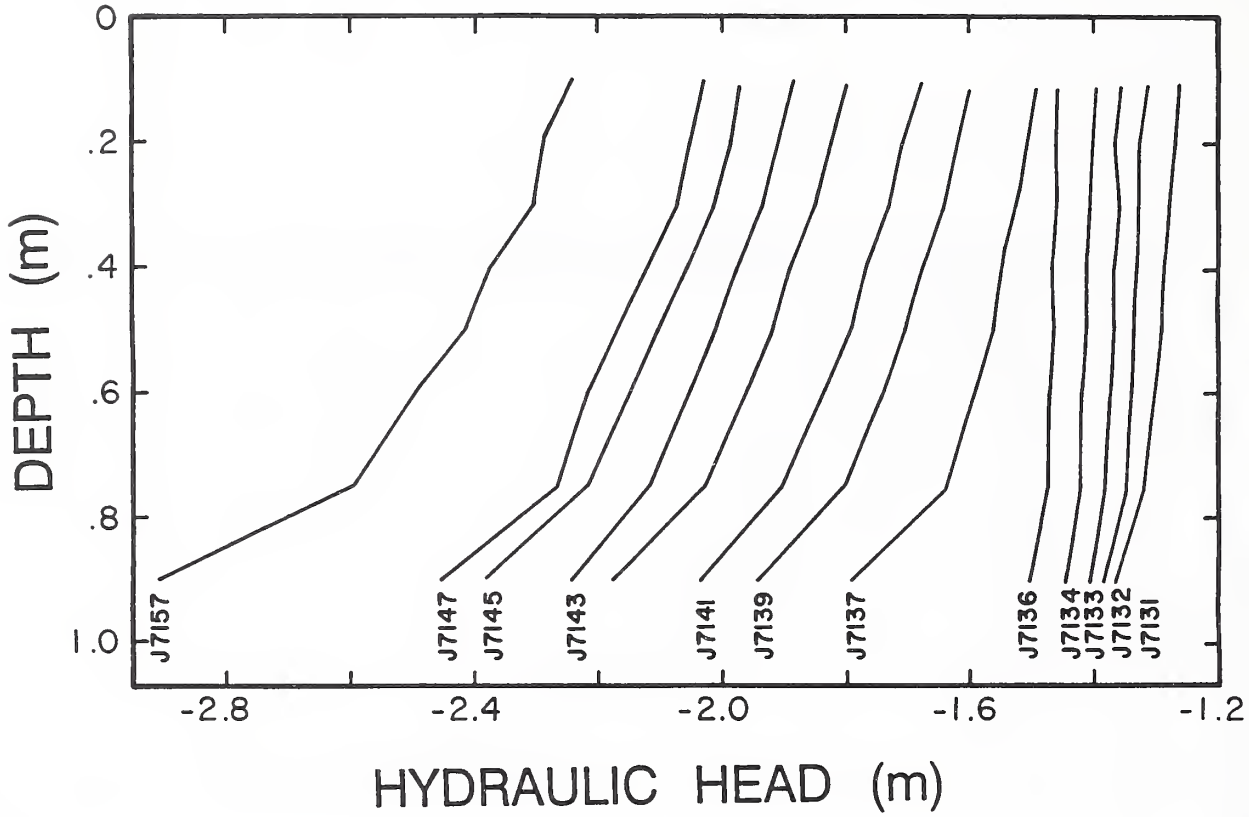

Fig. 2.12. Hydraulic head distributions at 0:00 in column C during drainage from J7131 through J7157.

Figure 2.12 shows hydraulic head distributions in column C at time 0:00 of the indicated days until J7157 when the plastic cover was removed to increase evaporative drying. The drainage tubes were put under suction at 16:00 hour on J7136; drainage before that time was under gravity alone. Figure 2.11 shows essentially unit hydraulic gradients during ponding. This situation corresponds to a hydraulic conductivity of about 8×10^{-6} m s^{-1}; the maximum observed water content was about 0.36 m^3 m^{-3}. These values were used to complement the sorptivity curve in Figure 2.9. A bulk density of 1550 kg m^{-3} corresponds with a total porosity of about 0.415 m^3 m^{-3}. Thus, the soil was not completely saturated with water, probably because of a combination of entrapped air and volume occupied by roots.

The data in Figures 2.10, 2.11, and 2.12 were used to indirectly determine the soil hydraulic properties at the end of the experiments by matching simulated and experimental results without having to account for the complicating effects of root water uptake. The data are suitable for applying inverse methods of parameter estimation which have been developed since the time of the experiments (e.g., *Kool et al.*, 1987), and recently were perfected by *Eching et al.* (1994), among others. Some of the transport experiments described in this report were simulated successfully using a newly developed simulation model for HYSteretic WAter and SOlute transport in the Root zone, HYSWASOR (*Dirksen, et al.*, 1993). The soil hydraulic property functions needed for these simulations were obtained by fitting the equations of *van Genuchten* (1980) to observed retention data. For drying (Fig. 2.7) we obtained the soil water retention parameters α = 0.00837, n = 1.931, θ_s = 0.360, and θ_r = 0.060, and for wetting α = 0.0767, n = 1.596, θ_s = 0.350. The wetting residual water content was adjusted by the program to prevent computational problems. Graphical displays of the fits are shown in *Dirksen* (1991). The hydraulic conductivity function in Figure 2.9 was approximated by two linear segments of $\log K$ vs θ going through the points (θ, K) = (0.10, 6.0 x 10^{-5}), (0.30, 1.8), and (0.35, 4.0), with K given in cm h^{-1}.

2.7.3. *Salinity Measurements*

A number of different types of measurements were made to evaluate the salinity distributions over time and space. Figure 2.13 shows distributions of the osmotic head, h_o, of the soil solution along five vertical rows in column F on J6014. The data were derived from the EC's of extracts from 1:1 soil-water mixtures of the core samples. Between the 0.50 and 0.90 m depths, the salinity increased monotonically from the center of the model to the end. Column F was located at the far end of the model and its canopy received light from the side as well as from above. The higher concentrations of the soil solution suggest that the uneven light intensity caused more root growth toward the end of the model.

Whereas Figure 2.13 adequately describes the spatial variability of the salinity in

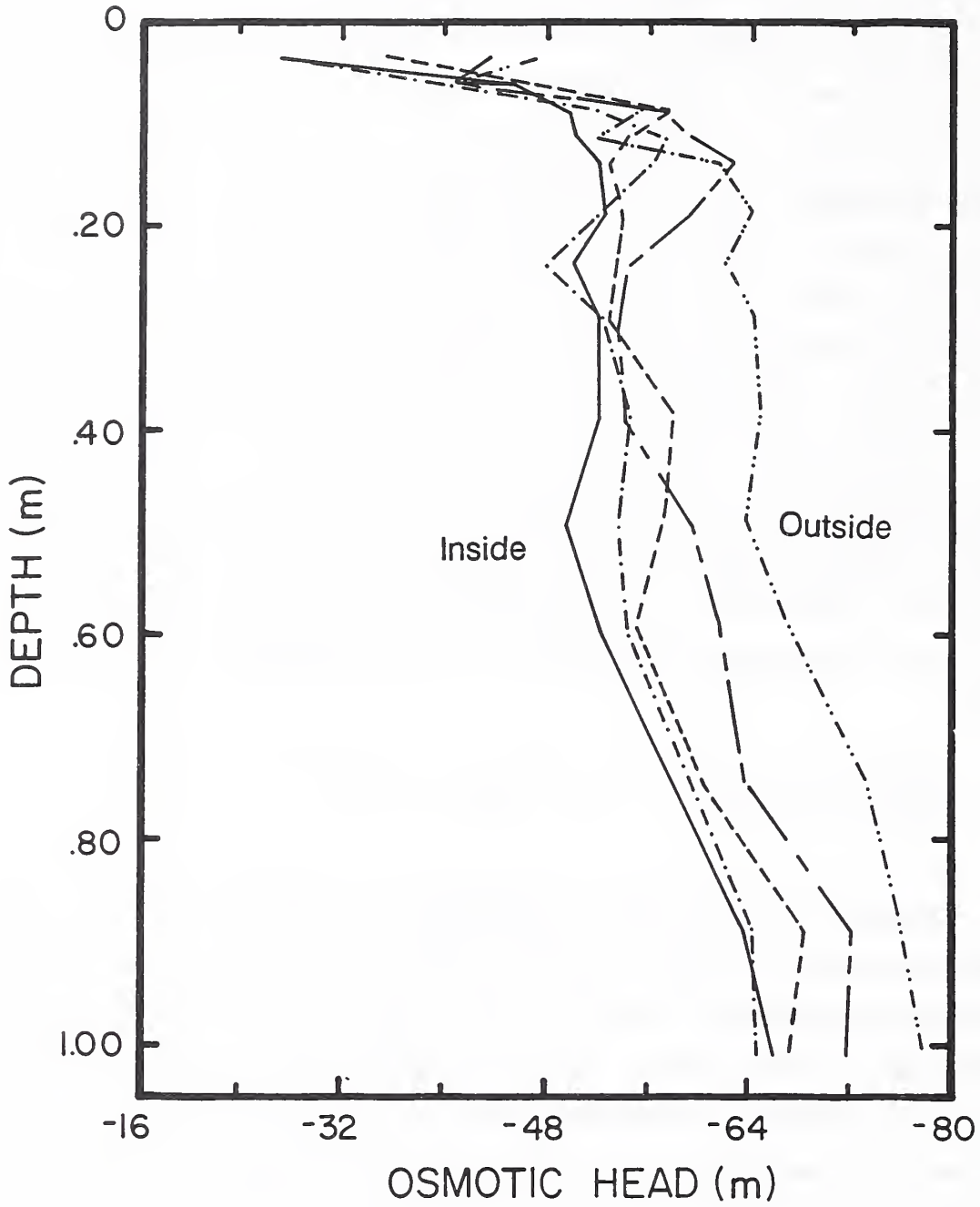

Fig. 2.13. Osmotic head distributions along five vertical lines in column F on J6014.

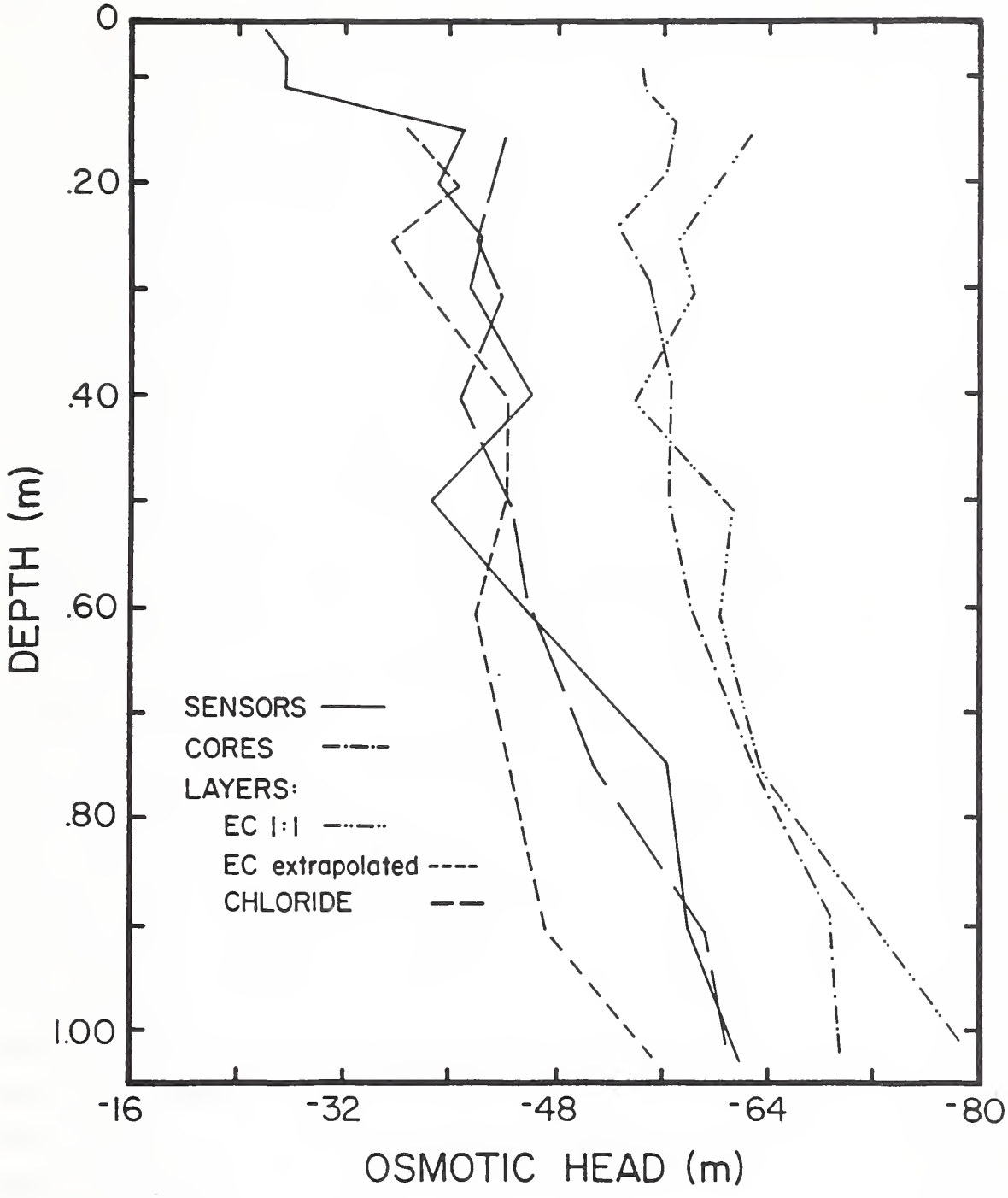

Fig. 2.14. Comparison of several methods used to determine the salinity in column F.

column F, the absolute values are too high. This follows from Figure 2.14, which gives the average h_o-values of the cores in Figure 2.13. They agree well with the h_o-values derived from the EC's of extracts from 1:1 soil water mixtures of 10-mm thick layers taken across the column. The water contents of the 1:1 soil water mixtures are much higher than those actually present in the column. As a result, the extracts probably contained salts that were precipitated in the column, thus making the salinity appear higher than it actually was. To evaluate this dissolution effect, EC's were also measured on extracts from 1:0.5 and 1:0.25 soil water mixtures. The three values for each layer were used to construct a second degree polynomial, which then was used to extrapolate to the h_o-value of the actual water content. The extrapolated h_o-values were much lower as shown in Figure 2.14. Also shown in this figure are h_o-values inferred from chloride concentrations on sub-samples of the 10-mm thick layers. Chloride concentrations are independent of soil water dilution and hence provide accurate estimates for the original in situ salinities. The salinity sensor readings taken just prior to sampling of column F were in excellent agreement with this standard. The extrapolated h_o-values agreed quite well with the chloride data in the top half of the soil column, but were too low in the bottom half. Absolute chloride concentrations were also obtained by titration with $Mg(NO_3)_2$. The corresponding h_o-values (not further shown here) differed little from the other chloride data, indicating that anion-exclusion was negligible.

Figure 2.15 gives similar comparisons for columns D and E sampled around J7173. The figure shows osmotic heads derived from EC's of saturated paste extracts, from chloride concentrations of 1:1 soil-water extracts, and from in-situ salinity sensors. The good agreement between the latter two indicates that the salinity sensors were still functioning well at the end of the experiments. Column E at the time of sampling was much drier than column D (Fig. 2.6), and its error in the osmotic head of the saturation extract hence was much larger. The salinity sensor readings at times were somewhat irregular, especially between the two vertical rows of measuring points. Often, a salinity sensor would temporarily deviate from the general trend and later fall in line again. This could be due to the presence of an active root in close proximity to the sensor. Because of the good agreements in Figures 2.14 and 2.15, and the significant variations in the data of Figure 2.13,

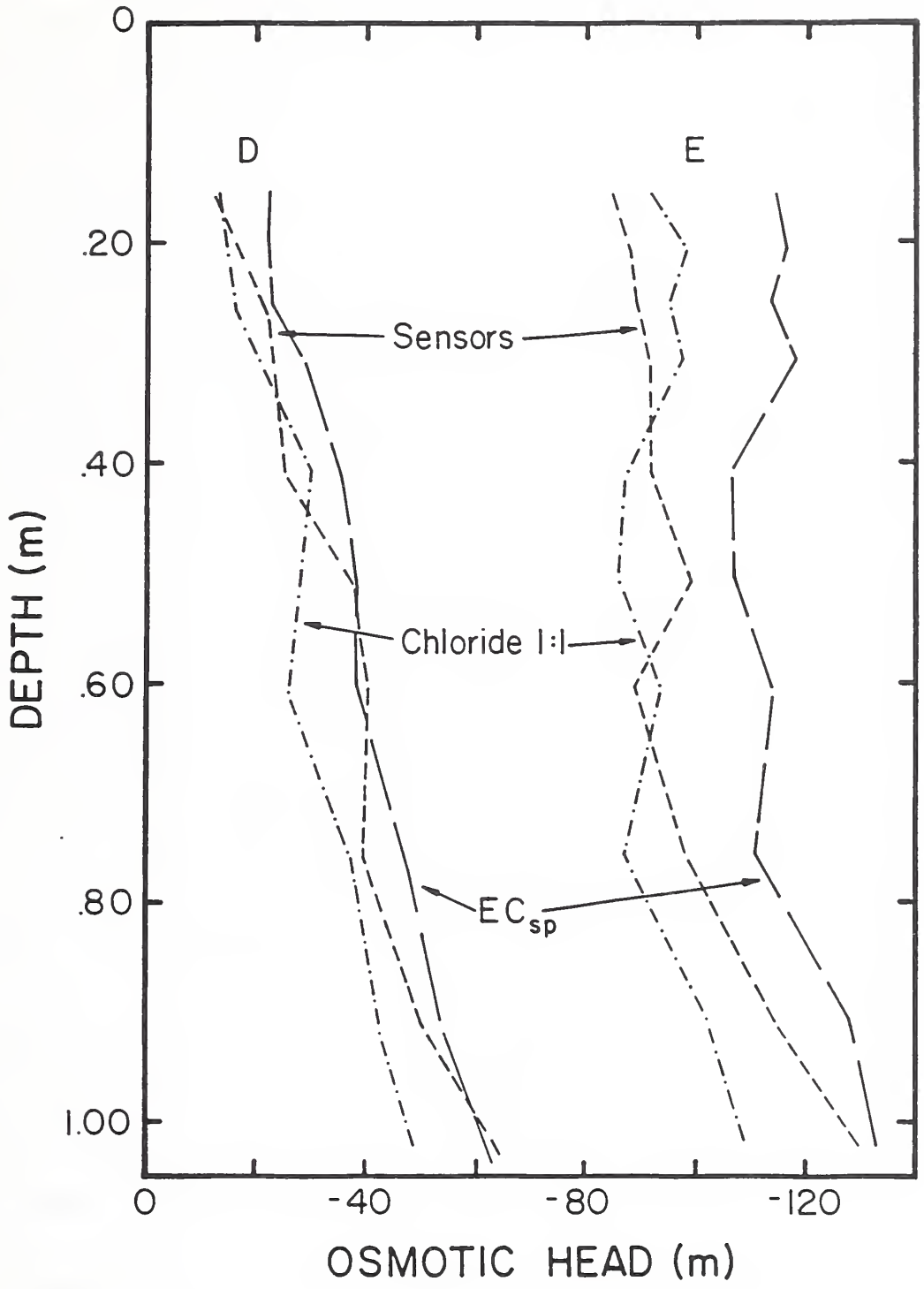

Fig. 2.15. Osmotic head distributions in columns D and E at the end of the experiments. The distributions were obtained with three different methods.

we believe that the irregularities in the salinity sensor readings generally reflected actual spatial variability.

2.8. *Conclusions*

This chapter summarized the experimental conditions, apparatus, procedures, and various soil properties. The illuminance decreased with time and was not uniform in space, especially at the start of the first set of lights. The columns could not be moved around to eliminate this factor. Consequently, results obtained with the various treatments can only be compared to a limited extent. This is also true because of a lack of replications. The objective of the experiments was to obtain data sets for a variety of experimental conditions that are as complete as possible, rather than to demonstrate statistically significant differences between different treatments. After an adjustment of the reference counts obtained before the first wetting, the gamma scanner appeared to give good results. Water content changes over relatively short time periods could be measured accurately. Although the absolute values were subject to some errors over the more than two-year time span, sampling at the end of the experiments showed that the water contents had been corrected adequately. Water contents near the surface were influenced by the not-insignificant volume occupied by root crowns. Analyses and simulation results reported elsewhere (*Dirksen*, 1987; *Dirksen et al.*, 1993) show that the hysteretic behavior of the soil cannot be ignored when one wants to simulate the complete wetting and drying cycles of the different irrigation regimes.

Destructive sampling of column F showed consistent differences in salinity over short distances. The salinity sensors also showed variations in salinity, e.g., between two vertical rows of measuring points in the same column. We believe that these variations generally reflected actual spatial variability in salinity, and that the salinity sensors yielded accurate in-situ soil water salinities throughout the experimental period. A comparison of various methods for measuring salinity indicated that one cannot obtain the true in-situ salinity from the extract of a wetter soil water mixture. The value must be corrected for a dissolution effect. Anion exclusion did not play a significant role in the experiments. Hydraulic

scanning valves used with the tensiometers worked well at first, but later had to be discarded because of leakage between ports. A set of solenoid valves proved unsuitable for hydraulic switching because of heating effects. Finally, only eight tensiometers were used, each one semi-permanently connected to its own pressure sensor. This procedure yielded hydraulic heads that were accurate to within a few mm of water.

Results presented in this Chapter 2 must be considered in conjunction with those on water and salt transport, root water uptake, leaf water potentials, crop yields, and root distributions, presented in the remainder of this report. Together, this information may be useful for developing and testing analytical and numerical models that describe the interactions in a salt-water-soil-plant system, and to gain insight into the interaction of plants with their physical environment.

3. DAILY IRRIGATIONS

This study was undertaken to obtain detailed quantitative information on how plants react and adjust to non-uniform salinity conditions in the rootzone. Chapter 2 gave a general discussion of the experimental conditions and the quality of data obtained during our laboratory experiments in which alfalfa was irrigated with saline water for more than two years. The present Chapter 3 reports results obtained during daily irrigation with different water salinities and at different leaching fractions, L. The study here covers growth periods and harvests I through IX (see Table 1.1 of Chapter 1), and also uses some data obtained during growth period XXVI.

3.1. *Daily Irrigation Experiments*

As explained in detail in Chapters 1 and 2, alfalfa was seeded in six laboratory soil columns (A through F) on Julian day 120 of 1975 (J5120). From J5148 to J6014 all columns were irrigated daily with water of different salinities and at different leaching fractions, L (see Table 1.1). The daily amounts of irrigation, $\bar{q}_i$, for columns A, B, E, and F, are given in the upper parts of Figure 3.1. The cycles in these daily irrigation quantities are associated with the different growth periods as marked on the horizontal axes. Initially we tried to keep all columns closely at a predetermined target L. Column A, irrigated with tap water (h_o= -2.4 m) at a target L of 0.25, served as a non-saline standard. To obtain a relatively high average salinity, column B was irrigated with water of h_o = -22.0 m at a target L of 0.50. Columns C and E were irrigated with water of h_o = -13.2 m at target L's of 0.18 and 0.08, respectively. Columns D and F received tap water at an average L of about 0.14 until J5273 at the start of growth period VI. These two columns were then quickly salinized by surface irrigation with water of h_o = -13 m, and by subsurface irrigation with waters of h_o = -20 and -40 m, respectively. Efforts to keep the target L's were not very successful because of difficulties in measuring ET accurately. Eventually we just maintained differences between the columns to insure a variety of salinity profiles, increased the

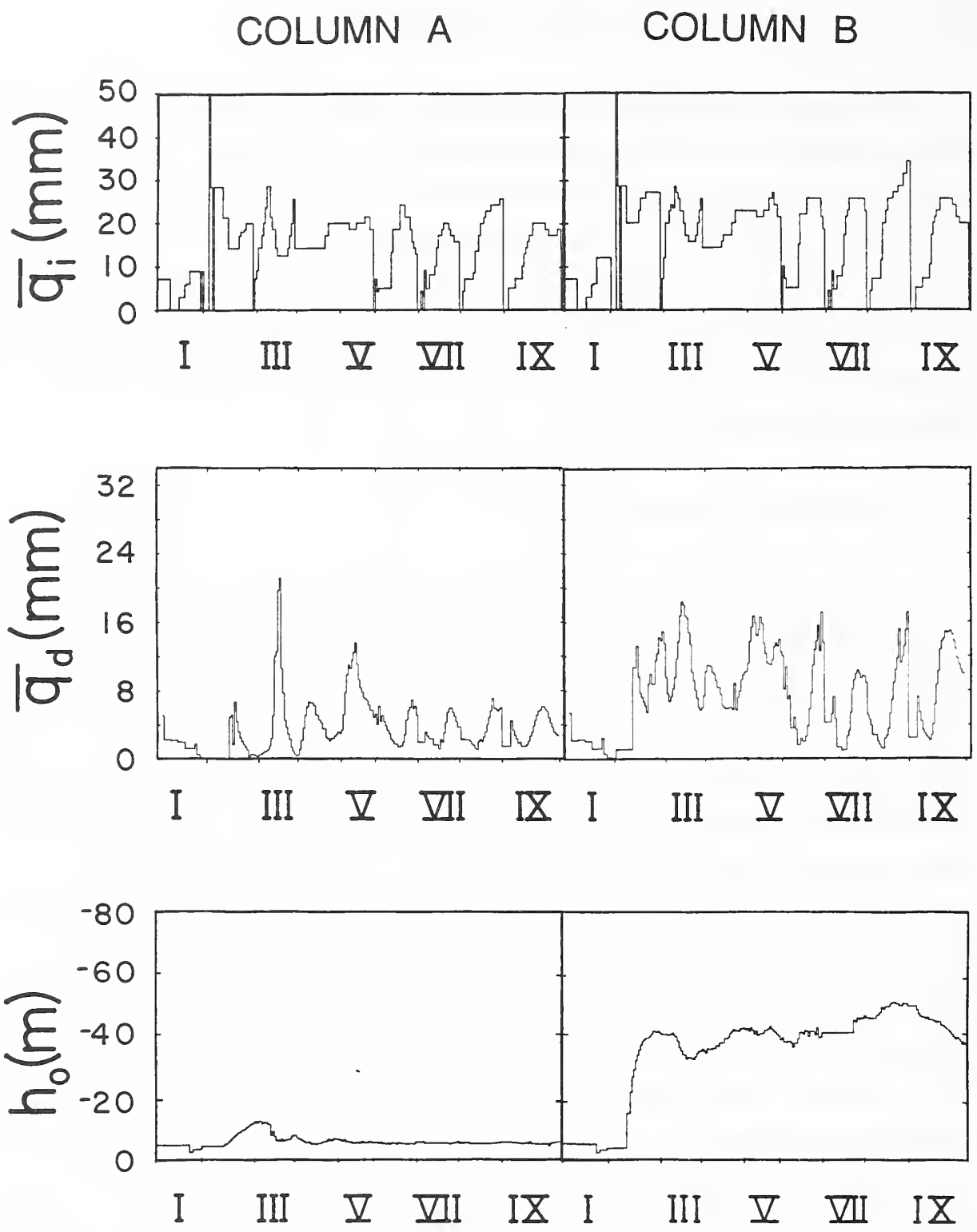

Fig. 3.1. Daily amounts of irrigation ($\overline{q}_i$) and drainage($\overline{q}_d$), and osmotic heads (h_o) of the drainage water for columns A, B, E, and F during growth periods I through IX.

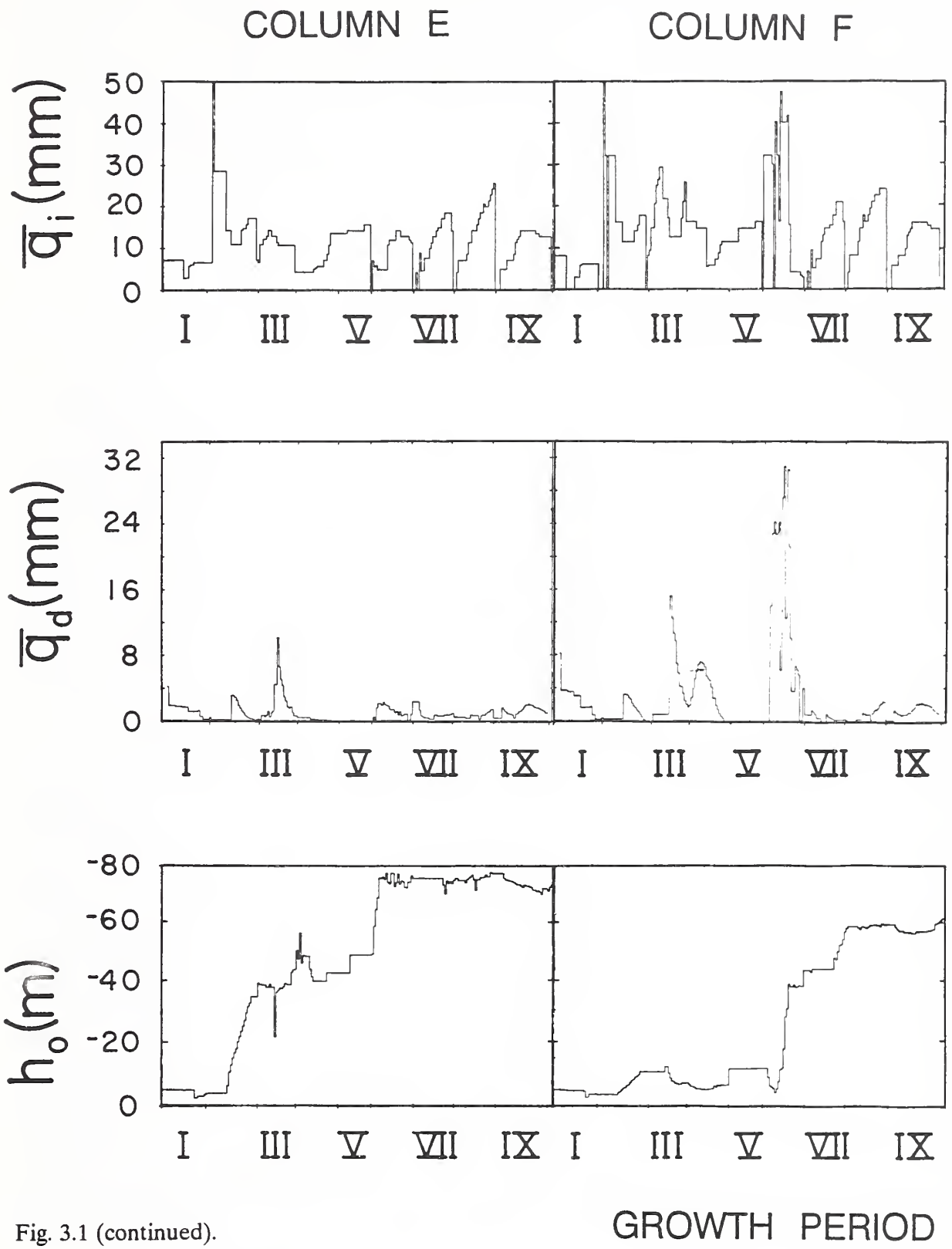

Fig. 3.1 (continued).

irrigation volumes with the growth of the alfalfa, and let the L's find their own values. Besides irrigation and drainage volumes, we also measured soil water contents, soil and leaf water pressure heads, soil water osmotic heads, and yields. Column F was sampled destructively on J6014 at the end of growth period IX to obtain direct measurements of bulk densities, soil water contents, soil water salinities and root lengths. Further details on the equipment and the experimental methods can be found in Chapter 2.

3.2. *Water and Salt Balances*

The average daily drainage rate, $\bar{q}_d$, reflects variations in the irrigation rate and *ET*-cycles due to cutting and regrowth (Fig. 3.1). The lower parts of Figure 3.1 show the osmotic heads of the drainage water. Figure 3.2 gives the cumulative amounts of irrigation and drainage for six columns. Column B received the most irrigation and also had the largest drainage volume. Column E was the lowest in both categories. Columns D and F showed the effects of the later, quick salinizations. Figures 3.3a and b give the cumulative amounts of salts in moles of charge per column in the irrigation and drainage waters, respectively. Column B is by far the highest in both categories, whereas column A received and lost as expected the least amount of salt. Figure 3.3c gives the difference between the cumulative amounts of salt in the irrigation and drainage waters, again in moles of charge per column. If we assume no salt uptake by plants and no salt precipitation or dissolution, this difference represents the amount of salt stored in the columns at any given time as a result of the irrigations. Column E, having the smallest leaching fraction (L = 0.08), became the most saline and was still increasing in salinity at the end of growth period IX, even though the osmotic head of the drainage water at that time reached a fairly constant value of about -75 m (see Fig. 3.1c). Because chlorides were used, this increase is the result of an upward shift in water uptake and not of salt precipitation. During non-daily irrigation, the plants concentrated the soil water solution to an osmotic head of -115 m. Columns B and C were more or less at a steady salinity prior to J5292 (growth period VI), but increased in salinity after that day. The drainage water from column B reached a fairly steady osmotic

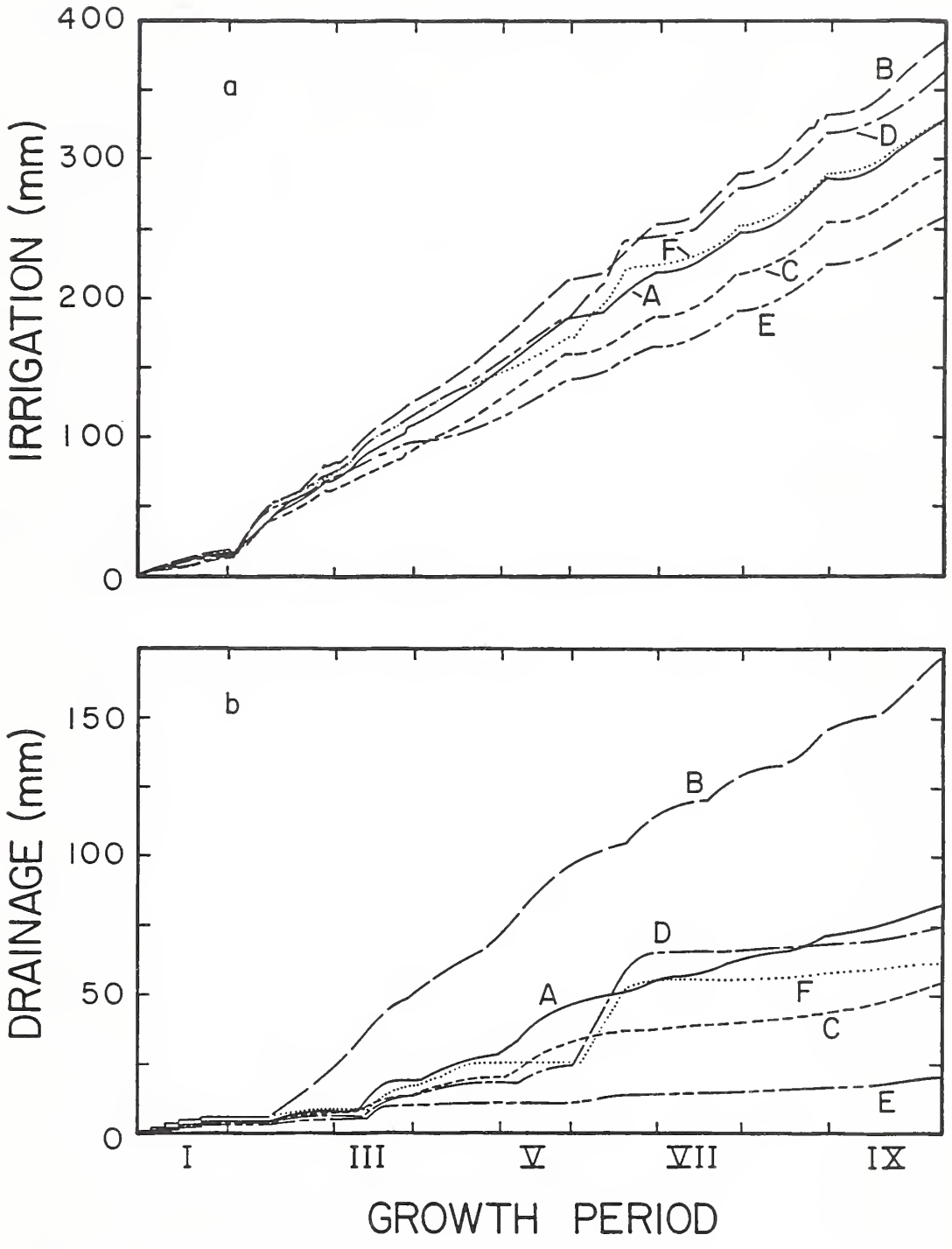

Fig. 3.2. Observed cumulative amounts of irrigation and drainage for six columns.

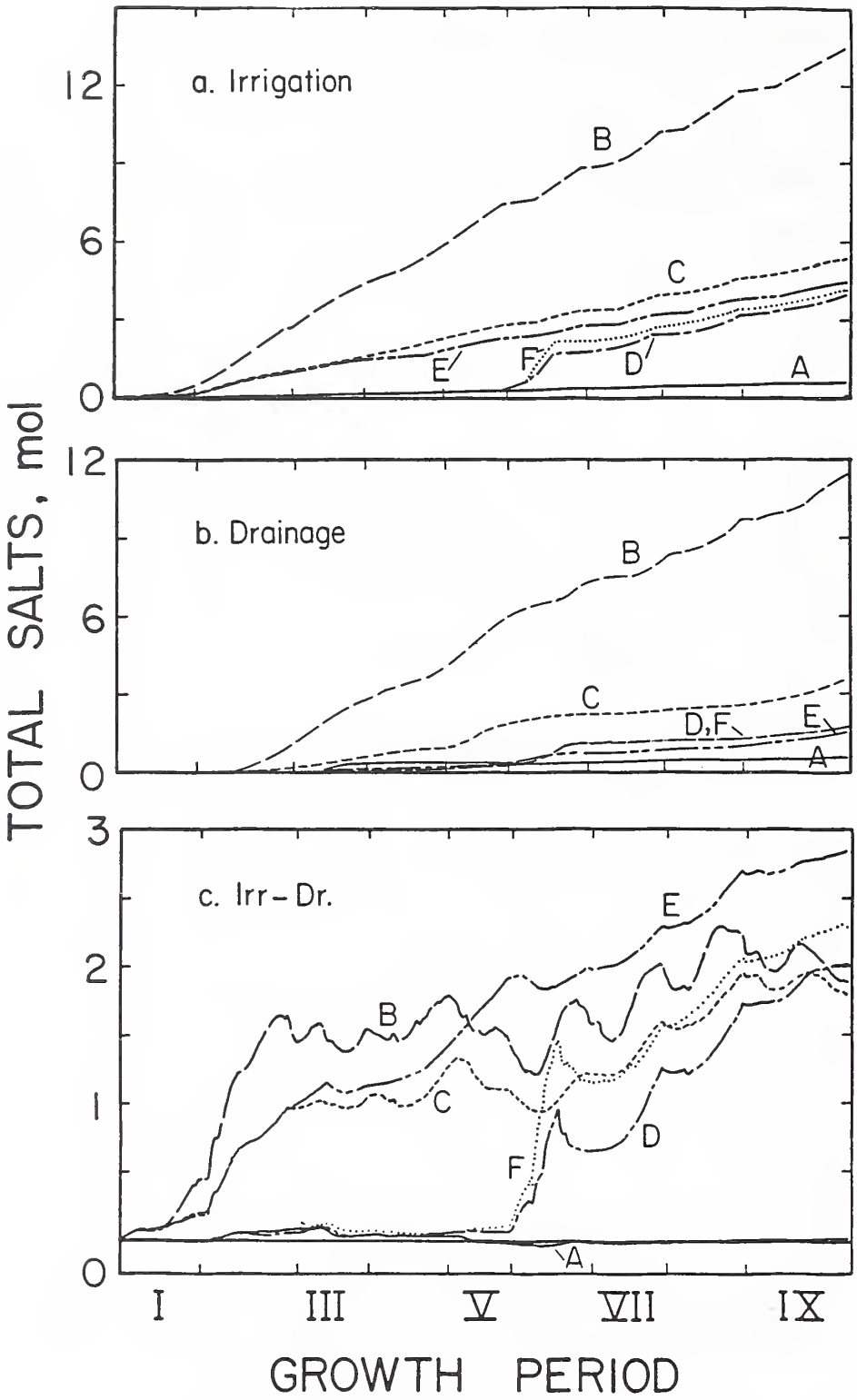

Fig. 3.3. Cumulative amounts of salt in irrigation (a) and drainage water (b), and total amount of salt (c) stored in six soil columns.

head of -40 m after 50 days, when L was still only 0.25. The effects of the various daily irrigation regimes and the resulting salinization processes on yields and transpiration ratios are discussed in Chapter 5.

Table 3.1 lists daily amounts of ET in mm at selected days during growth periods IV, V, and VI, as determined from the water balance for each column. The changes in ET with time, and even more so in the cumulative amounts of ET during the three growth periods, were very similar for the six soil columns. The decrease in ET toward the end for some of the columns were due to thrips or because of mechanical damage by the counter weight

Table 3.1. Evapotranspiration in mm on selected days of growth periods IV, V and VI.

	Growth	Day					
Column	Period	1	5	10	15	20	25
A	IV	4.11	7.47	10.23	12.39	13.95	14.91
	V	3.43	7.70	11.83	14.60	16.03	-
	VI	3.20	6.74	10.36	13.08	14.90	15.82
B	IV	4.93	6.76	8.78	10.50	11.92	13.04
	V	3.16	6.65	9.66	11.17	11.17	-
	VI	2.50	5.40	8.90	10.70	10.60	8.80
C	IV	5.02	8.36	11.72	14.18	15.74	16.40
	V	3.50	6.85	11.68	13.05	10.98	-
	VI	2.40	4.58	8.80	11.52	13.64	15.16
D	IV	3.71	9.02	13.91	16.84	17.83	16.86
	V	4.34	9.14	13.12	14.84	14.32	-
	VI	-	-	-	-	-	-
	IV	3.92	7.24	9.91	10.92	10.29	8.00
	V	3.39	6.51	9.60	11.80	13.08	-
	VI	3.27	4.99	7.01	8.87	10.59	12.15
F	IV	2.72	6.75	11.10	14.71	17.56	19.67
	V	3.12	7.55	11.74	14.43	15.62	-
	VI	-	-	-	-	-	-

cables of the gamma scanner. The most saline columns B and E had much lower *ET*-rates than the other columns. One day after the alfalfa was cut, all columns had daily *ET* amounts of about 3.5 mm. The average daily amount of *ET* for the full-grown canopies was about 11 mm for the saline columns and about 16 mm for the non-saline columns, with a maximum of nearly 20 mm. These values are high because they are based on a soil surface area of 0.070 m^2, while the canopy areas were much larger and also were exposed to light on the sides. In addition, the *ET*-data were obtained for 16 hours of light per day.

3.3. *Hydraulic Heads and Fluxes*

Figures 3.4a and 3.4b show hydraulic heads at various depths as a function of time in response to irrigations of 21.4 and 20.0 mm on the evenings of days J5270, and J6011,

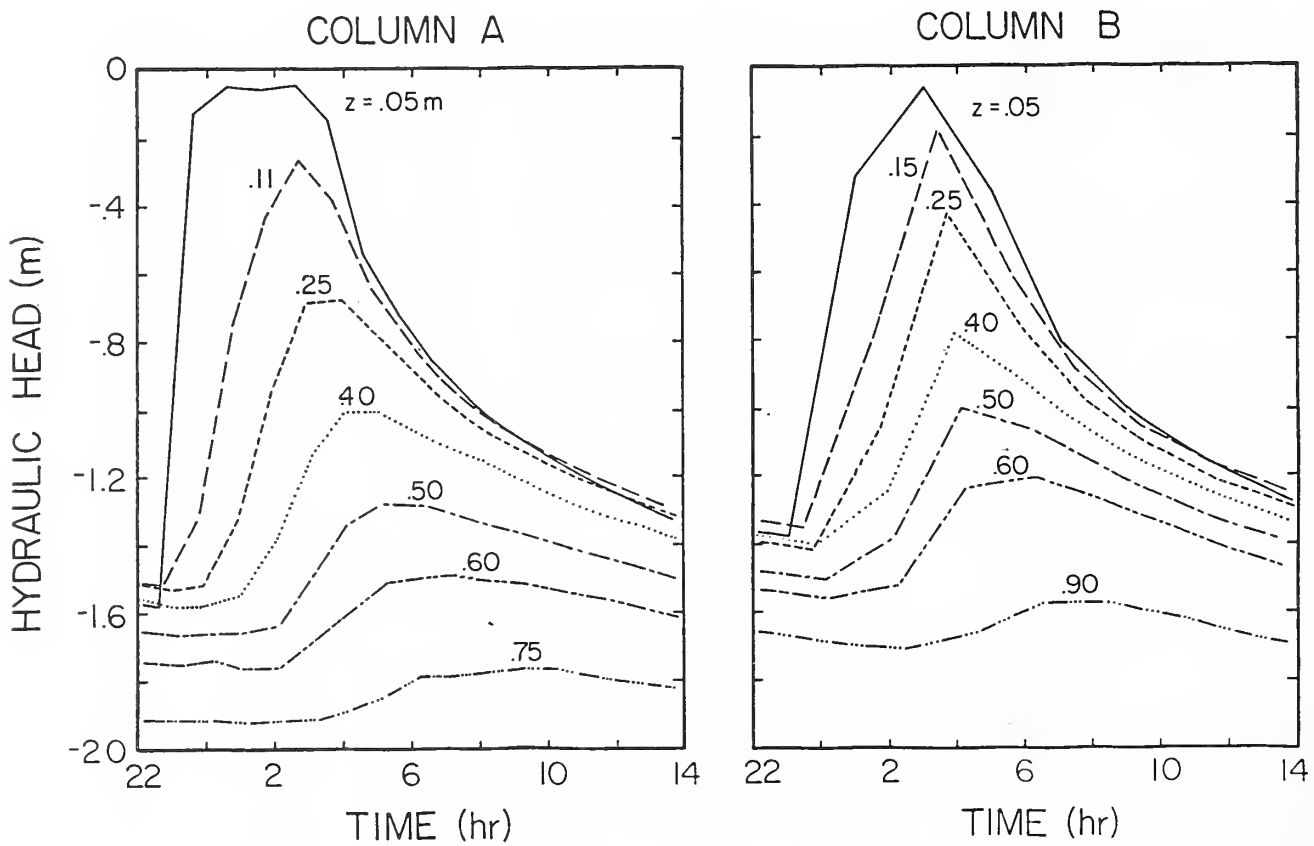

Fig. 3.4. Observed hydraulic heads at various depths, z, in columns A and B after the columns were irrigated with 21.4 mm water on J5270 (a) and 20.0 mm on J6011 (b), respectively.

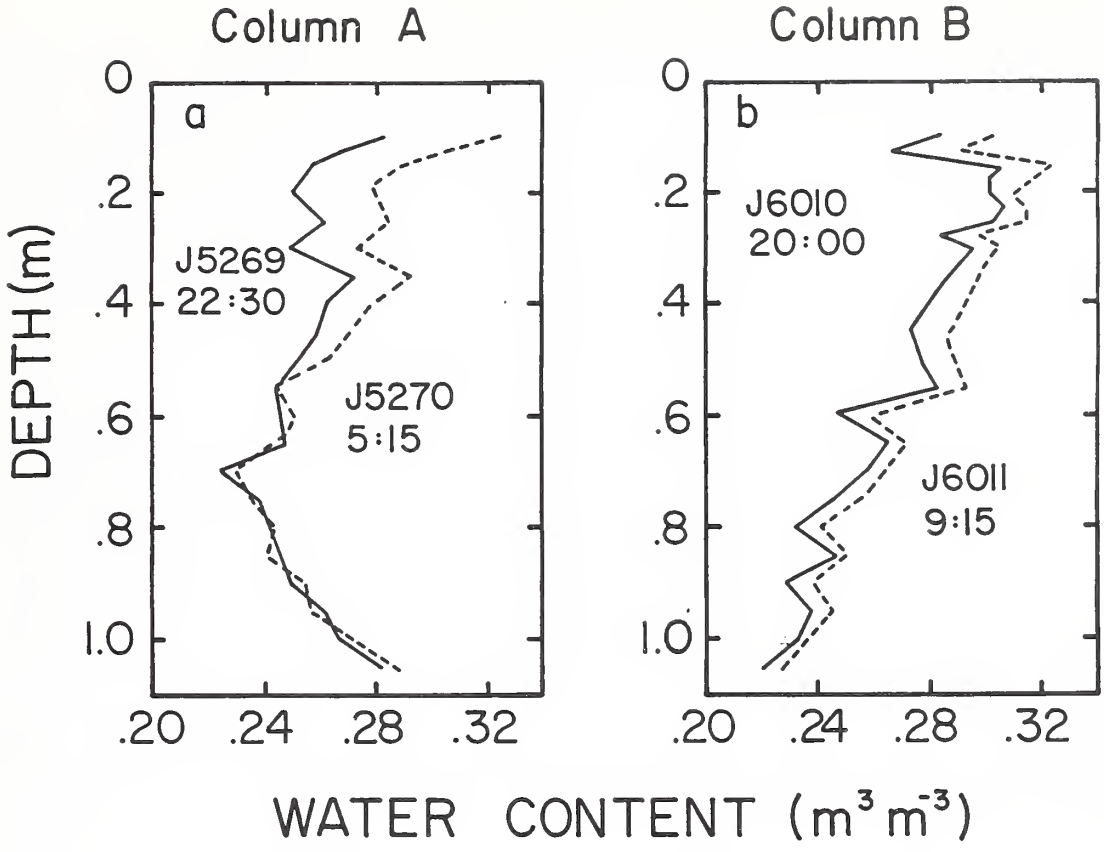

Fig. 3.5. Observed water content distributions before and after the irrigations of Figure 3.4

respectively, for columns A and B. Corresponding water content distributions are given in Figure 3.5. Column A received the most water per irrigation and, because it was kept non-saline, had relatively high yields, and high rates of evapotranspiration. As a result, the top half of the column each day dried out to such an extent that, with an irrigation of 21.4 mm, water contents increased only over a relatively shallow depth of about 0.60 m. The pressure pulse extended to below 0.75 m. Since the volumetric water content near the surface during irrigation was about 0.30, the actual irrigation water, assuming piston flow, would occupy initially only the top 0.07 m of the soil column. Non-piston flow and subsequent redistribution could possibly have moved the irrigation water twice as deep into the column, but this would still be far less than the depth to which the water contents increased. The consequences of this for salinization process will be discussed later in more detail. Column B was operated at the highest leaching fraction and, because of the high salinity of the irrigation water and the low illuminance, had relatively low yields and low *ET*-rates. As a

result, the entire column was wetted by the 20.0 mm irrigation. Drainage rates from this column were nearly equal to the water uptake rates, so that $\lambda(z,t)$ can be obtained only by rigorous calculation of the entire flow problem with a computer. This is not done here. Instead, we will describe some general features of the hydraulic head and flux density distributions during the daily irrigation cycles, and use these distributions to estimate root water uptake from observed rates of change of the water content.

The hydraulic head distributions for column C in Figure 3.6 are in response to a 17.1-mm irrigation that started at about 22:30 on the evening of J7076. Corresponding water content distributions are shown in Figure 3.7. The later date was chosen because the tensiometer data were more detailed and more accurate than during growth periods I through IX. The maximum hydraulic head started its increase at 0.75 m depth. There was

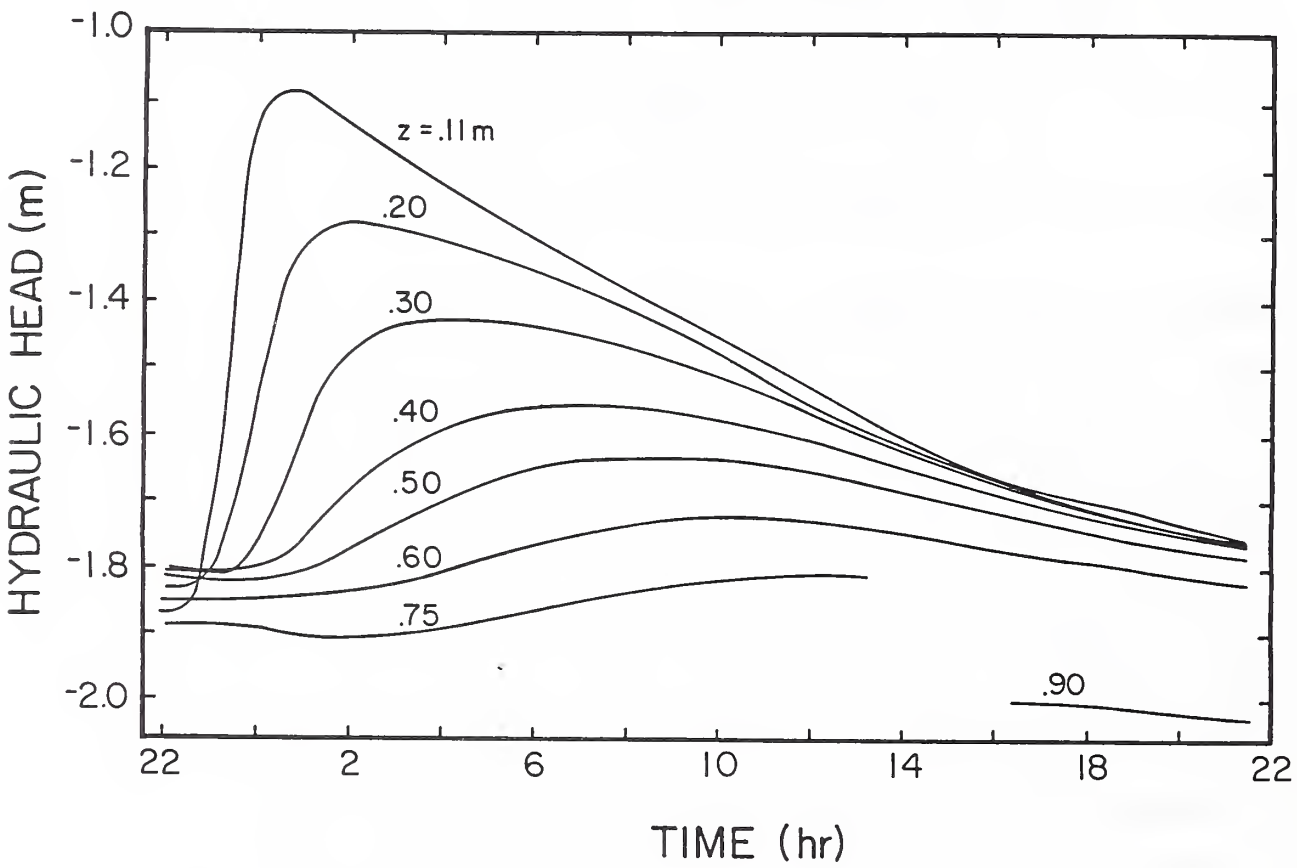

Fig. 3.6. Observed hydraulic heads in column C during and after an irrigation of 17.1 mm water on J7076

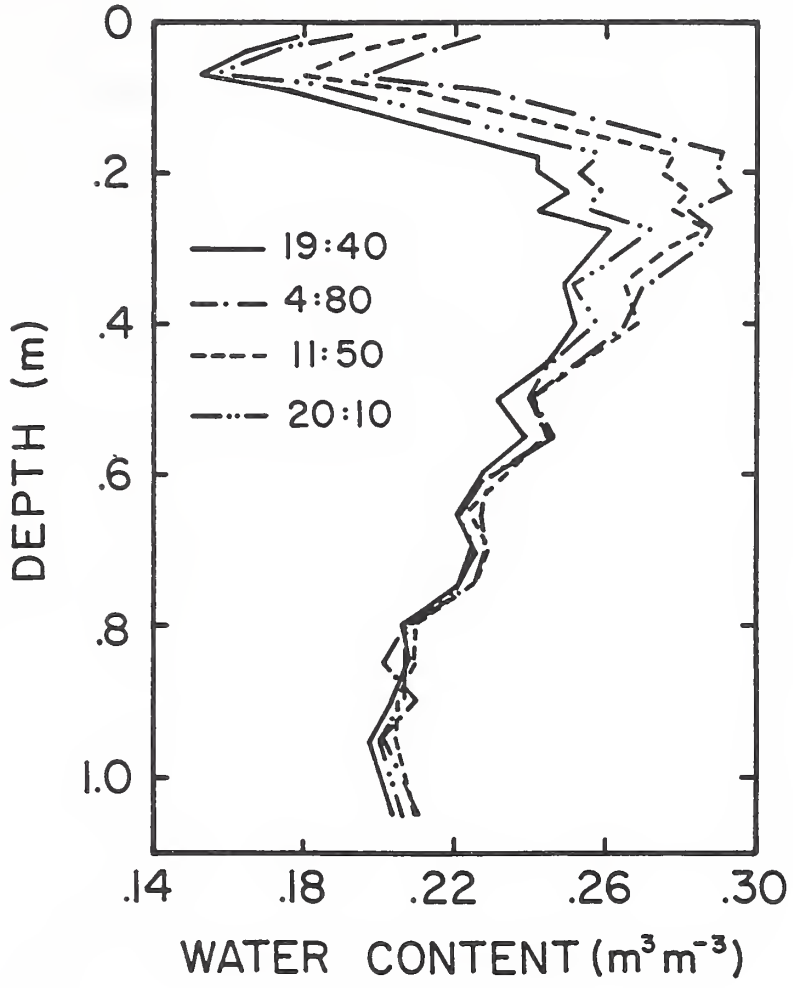

Fig. 3.7. Water content distributions in column C corresponding with Figure 3.6.

a time difference of about three hours between the initial responses at 0.11 m and 0.75 m depth, while the time difference between the peaks amounted to about 11 hours. As was observed often, the pressure head h_p between 0.20 and 0.60 m depths reached successively nearly the same maximum value, in this case h_p = -1.13 m. Another feature, often more pronounced than in Figure 3.6, is the distinct increase in the rate of decline of the hydraulic heads when the lights were switched on (at 8:00 a.m. on this day). The daily irrigations normally were applied soon after the lights were turned off. Later in the day, the hydraulic

head gradients in the zone with the largest water uptake rates became very small, and often were reversed. The hydraulic head gradients in Figure 3.6 between 0.11 and 0.30 m depths after 14:00 were only about 0.1 or less. Except during and shortly after irrigations, the gradients were always smaller than unity down to 0.75 m. The tensiometers at 0.75 and 0.90 m depths could not be read at the same time, and were interchanged from time to time. Extrapolated h_h-values for the same time on J7077 as well as on J7078 indicate a unit gradient between these two depths. The water content in 0.75 - 0.90 m depth zone was approximately 0.205 $m^3\ m^{-3}$ (Fig. 3.7), giving a hydraulic conductivity of 3.5×10^{-8} m s^{-1} (Fig. 2.8). The measured daily-averaged drainage rate was also 3.5×10^{-8} m s^{-1}. In view of the unit hydraulic gradient below 0.75 m, this is an excellent agreement. Based on the

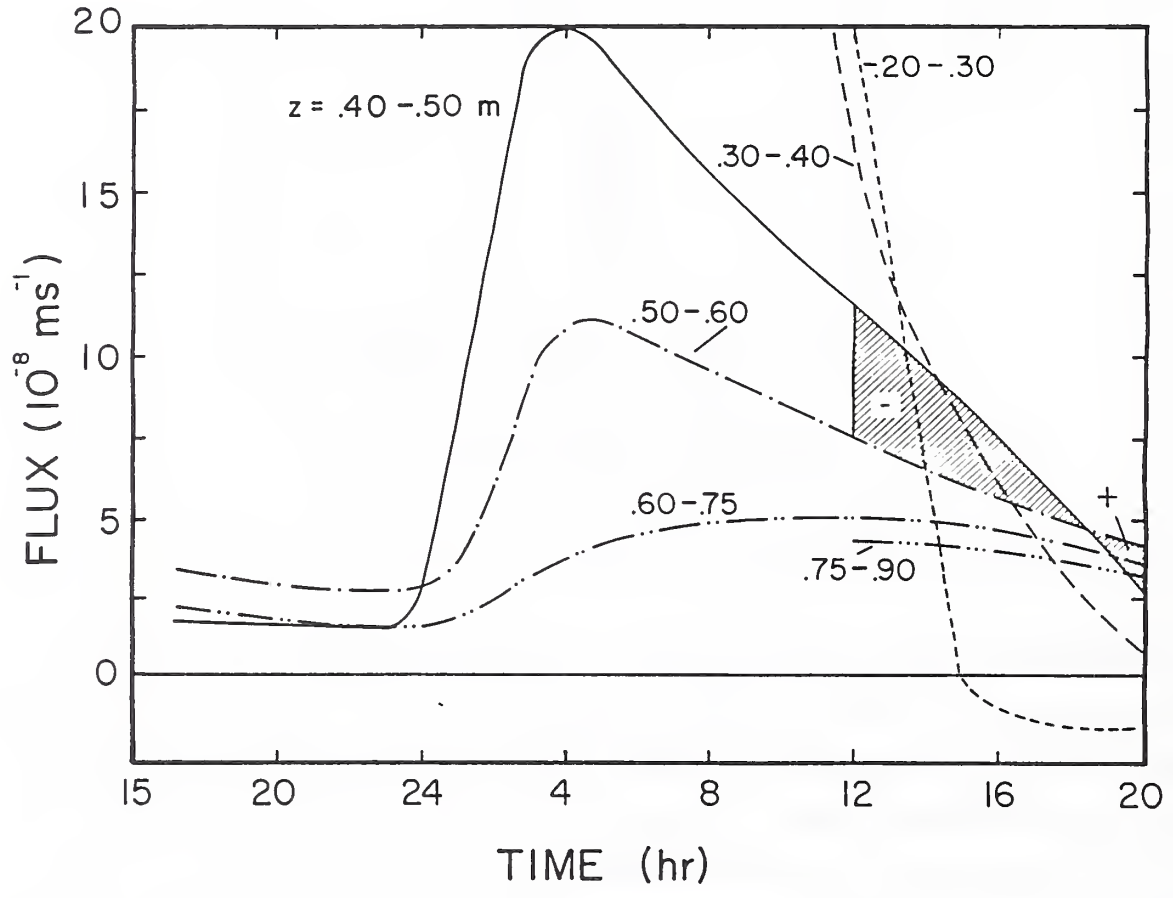

Fig. 3.8. Average water flux densities at various depth intervals corresponding with Figure 3.6. The shaded portion of the figure was used to derive the divergence of the flux density, DF (see text).

measured hydraulic heads in Figure 3.6 and the $K(\theta)$ function in Figure 2.8, average water flux densities as a function of time were calculated with Eq. (1.3) for various depth intervals; these flux densities are presented in Figure 3.8. The small variations between 0.60 and 0.75 m suggest that the instantaneous drainage rate from the column varied somewhat around the average value of 3.5×10^{-8} m s^{-1} but, unfortunately, this was never monitored. The high flux densities in the top of the column during and immediately after irrigation could not be calculated accurately because of rapidly changing water contents and hydraulic conductivities. For instance, the flux density between 0.30 and 0.40 m around 05:00 was still in excess of 100×10^{-8} m s^{-1}. Relatively high conductivities coupled with small gradients make an accurate calculation of the divergence of the flux difficult. To keep Figure 3.8 useful for estimating the divergence of the flux density, its ordinate was limited to 20×10^{-8} m s^{-1}.

3.4. *Root Water Uptake Distributions Derived from Hydraulic Data*

The irrigation cycle during infrequent irrigation can be divided roughly into two phases: one in which infiltration and redistribution dominate, and one in which water uptake by roots dominates. We will explore whether this partitioning can be used to obtain water uptake distributions also during frequent (daily) irrigation. Equation (1.6) will be used for that purpose. The first term (RCWC) on the right-hand side of this equation follows directly from observed water content distributions (e.g., from Fig. 3.7), while the second term (DF) can be obtained from such plots as shown in Figure 3.8. The integral in the numerator of DF is simply the area between two curves with appropriate signs, as indicated by the shaded area in Figure 3.8 for the period between 12:00 and 20:00 hours, and for the zone between average depths of 0.45 and 0.55 m. DF is at first negative, but becomes positive when the two curves cross. Figure 3.8 shows that later in the irrigation interval the absolute value of DF decreases with time. Since DF introduces by far the largest errors in the calculation of λ, we will investigate whether during the latter part of the irrigation interval DF can be neglected with respect to RCWC. Figure 3.9 shows in block diagram average values of DF derived from Figure 3.8 for six depth layers and for the time period between 12:00 to 20:00. Also plotted is the slightly smoothed RCWC-distribution

derived from the data in Figure 3.7 for the same time period. For example, the shaded area in Figure 3.9 represents the algebraic sum of the two shaded areas in Figure 3.8. The λ-distribution in Figure 3.9 was drawn consistent with these data according to Eq. (1.6) and with the assumption that no root water uptake took place below 0.75 m. This assumption was based on the fact that the average water flux density under unit gradient below 0.75 m was found to be equal to the average drainage rate of 3.5×10^{-8} m s^{-1} (section 3.3). For the 8-hour time period considered here, this rate is about equivalent to the area between the RCWC-curve, the λ-curve and the *z*-axis below 0.75 m.

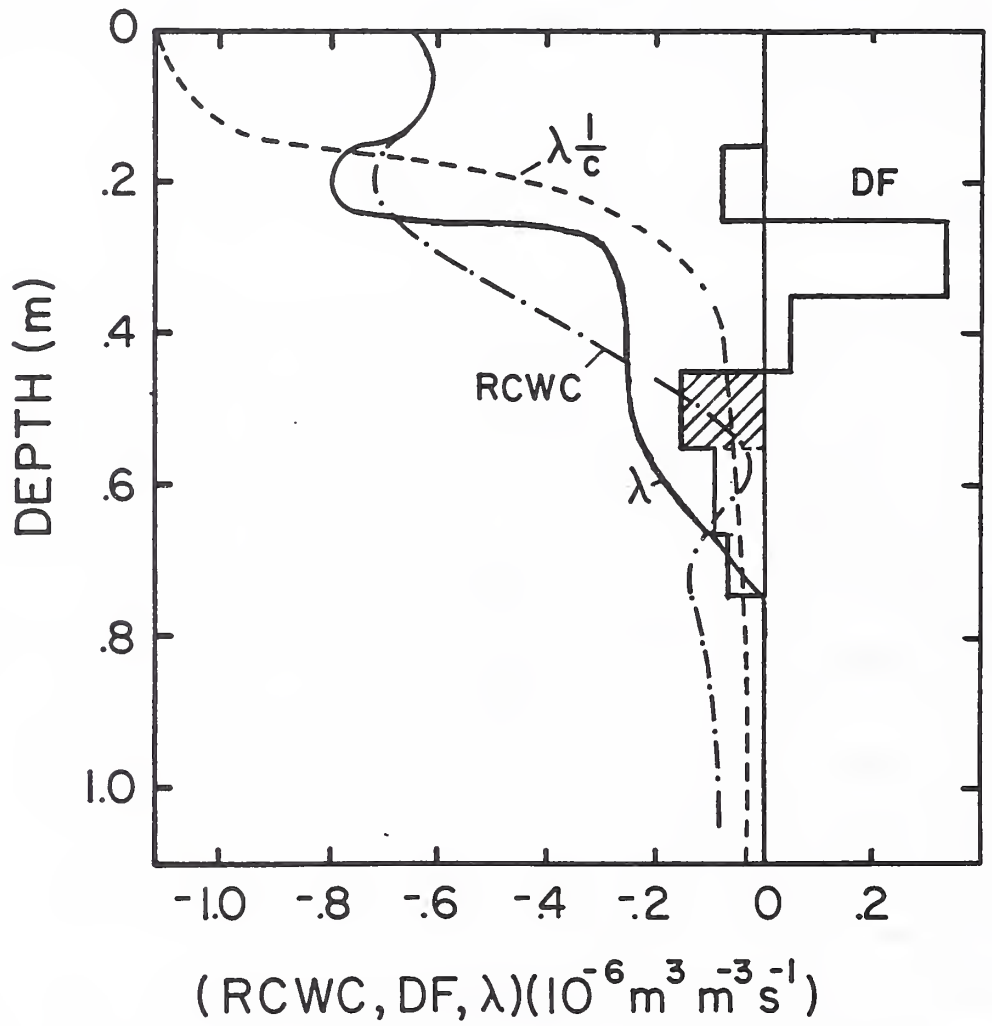

Fig. 3.9. Water uptake distributions derived from hydraulic data (λ) and from the salt dilution profile ($\lambda_{1/C}$). The distributions of RCWC and DF are also shown.

Figures 3.6 and 3.8 show that the flux densities in the bottom part of the column are about 12 hours out of phase with the irrigation rates; it appears therefore reasonable to account for drainage between 12:00 to 20:00 by the decrease in water content at the bottom. This treatment of the data infers that during other parts of the day water contents below 0.75 m increased again in such a way that over 24 hours the net change in water content below 0.75 m was zero, and hence that the average flux density through this zone was equal to the average drainage flux density from the upper 0.75 m. The required increase in K, and thus in θ to accommodate the increase in drainage flux density under the unit gradient assumption towards the bottom between 12:00 and 20:00, is hardly measurable. The shape of the RCWC-curve suggests a transition from the bottom of the root water uptake zone to the top of the drainage zone between about 0.60 and 0.70 m depth. However, the measured differences in θ are too close to the errors in the gamma data to permit more than speculation about this. The salinity profile in column C prior to J7077 appeared sufficiently steady to derive the λ-distribution also from Eq. (1.7). The resulting $\lambda_{I/C}$-curve in Figure 3.9 shows an even shallower root water uptake distribution. The most significant agreement between the two λ-profiles is the sharp increase towards the surface starting from a depth of about 0.30 m.

The water balance of column C as a whole indicated that the ET-rate was relatively constant at 28 x 10^{-8} m s^{-1} so that the estimated total transpiration during the 12 hours of light on J7077 was 12.0 mm. With a total drainage of 3.0 mm and an irrigation of 17.1 mm this means a net increase of 2.1 mm water in the column. This is consistent with the fact that the 17.1-mm irrigation was the first of this magnitude after a long period of daily irrigations of 14.3 mm.

The local value of DF had an absolute maximum at around 0.30 m depth, and was about 50% of the local value of RCWC. This may seem a large correction for RCWC. However, for purposes of irrigation management and salinity control one is mostly interested in the integral of λ with respect to z above a certain depth, since this integral determines the salinity at that depth. The maximum correction for DF on the integral of $\lambda(z)$ occurred at 0.45 m depth and was only about 14% of the calculated integral of $\lambda(z)$ to that depth, and

about 11% of the total transpiration rate for the entire column. These values are probably higher than normally expected for our experiments because of a net wetting of column C on this day (J7076), and because this column was already operated at a relatively high L of about 0.20. This is supported by other data which indicate that redistribution was very small. For instance, Figure 3.5 in *Dirksen and Raats* (1985) shows that the water content just below the wetted zone (0.50-0.60 m) remained constant for about 5 days after a large irrigation.

The preceding discussion suggests that RCWC-distributions during later parts of the light periods provide reasonable approximations for the actual $\lambda(z)$ distributions, especially from the point of view of salinity control and for columns operated at low L. Therefore, RCWC-distributions presented in this report are treated as if they were the actual $\lambda(z)$ distributions.

3.5. *Effect of Sudden Salinization on Water Uptake Distribution*

Almost immediately after the salinity treatments were started, some interesting differences developed in the water uptake distributions. These differences were enhanced by unintended under-irrigations and are illustrated by the water content distributions on J5164, J5168, and J5174 in Figure 3.10. Column F (Fig. 3.10a) was under-irrigated with tap water and the entire column dried out nearly uniformly. On J5174, the water content was 0.08 m^3 m^{-3} down to a depth of about 0.80 m. The increase in water content below that depth was probably due to a smaller local root density. Visual observations through the glass walls on J5169 indicated that the roots had not yet fully developed in the bottom of the column. Column E (Fig. 3.10b) was irrigated with water of h_o = -13.2 m. The water content at 0.25 m depth in this column changed little during the entire 10-day period from J5164 to J5174. The soil water content above this depth first increased each day as a result of the 6.5-mm irrigations, and then decreased again because of root water uptake. Salts displaced from the daily replenished part of the root zone salinized the lower layer quickly. As a result, rather than drying out this part of the soil profile, plants augmented deficit

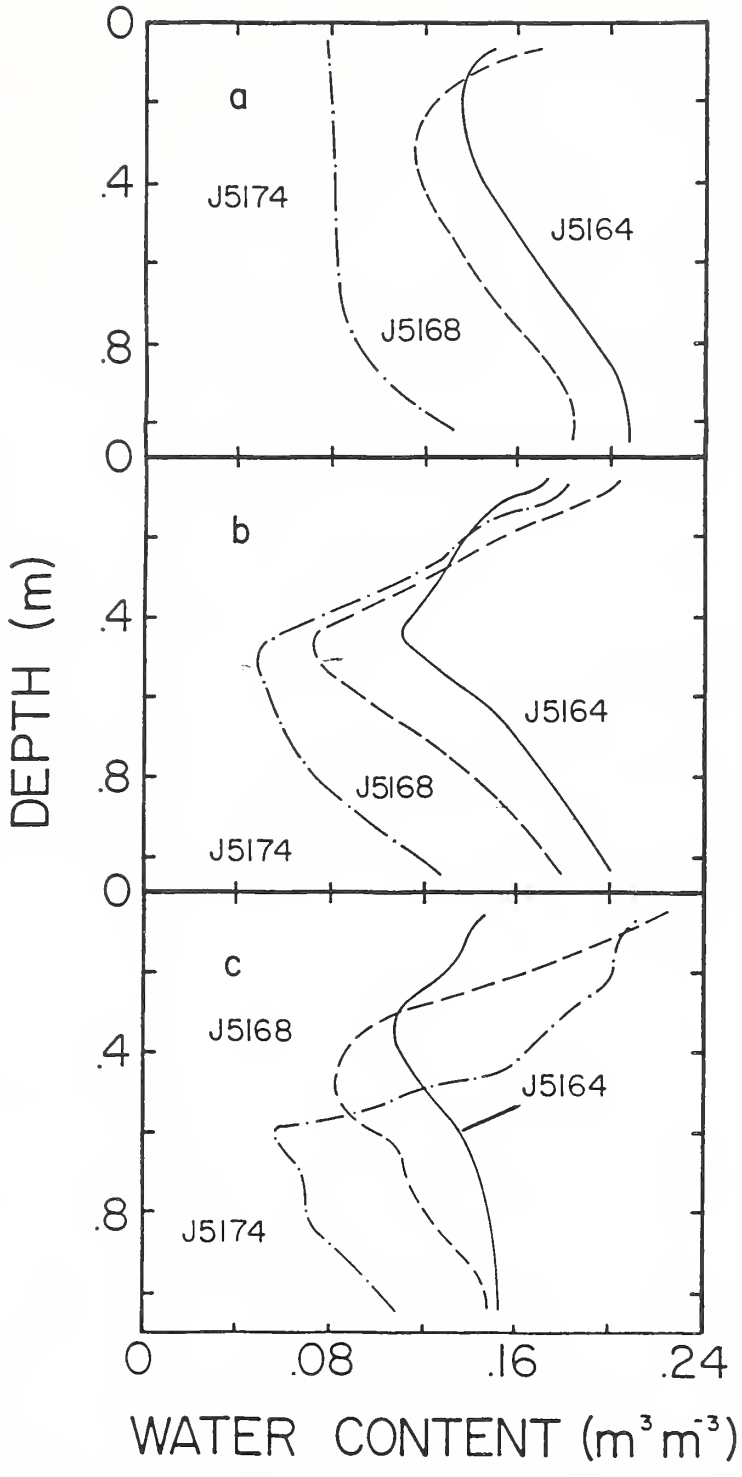

Fig. 3.10. Effect of different salinizations on resulting water content distributions in columns F (a), E (b) and B (c). The columns were salinized with water having osmotic heads h_o of -2.4, -13.2 and -22.0 m, respectively.

irrigation with non-saline water from the bottom part that was left there from before salinization was started. The sharper increase in θ with depth than in column F agrees well with visual observations that the vertical root development was much slower in column E than in column F. Column B (Fig. 3.10c) was irrigated daily with water of h_o = -22.0 m: 6.0 mm per irrigation until J5166 and 12.0 mm thereafter. The zones of rapid water content changes for these amounts were approximately 0.30 and 0.60 m deep, respectively. Apparently, the irrigation water was much more saline than the soil water at the bottom of the column. As a result, the top part of the column became even wetter in time while the roots dried out the bottom part. These water uptake distributions for column B are unusual and resulted from the sudden salinization by irrigation water.

Salinity generally increased and water uptake decreased with depth as the experiments progressed. The columns went through a few more net drying and wetting cycles in addition to the imposed daily fluctuations due to irrigation. We will discuss now the interactions between over- and under-irrigation, salt and water transport and RCWC-distributions during the gradual salinization of the most saline column E. This column was operated at the lowest L and its RCWC-distributions needed therefore the smallest corrections for DF to obtain λ-distributions.

3.6. *Gradual Salinization at Low Leaching Fraction*

Figure 3.11 shows the net drying of column E from J5215 to J5249 as a result of daily irrigations that did not meet evaporative demand. Similarly, Figure 3.12 shows the net wetting of column E from J5249 to J5275 as a result of daily over-irrigations. Notice the difference in drying patterns (λ-distributions) between Figures 3.11 and 3.10b. This was caused by differences in salinity distributions. Figure 3.13 shows somewhat smoothed osmotic head distributions in column E on J5205, J5225, J5244, J5292, and J6008. These distributions indicate that the column became considerably more saline during the under-irrigations before J5249. Subsequent over-irrigations leached salts from the top and accumulated them in the bottom part of the column. The salinization process continued in time as indicated by the osmotic head profile on J6008 and by the curve for column C in

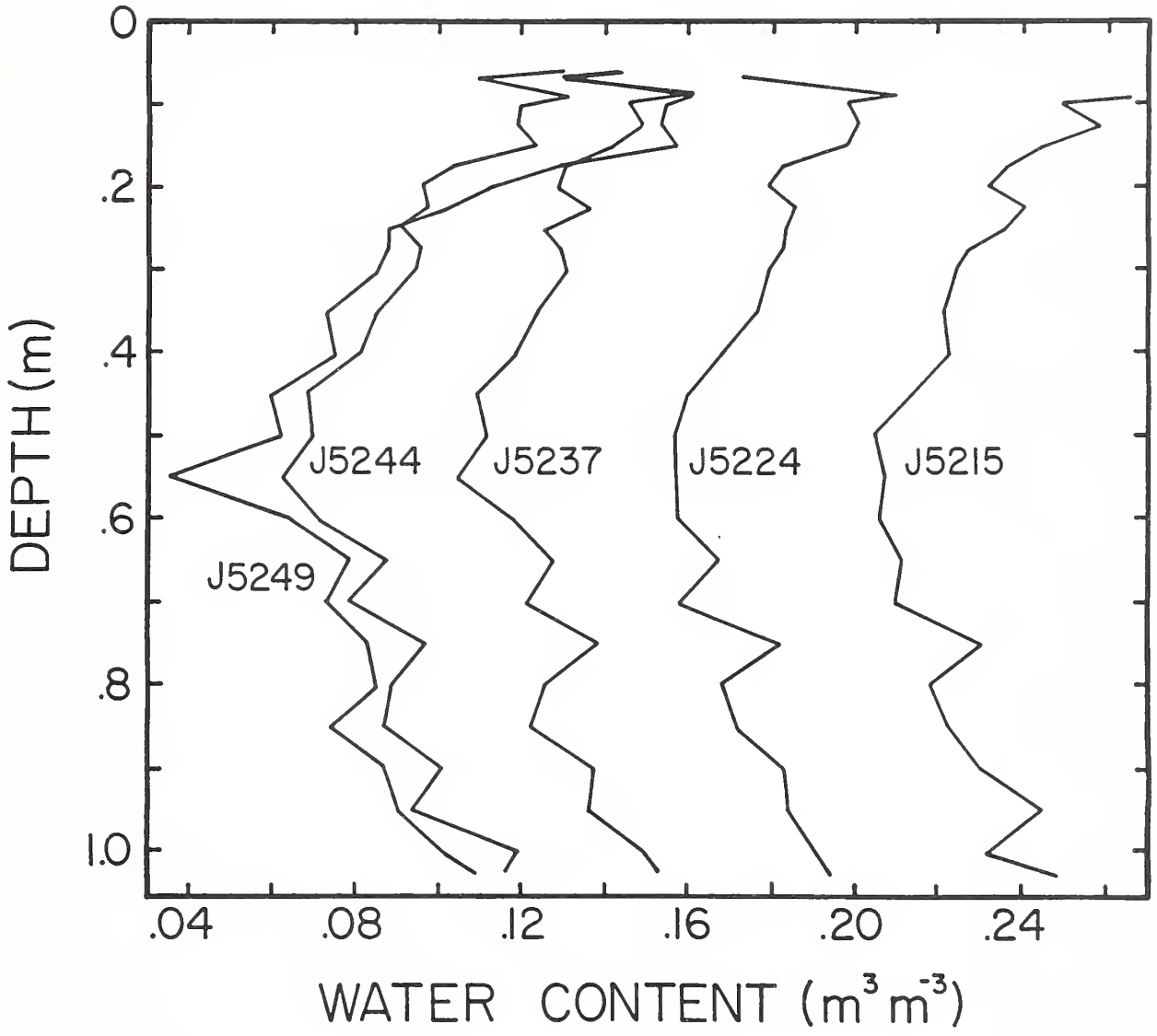

Fig. 3.11. Net drying of column E from J5215 until J5249 as a result of daily under-irrigations.

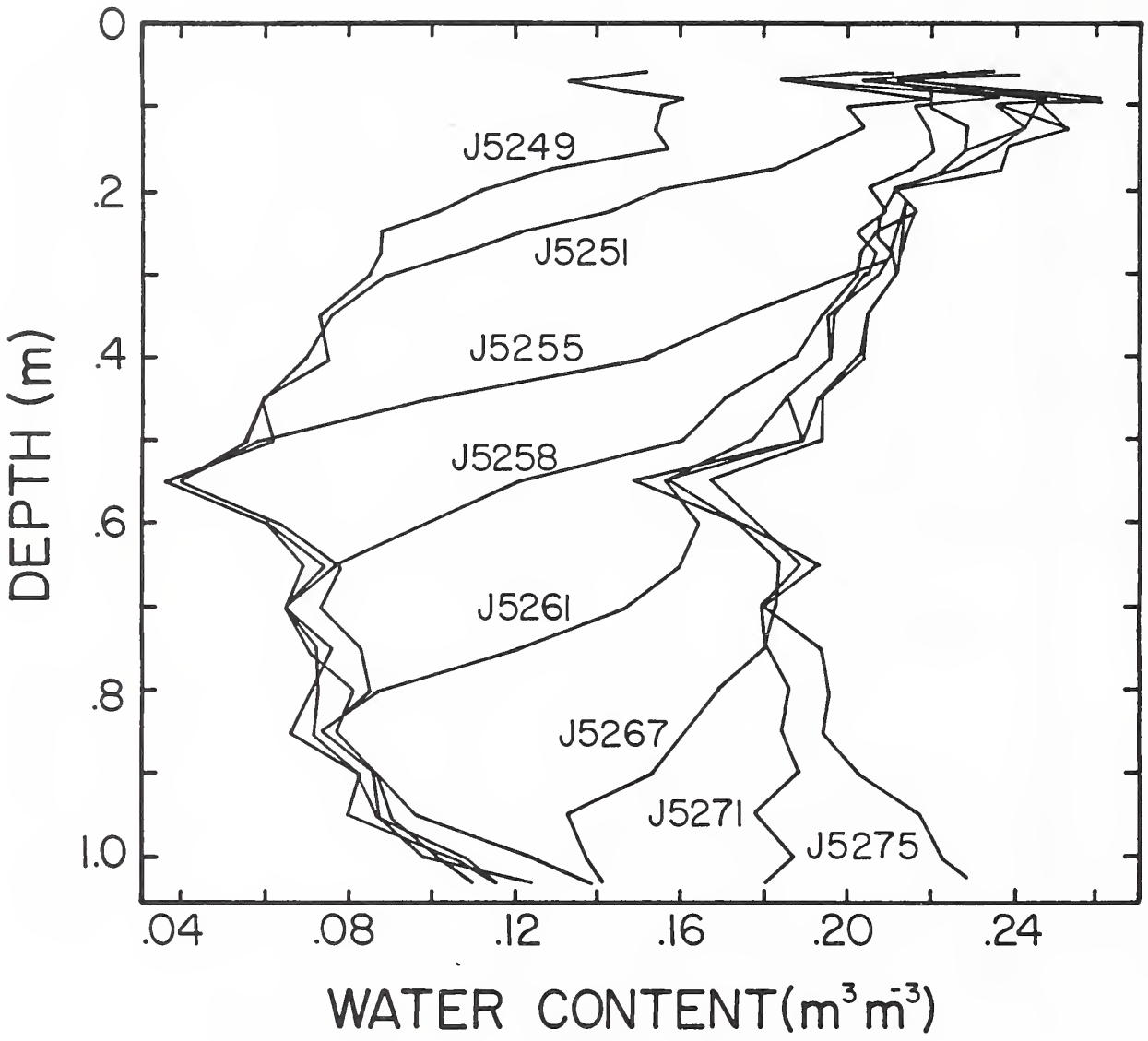

Fig. 3.12. Net wetting of column E from J5249 until J5275 as a result of daily over-irrigations.

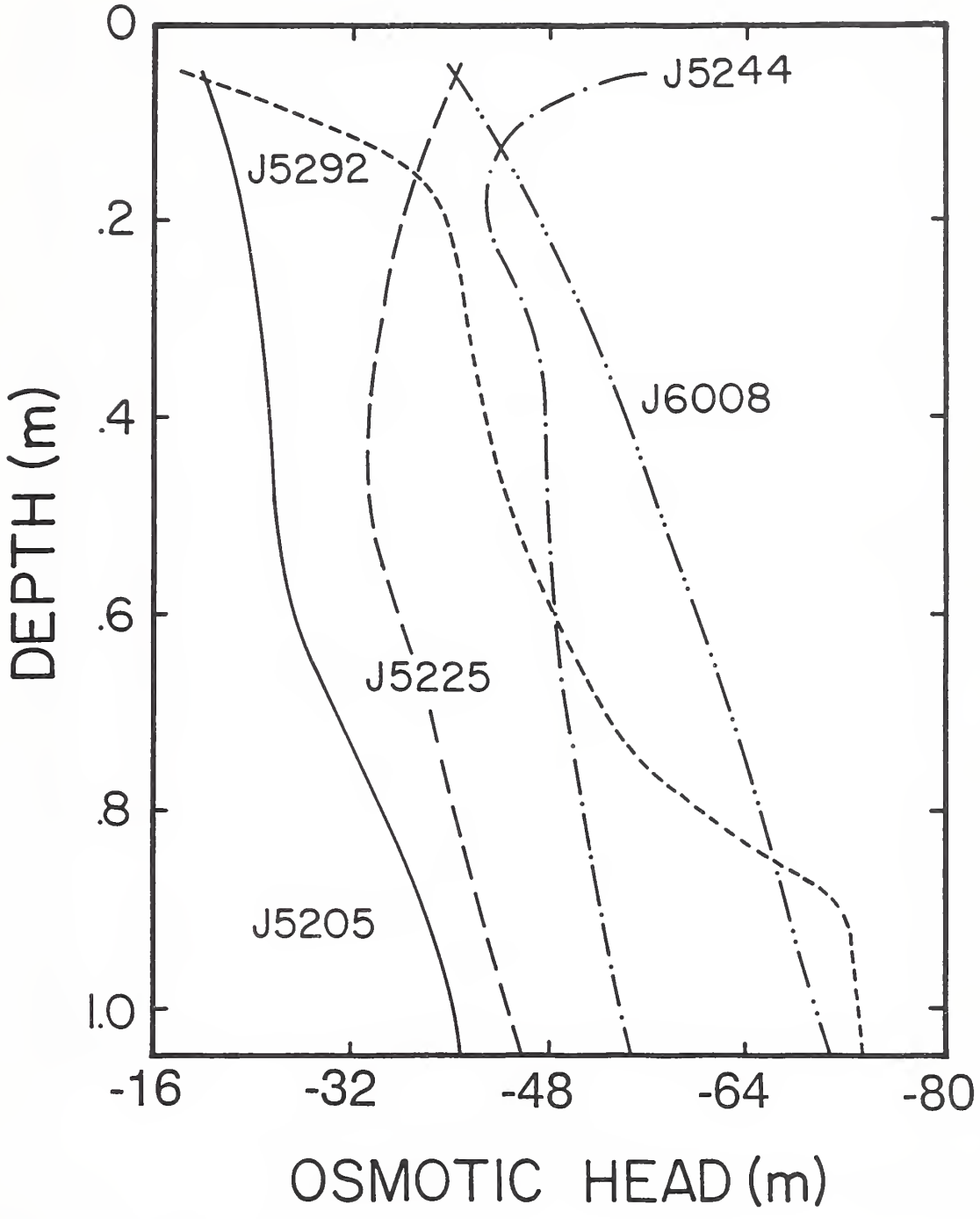

Fig. 3.13. Osmotic head distributions in column E on five different days in 1975.

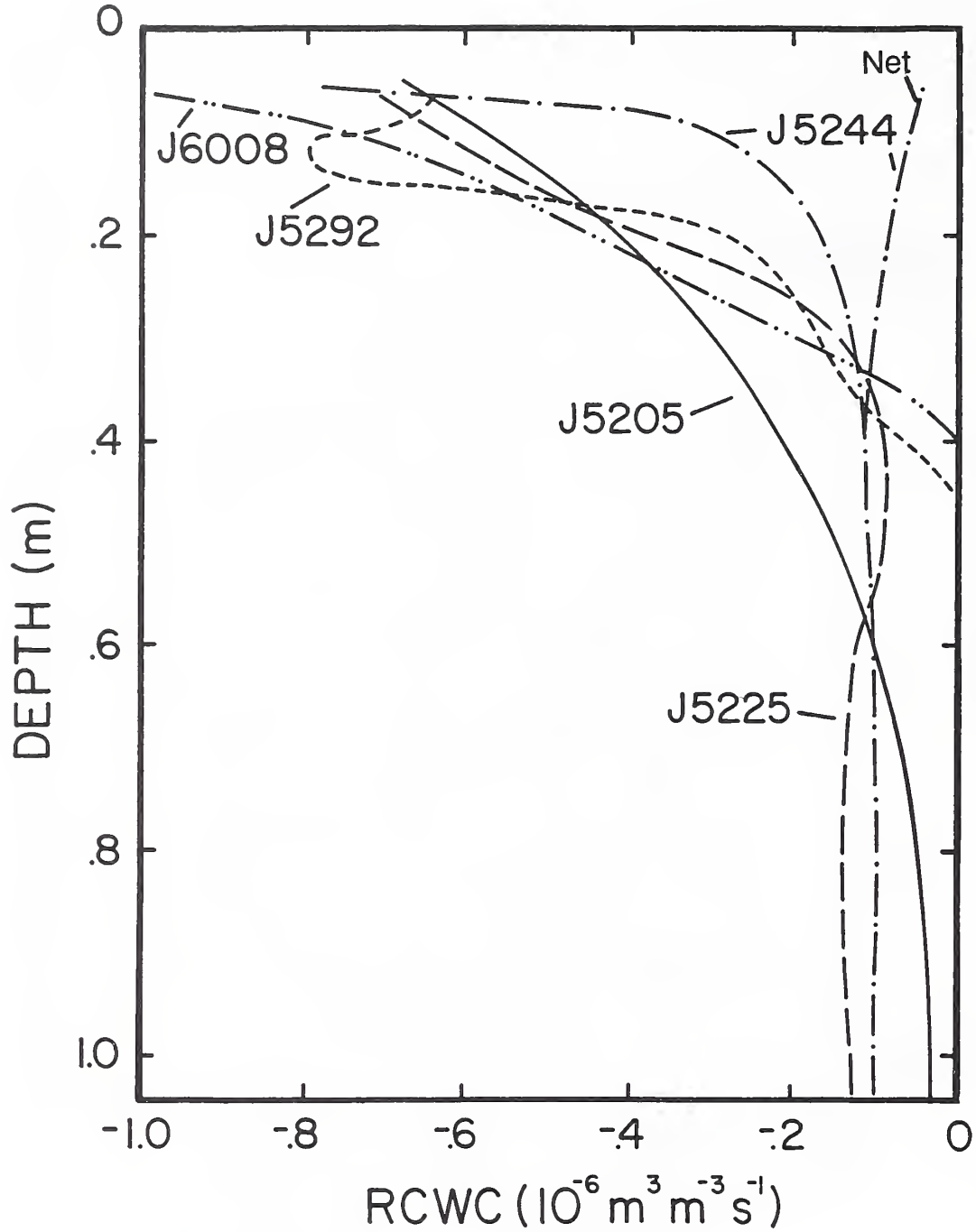

Fig. 3.14. Distributions of RCWC (rate of change of water content) in column E corresponding with the salinity distributions in Figure 3.13. The net rate of water loss for J5244 ("net") is also indicated.

Figure 3.3c. The relative speeds of the wetting and salinity fronts during the wetting phase from J5249 to J5282 were analyzed in a separate paper (*Dirksen*, 1980).

Figure 3.14 shows measured RCWC-distributions in column E on the same days as the salinity profiles in Figure 3.13. The curves are all averages for approximately 8 ½-hour periods towards the end of the 16-hour light periods when, as discussed earlier, the redistribution fluxes in the soil were small, especially in the relatively dry column E. Thus, the RCWC-distributions all are good approximations of the λ-distributions. Figure 3.14 demonstrates the steepening of the λ-distribution as a result of the gradual salinization of column E. For J5244, the net rate of water loss is also indicated. This was determined by

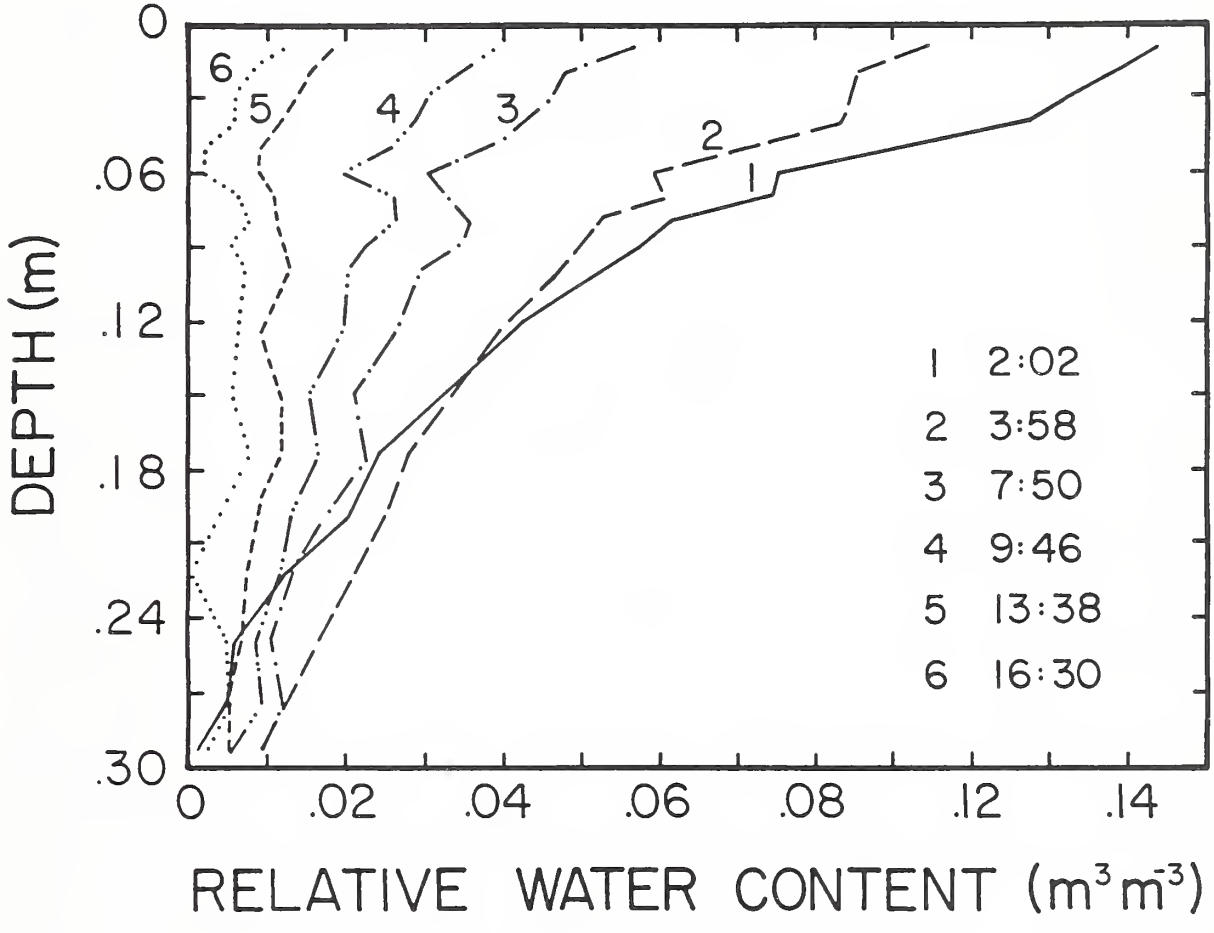

Fig. 3.15. Water contents in the top 0.3 m of column E relative to values before a 12.9-mm irrigation just before midnight. The curves are given for several times on J6008.

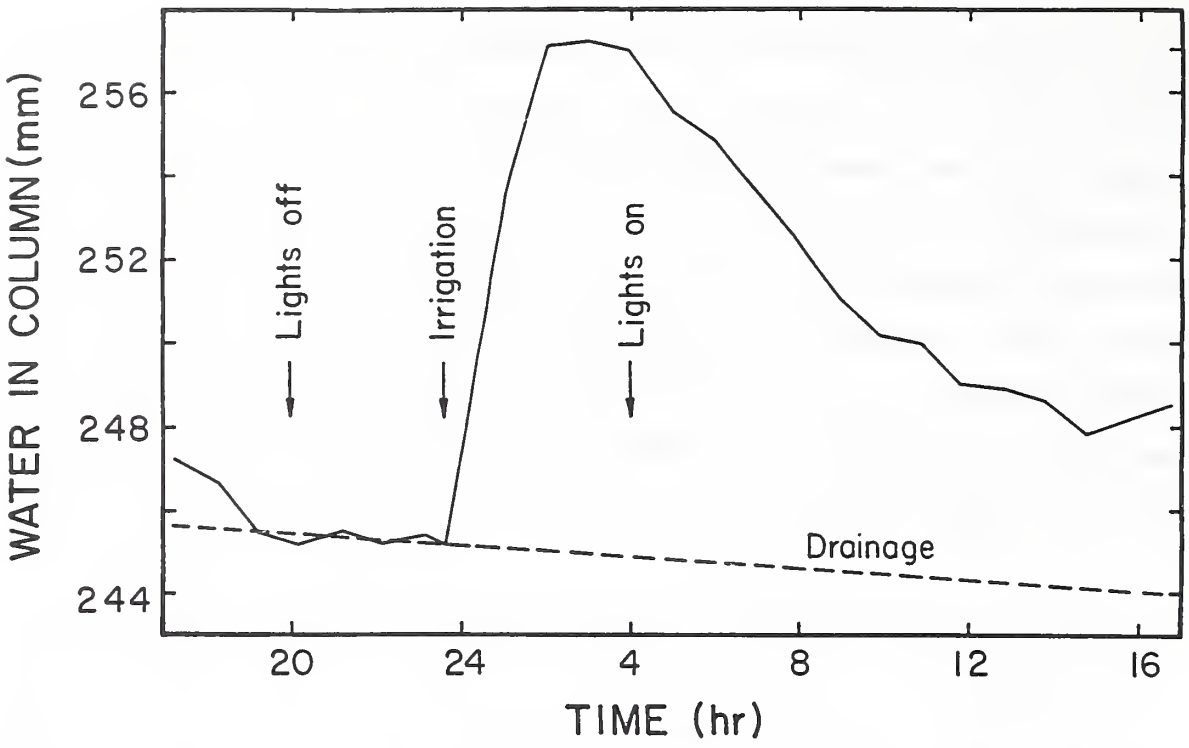

Fig. 3.16. Total amount of water in column E on J6007 and J6008.

gamma scans just prior to the daily irrigations. The difference between the two curves for J5244 in the top part of the column represents water supplied by irrigation.

The measured differences in absolute water contents near the surface could in general not be shown graphically with adequate resolution. Changes in water content relative to those just prior to irrigations, however, were usually very regular. Figure 3.15 shows these relative water contents in the top 0.30 m of column E before, during and after a 12.9-mm irrigation starting near midnight on J6007. The times are indicated in the figure. Some redistribution of water was apparent between 2:02 and 3:58, but not much thereafter when the lights were switched on and evapotranspiration took place. Figure 3.16 shows the total amounts of water in column E on J6007 and J6008 derived from the gamma data. The average rate of drainage is indicated also. This drainage took place without measurable changes in θ below 0.40 m. There was a decrease in the evapotranspiration rate from a maximum of about 33×10^{-8} m s^{-1} to about 14×10^{-8} or 3×10^{-8} m s^{-1}, depending on which of the last two data points in the figure is taken (the gamma scanner developed a minor

problem at the time). Why the evapotranspiration rate decreased so much compared to the rate of about 19 x 10^{-8} 8 m s^{-1} at the end of J6007 is not clear; there was still more water present in the column than at the end of the previous day.

3.7. *Root Water Uptake Distributions Derived from Salinity Profiles*

Figure 3.17 shows osmotic head profiles in columns B, C, E, and F on J6013 near the end of the nine growth periods. Column E was by far the most saline. The lowest osmotic

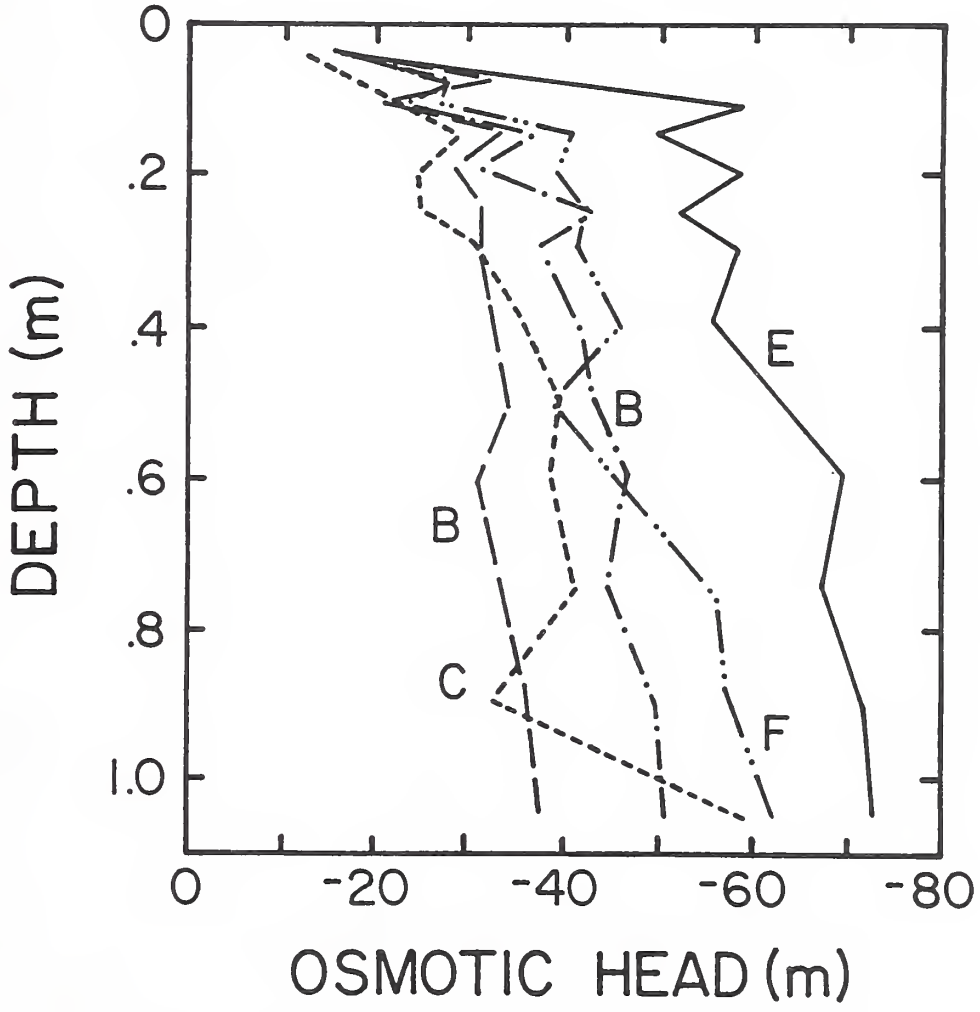

Fig. 3.17. Osmotic head distributions in four columns on J6013. The most saline profile, observed for column B on J5330, is also given (dash-dotted line).

heads in column B were observed on J5330 and are also shown. The steepest increase in salinity in these columns occurred near the surface. The reason for this becomes clear when one considers the rate of movement of actual water particles rather than the maximum zone over which the water content increases as a direct result of daily irrigations. As an example, take an irrigation of 20 mm, which is rather high for a daily dose, and a surface layer water content of 0.25 m^3 m^{-3} during irrigation, which is rather low. If we assume piston flow, the new water particles initially will occupy only the top 0.08 m layer of the column, while the water content itself may increase to a depth exceeding 0.50 m. Between irrigations, the fresh irrigation water will be taken up preferentially since it has the lowest salinity. With the next irrigation, this water will be pushed further down to below the surface layer that is replenished with newly applied irrigation water. Since there is less water than originally, it will occupy a thinner layer than on the first day. This water will be subject to additional concentration by root uptake. Non-piston flow behavior and redistribution may increase the travel distance of an individual irrigation somewhat, especially during the first irrigation, but these two effects will tend to balance each other over several irrigations. The concentration process repeats itself with the net result that water becomes quite saline before it has reached the maximum depth to which the water content increases daily. The concentration process is enhanced further by the fact that, starting from a given concentration C_o, further doubling of the concentration during a particular step requires only half the amount of root water uptake of the previous step. This means that an increase in concentration from 8 C_o to 16 C_o requires only one-eighth of the root water uptake involved in an increase from C_o to 2 C_o. Thus, the increases in salinity with depth below 0.30 m in Figure 3.17 are associated with very little water uptake.

For steady state conditions the processes described above are represented by Eq. (1.7). Figure 3.18 gives the λ-distribution calculated from the salinity distribution in column F on J6006 using Eq. (1.7) and the time-averaged boundary condition q_oC_o = 5.31 x 10^{-6} mol m^{-2} s^{-1} (= 45.9 x 10^{-3} meq cm^{-2} day^{-1}). The slope of this distribution differed only slightly from the slope of the salinity profile on J6013 shown in Figure 3.17. The small uptake below 0.40 m caused a decrease in osmotic head h_o from about -35 m to -55 m. The date of J6006 was chosen because the salinity sensor readings had been fairly steady for more

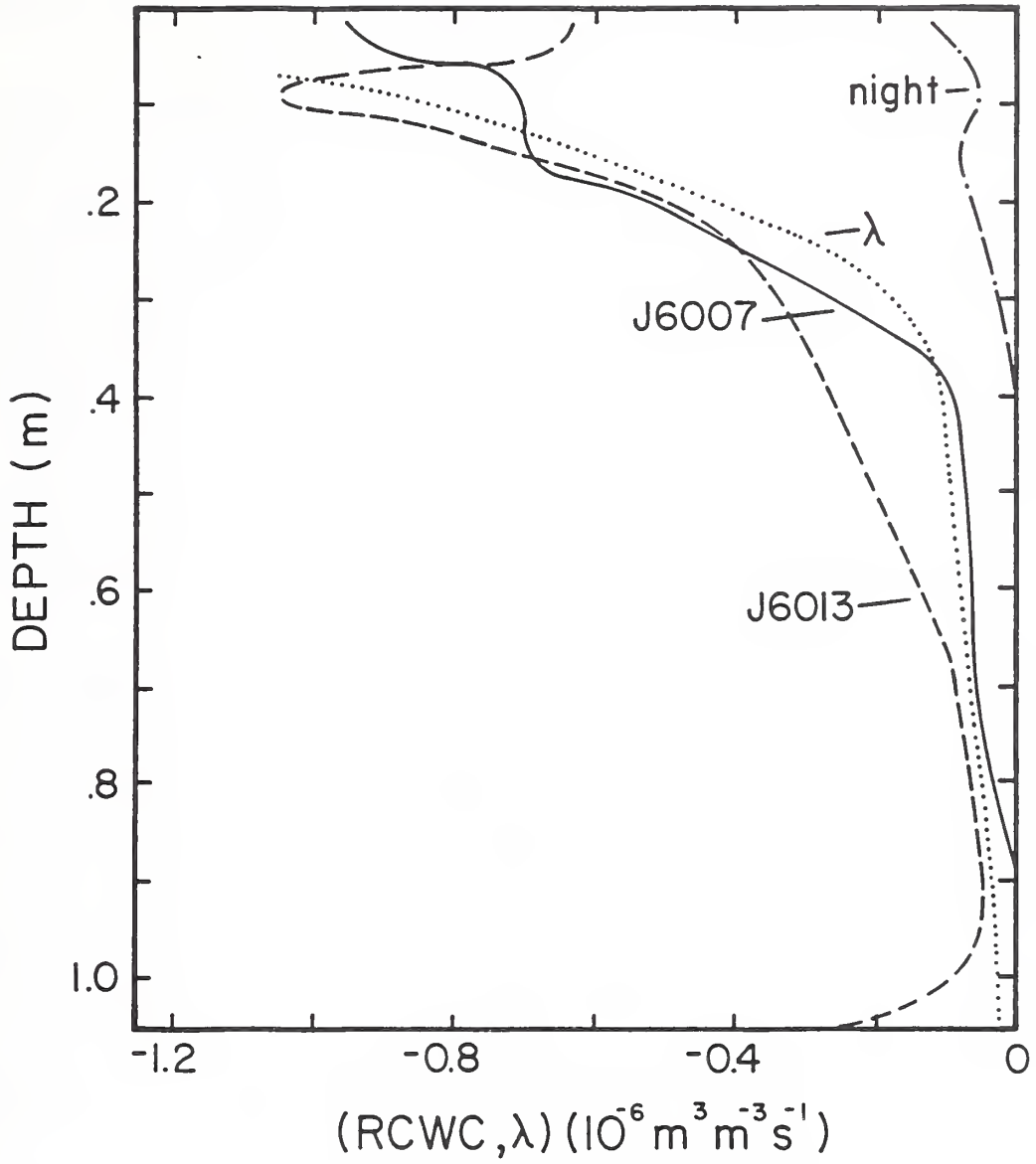

Fig. 3.18. Comparison of RCWC-distributions in column F on J6007 with the water uptake distribution (λ) derived from the dilution profile (Eq. 1.7) on J6006. Also shown are RCWC-distributions during night and day without irrigation (J6013).

than 40 days prior to this date. This means that Eq. (1.7) can be tested experimentally by comparing this λ-distribution derived from salinity data with the RCWC-distribution obtained from gamma scans on J6007. The agreement shown in Figure 3.18 is very satisfying indeed. The correction of RCWC for DF would make the agreement even better. The root length density distribution of this column F was determined on J6014 and is given

in Figure 5.1. Except for a slight increase in root lengths near the bottom, the λ-distribution was nearly proportional to the root length density distribution.

During the last week prior to sampling on J6014, under-irrigation of column F resulted in a general increase in salinity levels. To keep the column dry for sampling, column F was not irrigated during the night from J6012 to J6013. This offered a rare opportunity to measure the RCWC-distributions during the night and the following day without interference by hydraulic flow due to irrigation. There are indications that the small RCWC values in the top of the column during the almost 8 hours of darkness (night) reflect water uptake to restore plant water deficits, rather than water redistribution. The RCWC-distribution during the almost 9 hours of light on J6013 indicate that the plants, without the regular supply of irrigation water, took up appreciably more water between 0.40 m and 0.70 m depth than a week earlier.

The effect of the under-irrigation on the salt balance of column F is shown in Figure 3.19. The product of volumetric soil water content and concentration in mol salt per m^3 of bulk soil below 0.40 m depth was essentially the same on J6013 as on J6006, whereas above 0.40 m the absolute salt content of the soil column increased as a result of under-irrigation. This again indicates that root uptake took place primarily in the upper 0.40 m of the column. The total salinity increase above 0.40 m amounted to about 0.068 mol. Irrigations between J6006 and J6013 added about 0.155 mol to the column, while the drainage carried off about 0.100 mol. The difference of 0.055 mol is in reasonably good agreement with the 0.068 mol increase above 0.40 m, especially in view of the variability in salinity that was encountered during sampling (Chapter 2).

3.8. *Conclusions*

Under daily irrigation, soil water pressure heads and water contents never attained very low values. The water content was always somewhat above field capacity such that the average daily flux density below the root zone corresponded to the leaching fraction. The experiments indicated that some 10 hours after the irrigations the hydraulic gradients became very small or nearly zero in the most active part of the rootzone, down to a depth

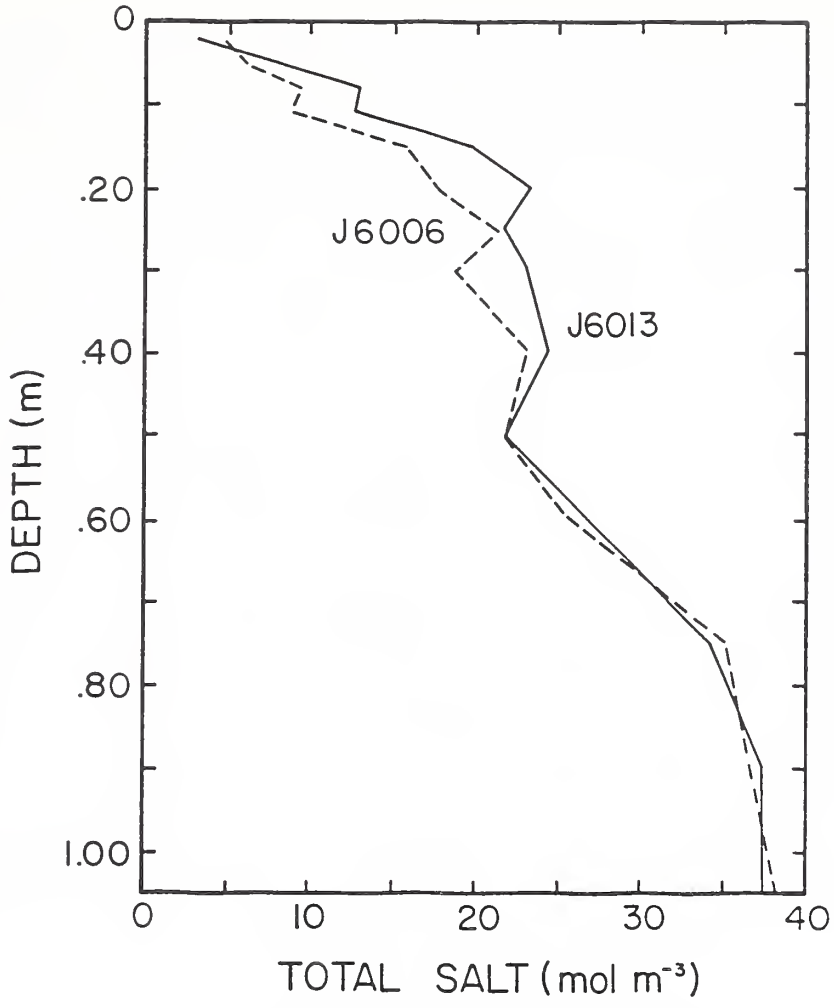

Fig. 3.19. Salinity distributions in column F on J6006 and J6013.

of about 0.30 m. This made it possible to estimate the root water uptake distributions based on measured gradients and the known hydraulic conductivity as a function of water content. The calculations indicated that for not too high leaching fractions, the rate of change of water content later in the irrigation interval was a good approximation for the rate of root water uptake. This was especially true for the cumulative root water uptake above a certain depth, a parameter that is of considerable interest for salinity control since it determines the salinity level at that depth. The data confirmed that water uptake distributions can be derived quite accurately from observed salinity (or dilution) profiles under steady-state conditions. In turn, root water uptake was adversely affected by salinity. During the initial phase of salinization, root water uptake occurred preferentially in the bottom part of the

rootzone while the water content in the top part was increasing. Although the water content increases over a considerable depth with each daily irrigation, the water particles themselves travel only a short distance. As a result, the salinity increases slowly towards a steady-state, characterized by a rapid salinity increase with depth near the surface. Root water uptake occurs then mainly in this shallow surface layer. In these experiments, salinity was still increasing after 230 days of irrigation at an average leaching fraction of 0.08. Thus, the high soil water contents and pressure heads maintained under daily irrigation are at the cost of much higher average salinities for the soil columns as compared to infrequent irrigation (Chapter 4). The effects of higher average salinities on yields and uptake-weighted mean salinities of the root zone are investigated in Chapter 5.

The results for column E alone were also analyzed by *Dirksen* (1987) who showed that the observed water and solute transport data in the root zone during frequent irrigation could not be simulated accurately without taking hysteresis into account. The transport processes under such conditions apparently may become so complex that they, even qualitatively, can be understood only with the help of numerical simulations. *Dirksen et al.* (1993) described a hysteretic simulation model which could handle such complexity, and present simulation results for column E during growth period IV (J5251 to J5272).

4. NON-DAILY IRRIGATIONS

The previous Chapter 3 reported results for daily irrigations at different leaching fractions and salinities. This Chapter reports results for the non-daily irrigations.

4.1. *Non-Daily Irrigation Experiments*

After soil column F was sampled at the end of growth period IX on J6014 (see Table 1.1 and Chapter 2), observations on the remaining 5 columns under daily irrigation were continued for 56 days, covering growth periods X and XI. Subsequently, from J6070 until J6156, columns A through E were irrigated at intervals of 3, 3, 7, 2, and 5 days, respectively. All columns received the same average daily amount of water: 14.3 mm. This amount was reduced by 10% on J6123. New 2.44-m long lights were installed on J6126, and additional 1.22-m long, high-intensity lights were suspended across the junction of the two main light banks on J6167. Starting on J6135, the columns received fertilizers with the irrigation water. These and a few additional changes made during the interim period resulted in significant yield increases. On J6149 (harvest XIV), column A recorded the highest yield of the entire study: 0.396 kg green matter and .0766 kg dry matter in 28 days.

On J6156, the irrigation frequencies were changed to 6, 4, 8, 12, and 6 days for columns A through E, respectively. The average daily amount of irrigation, $\bar{q}_i$, reduced from 14.3 to 12.9 mm/day on J6123, was too low for the new lights and with fertilization. Alfalfa on column A was wilting severely on harvest day J6173 of growth period XV. Therefore, irrigations were increased on J6174 to the previous average daily amount of 14.3 mm, and on J6181 the light periods were shortened from 16 hours to 12 hours per day.

This was the start of nine growth periods (XVI through XXIV), each lasting 24 days except the last one, with no further changes in experimental conditions except for the following two. First, the light intensity decreased with time as discussed in Chapter 2. Second, a plastic cover was placed over column E during the first 12 days of growth period XXII to prevent evapotranspiration (ET); this was done in an attempt to measure the soil hydraulic conductivity (K) after salinization and soil compaction by roots. Unfortunately,

the solenoid valves of a new hydraulic tensiometer switching system, installed at that time, developed too much heat. This caused the pressure to drift so much that the attempt to measure K had to be abandoned. The plastic cover reduced ET and increased drainage not only directly during the 12 day period, but also indirectly due to molds and fungi that developed in the 100 percent relative humidity. They continued to damage the canopy for the next two growth periods. The present Chapter 4 deals with salt and water fluxes and accumulations, and their effects on root water uptake distributions, during the nine growth periods of non-daily irrigation. Further details about the experiments can be found in Chapter 2.

4.2. *Water and Salt Balances*

Table 4.1 summarizes a number of experimental parameters for the nine growth periods XVI through XXIV as a whole. For convenience, the irrigation intervals (4 to 12 days) are added to the letter designations of the five columns used earlier. All columns received the same total amount of water, namely 3090 mm, which corresponds to a daily average of 14.2 mm. The non-saline column was irrigated at 6-day intervals (A-6) and had by far the lowest drainage volume, the highest yield and the lowest transpiration ratio (kg of water transpired per kg of dry weight produced). Column C-8 was at the other end of the scale in these three categories. The illuminance values in Table 4.1 are averages for four heights above the soil surface (corresponding to values at about 40 cm height, see also Figure 2.2). They were reasonably uniform, except for the two outside columns, A-6 and E-6, which received some additional light from the sides. This resulted in relatively more growth, higher ET values, and lower drainage rates. The lower drainage rate, in turn, caused the salinity in column E-6 to become relatively high, which probably reduced ET later below its maximum. Further details about yields and transpiration ratios are reported in Chapter 5.

The irrigation regimes are completely determined by the irrigation intervals given in Table 4.1. The drainage patterns, shown in Figure 4.1 for columns B-4, C-8, and D-12, exhibited the same periodicity as the irrigation patterns, with time lags increasing with the

Table 4.1. Summary and totals for growth periods XVI to XXIV.

Column:	A-6	B-4	C-8	D-12	E-6
Irrigation interval, days	6	4	8	12	6
Irrigation water h_o, m	-2.4	-12.0	-12.0	-12.0	-12.0
Irrigation, mm	3090	3090	3090	3090	3090
Evapotranspiration, mm	2929	2609	2401	2463	2736
Drainage, mm	161	481	689	627	354
Leaching fraction	0.052	0.156	0.223	0.203	0.115
Dry weight, kg	0.364	0.299	0.239	0.265	0.317
Dry matter, percent*	15.9	15.9	14.8	15.2	16.4
Transpiration ratio, kg/kg	563	611	703	650	605
Illuminance, beginning, lux	23000	22350	21700	21550	22350
Illuminance, end. lux	18000	16900	17250	17600	18200

*Harvest XXIV not included.

duration of the irrigation intervals. The drainage pattern of column B-4 was the least variable. In column D-12, periods of high rates of drainage alternated with periods of little or no drainage. The maximum drainage rates decreased somewhat with time, especially in column B-4. The highest drainage rates usually occurred after the second irrigation in each growth period. The columns were then still wet from the first irrigation and *ET* had not yet increased to the high values for a full-grown canopy.

Cumulative drainage amounts for five columns are shown in Figure 4.2a. Column A-6 yielded little drainage after growth period XVIII. Drainage during growth periods XVI and XVII was higher in column C-8 than in column D-12; thereafter the rates differed little between the two columns. Column 8-4 produced less drainage than columns C-8 and D-12, the difference increasing with time. Drainage from column E-6 was much lower than expected as compared to B-4, C-8, and D-12. The apparent reason for this is that E-6 was an end column that received illumination also from the side. This increased the size of the

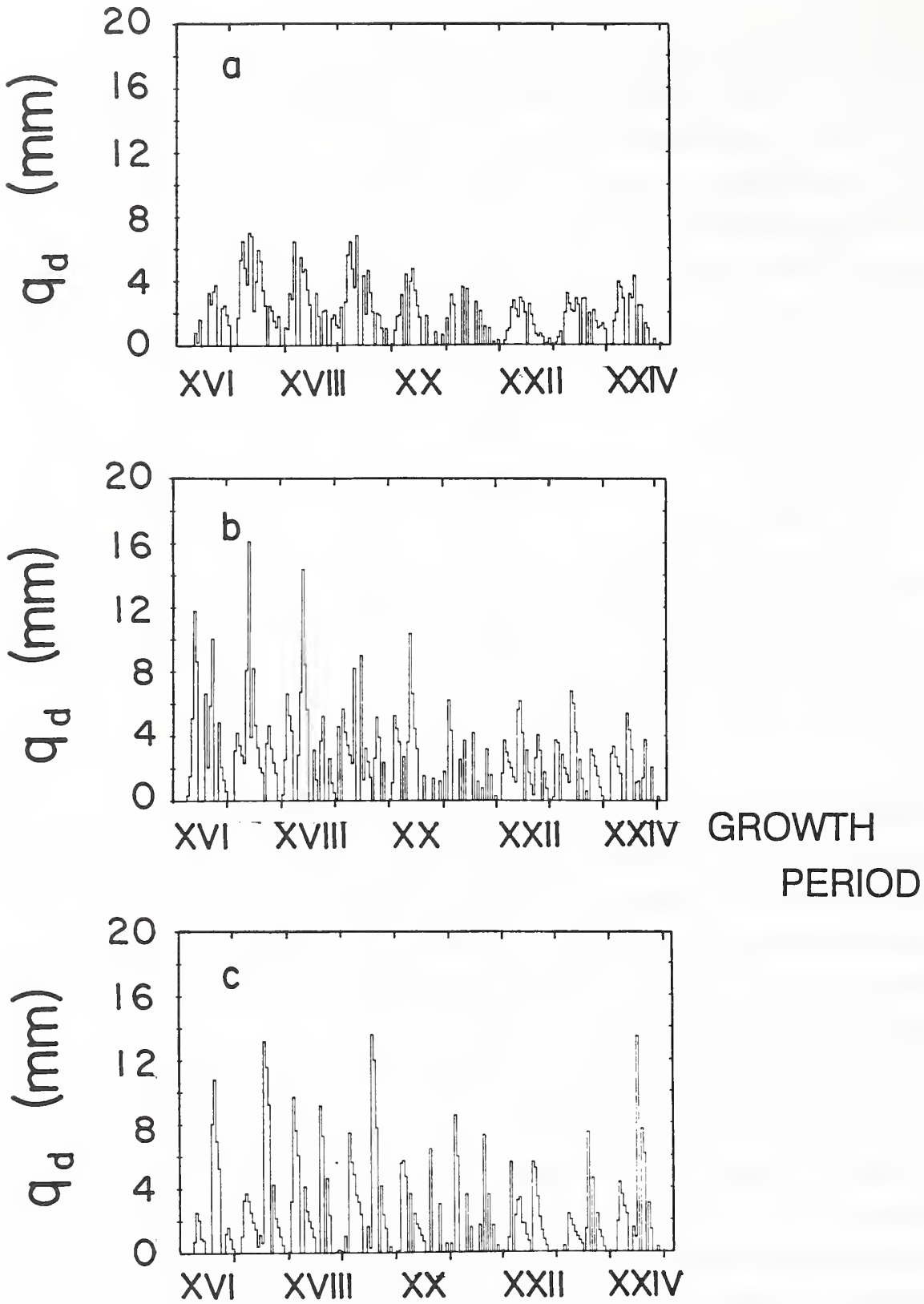

Fig. 4.1. Daily amounts of drainage ($\overline{q}_d$) for columns B-4 (a), C-8 (b) and D-12 (c).

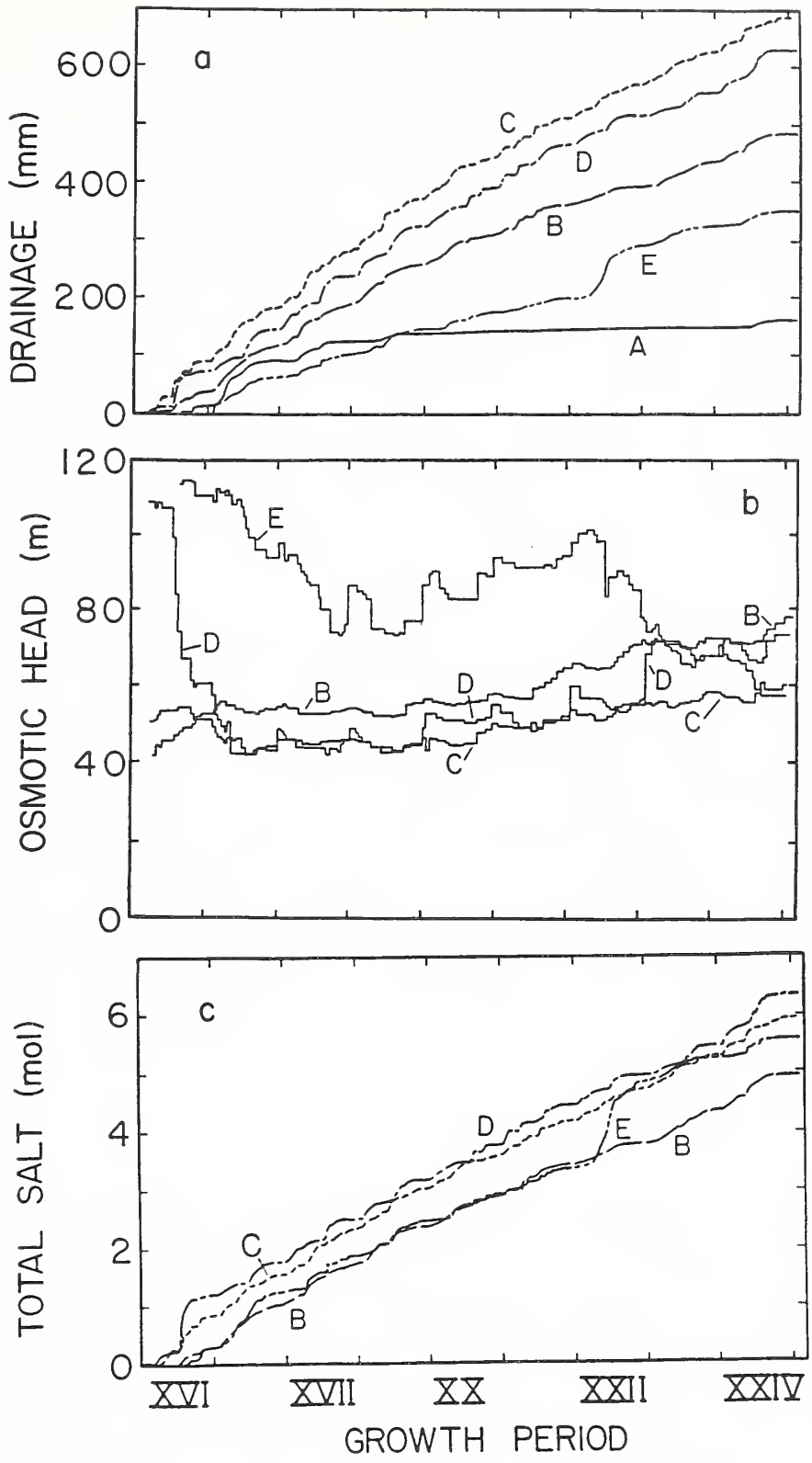

Fig. 4.2. Cumulative amounts of drainage (a), osmotic head of drainage water (b), and cumulative amount of salt collected in drainage water (c) for five soil columns

canopy and the amount of ET, and thus decreased drainage and the leaching fraction. The irregular behavior of column E-6 during growth period XXII was due to the plastic cover already discussed.

Figure 4.2b shows the osmotic heads of the drainage water of columns B-4 through E-6, while Figure 4.2c gives the total amount of salt in moles that was discharged in the drainage water. Differences in the discharged amount of salts between columns C-8 and D-12 were even smaller than those in the drainage volumes. Columns B-4 and E-6 were almost identical in their salt discharge up to the time of the plastic cover. Compared with column B-4, the higher salt concentrations in the drainage water of column E-6 were compensated for by the lower drainage volumes, such that the products (moles of salt) remained about the same.

The differences in discharged salts are reflected in the more or less steady osmotic head distributions on J7017 towards the end of the non-daily irrigation phase (Fig. 4.3). Columns B-4 and E-6 were the most saline, while column D-12 had the least salinity. The shape of the osmotic head profile in column D-12 is convex downward, in contrast to that in column B-4 which is convex upward. Therefore, the average salinity in the column with the 4-day irrigation interval was much higher than in the column with the 12-day interval. This important feature of high frequency irrigation was already encountered in Chapter 2 and Chapter 3 for daily irrigation; its dependence on the irrigation interval is explored next.

4.3. *Individual Irrigation Cycles*

The drainage patterns of Figure 4.1 can be understood better by considering also the typical depths of wetting for the various amounts of irrigation. Figure 4.4 shows water content (θ) distributions following irrigations on three of the columns, and Figure 4.5 shows the corresponding changes in hydraulic head at various depths in the columns. In each case, the data relate to the second irrigation of growth period XXIII. The 57.2-mm irrigation on column B (Fig. 4.4a) initially increased the water content to about 0.75 m depth, while redistribution also caused a slight increase in θ near the bottom of the column. Later irrigations during the same growth period increased θ only to about halfway down the

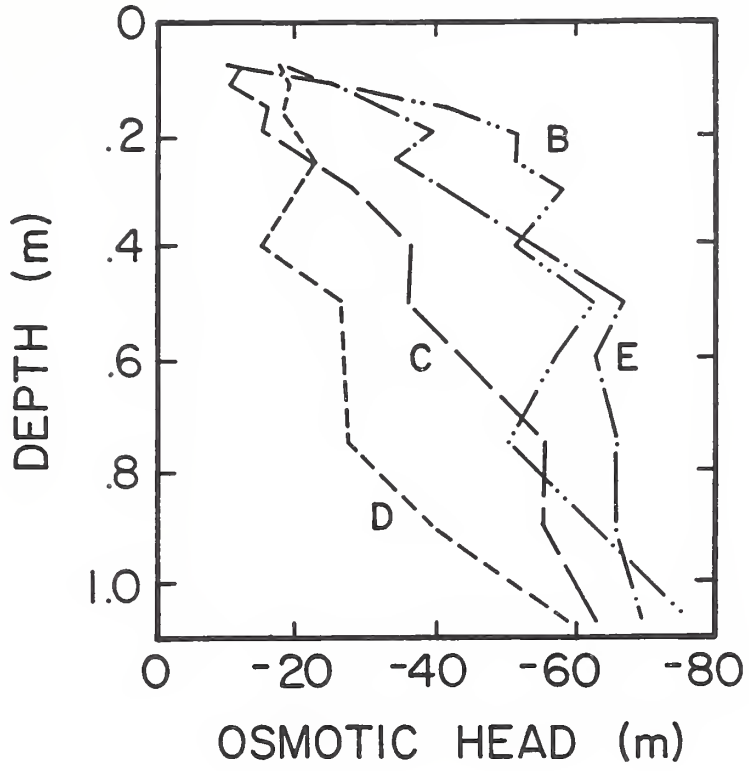

Fig. 4.3. Osmotic head distributions in J7017 of growth period XXIV.

column; this depth is about the same as that observed for the daily irrigations in column A (Fig. 3.5a). The drier soil at the start of the irrigation compensated for the higher amount of irrigation with the four-day as compared to the one-day cycle. The average water content in the top 0.25 m following irrigation on column B-4 was about 0.28 m^3 m^{-3}. If we assume piston flow, the 57.2 mm of irrigation water proper must have infiltrated initially about 0.20 m. Root water uptake causes this water and that of subsequent irrigations to salinize over a relatively short depth interval. This makes the salinity profile of column B-4 on J7017 in Figure 4.3 very similar to that of column E under daily irrigation (Fig. 3.17). Thus, the salinization process and the water content distributions of column B-4 were not much different from those under daily irrigation and it seems therefore that the four-day irrigation cycle in this study can still be considered frequent.

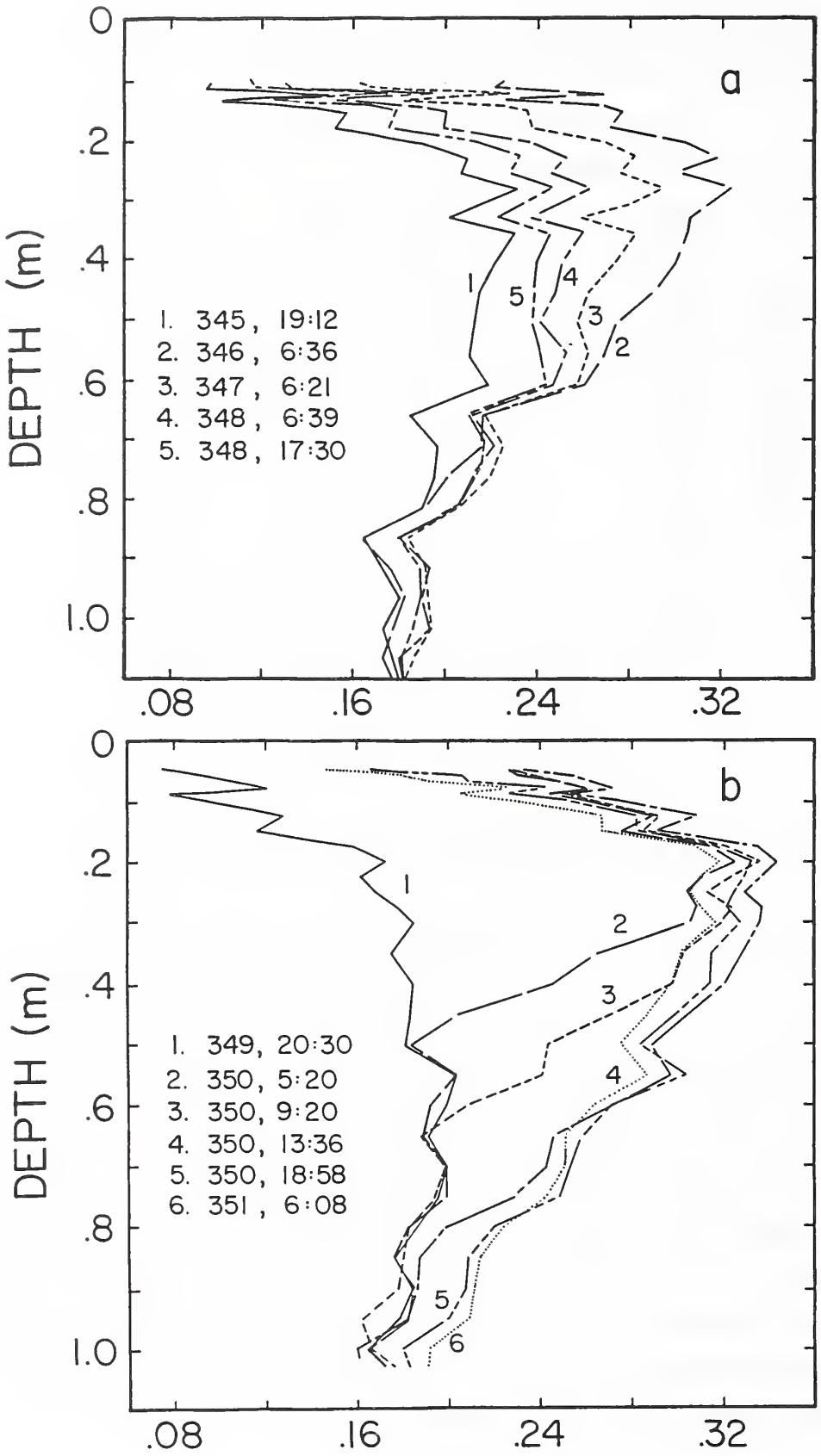
a
DEPTH (m)
0
.2
.4
.6
.8
1.0
.08
.16
.24
.32
1. 345, 19:12
2. 346, 6:36
3. 347, 6:21
4. 348, 6:39
5. 348, 17:30
b
1. 349, 20:30
2. 350, 5:20
3. 350, 9:20
4. 350, 13:36
5. 350, 18:58
6. 351, 6:08

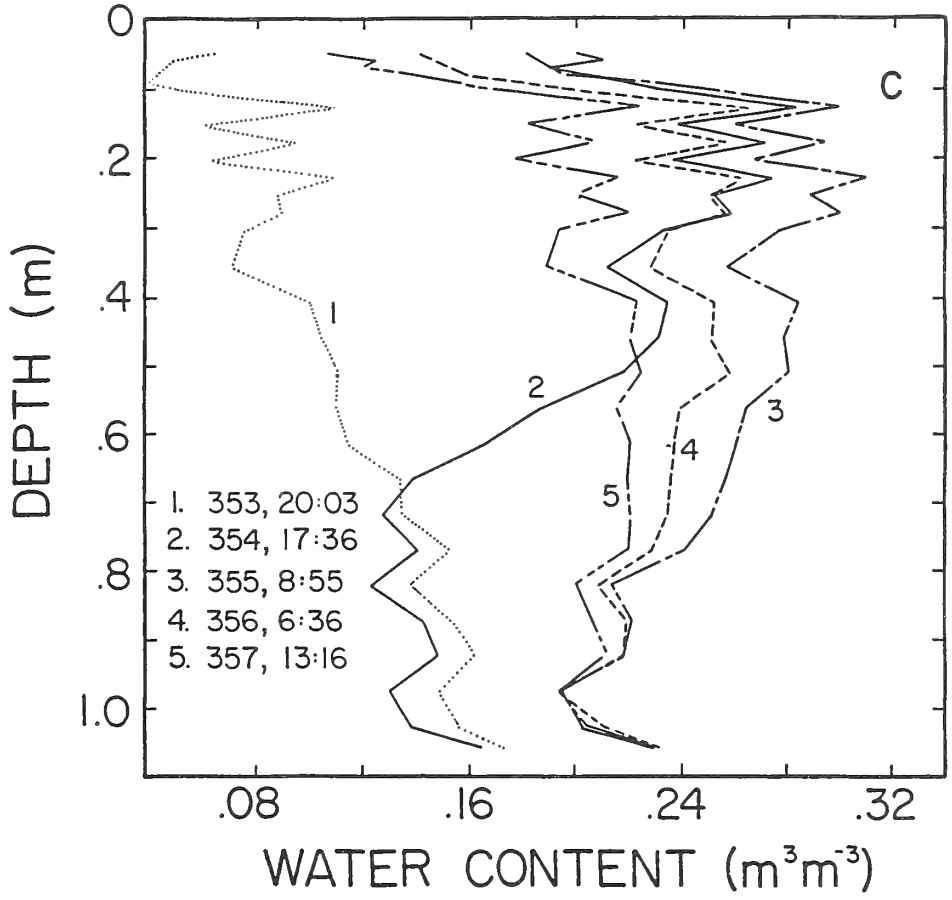

Fig. 4.4. Water content distributions during and after the second irrigation of growth period XXIII. The distributions are for (a) column B-4 following a 57.2 mm irrigation that started on J6345, (b) column C-8 after a 114.3 mm irrigation on J6349, and (c) column D-12 after a 171.4 mm irrigation on J6353.

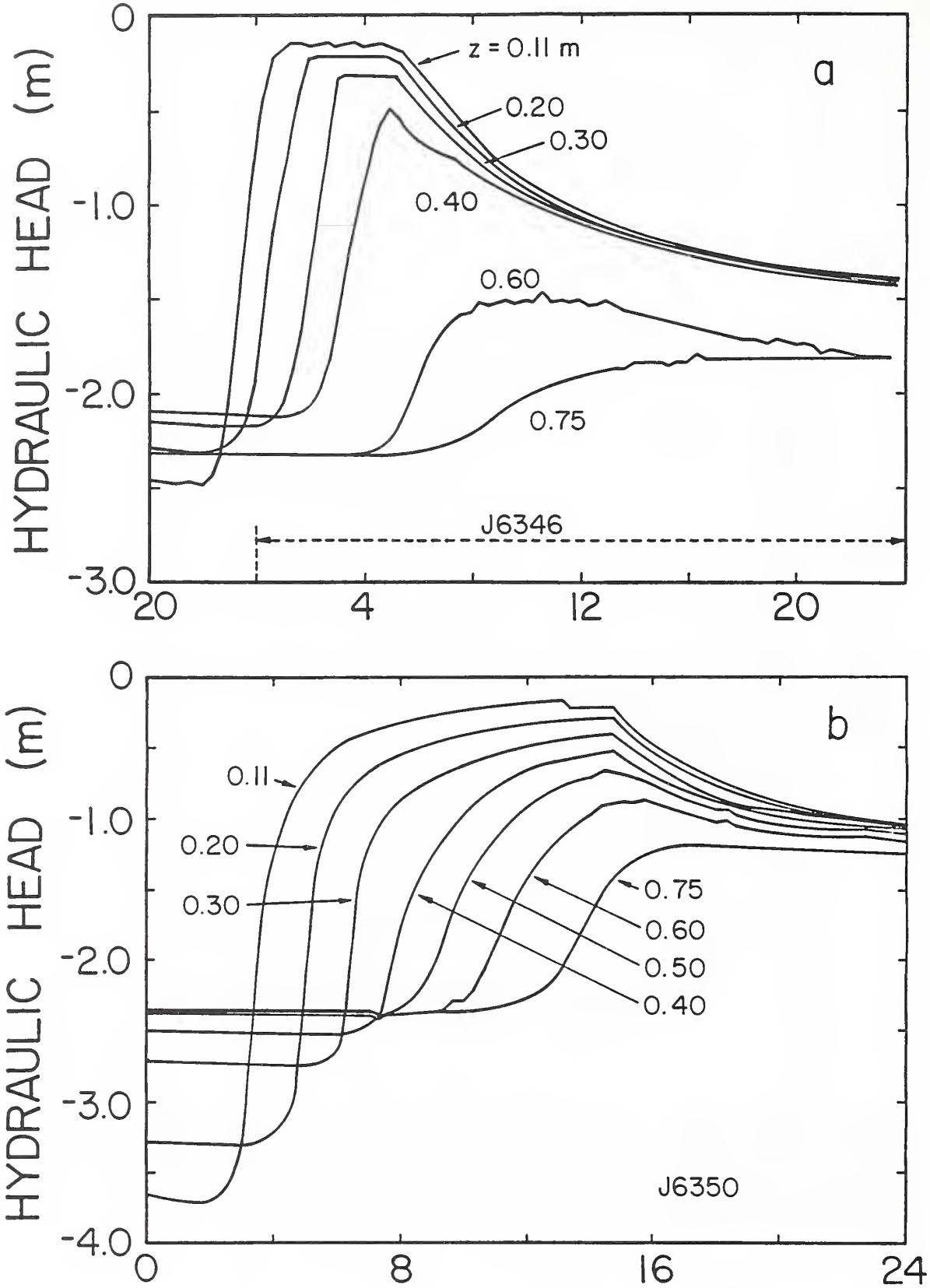
HYDRAULIC HEAD (m)
0
-1.0
-2.0
-3.0
z = 0.11 m
0.20
0.30
0.40
0.60
0.75
a
J6346
20
4
12
20
HYDRAULIC HEAD (m)
0
-1.0
-2.0
-3.0
-4.0
0.11
0.20
0.30
0.75
0.60
0.50
0.40
b
J6350
0
8
16
24

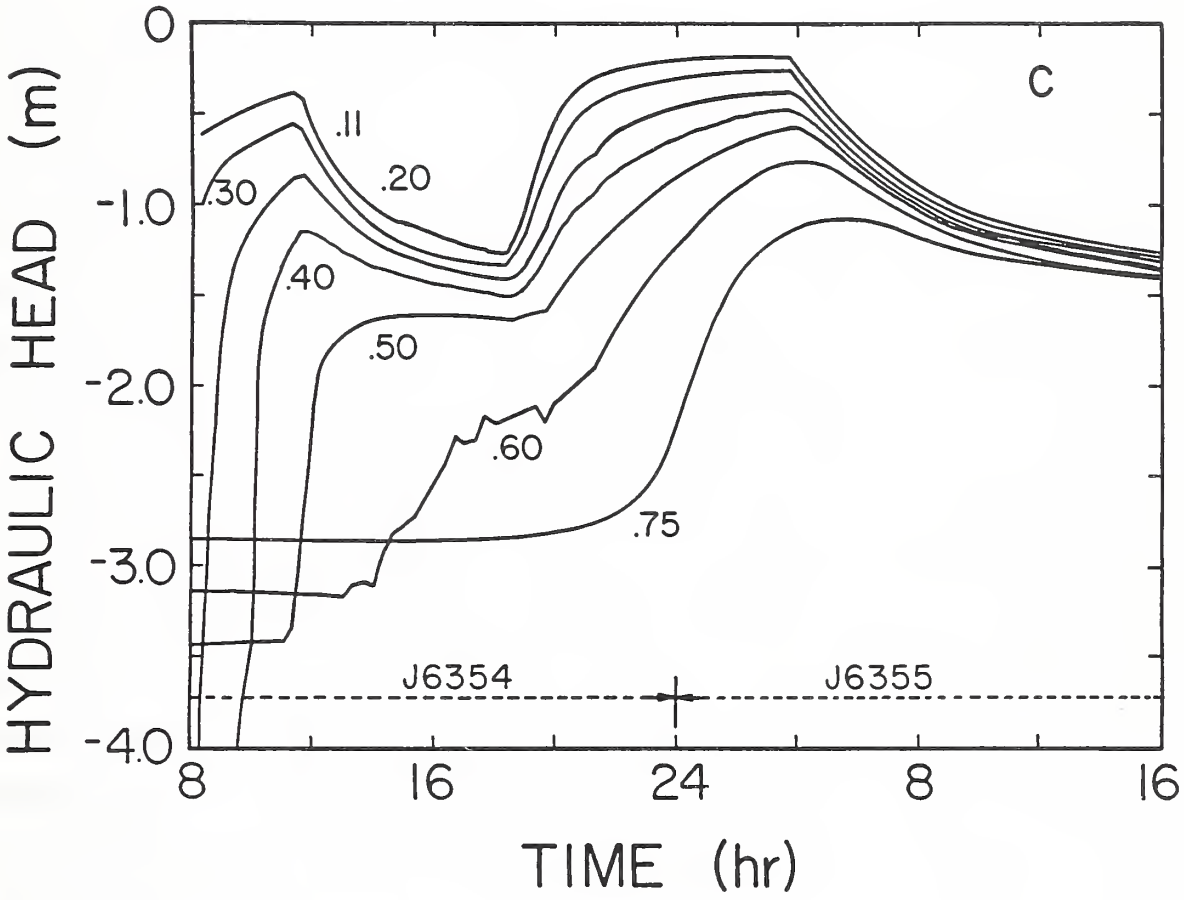

Fig. 4.5. Observed hydraulic heads in columns B, C and D corresponding with the irrigations of Figure 4.4

Figure 4.5a shows that the hydraulic heads (h_h) in column B-4 near the surface exhibited steady maximum values for some length of time. This time length decreased with depth; at z = 0.40 m, h_h started to decrease again just before reaching a steady value. The response at 0.75 m depth was still considerable. The time period between the initial increase and the first decline in h_h at 0.11 m depth was a little over 7 hours, which agrees well with the actual irrigation period. Before the irrigation, the hydraulic gradient was reversed down to a depth of at least 0.40 m; the gradient between 0.60 m and 0.75 m depth was essentially zero.

Figure 4.4b shows that the 114.3-mm irrigation on column C increased θ at the bottom of the column by about 0.03 m^3 m^{-3}, a sufficient change to cause a strong increase in the drainage rate (Fig. 4.1b). The water contents in the top part of the column during irrigation indicate that the irrigation water must have infiltrated initially about 0.38 m, while redistribution moved it somewhat deeper into the column. The salinities in column C-8 were intermediate (Fig. 4.3); its osmotic head distributions were shaped like those of column B-4 just before an irrigation, and like those of column D-12 shortly after an irrigation. The osmotic head of the drainage water from column C-8 was generally the highest (Fig. 4.2b), consistent with the lowest total yields, the lowest total ET, and the highest drainage.

The hydraulic head response at 0.11 m indicates that the irrigation on column C-8 lasted for about 12 hours (Fig. 4.5b). Contrary to column B-4, h_h never reached steady values. Figure 4.6 shows hydraulic head distributions in column C-8 immediately before and during the second eight-day irrigation cycle. The hydraulic gradient before irrigation was reversed to as deep as 0.50 m and was nearly zero below that depth (see the dashed curve). The gradient in the entire column again was reversed at the end of the irrigation interval. About 10 hours after the irrigation, the overall hydraulic head gradient between 0.11 and 0.75 m was less than 0.4 m^{-1}, and later decreased even more. The figure shows that there was a net drying of the column during the interval. The effect of water uptake on the rate at which the hydraulic head decreased is apparent. This decrease was much smaller during the night than during the day. The amount of drainage between J6350 and J6353 decreased from 6.8 to 4.2 mm per day.

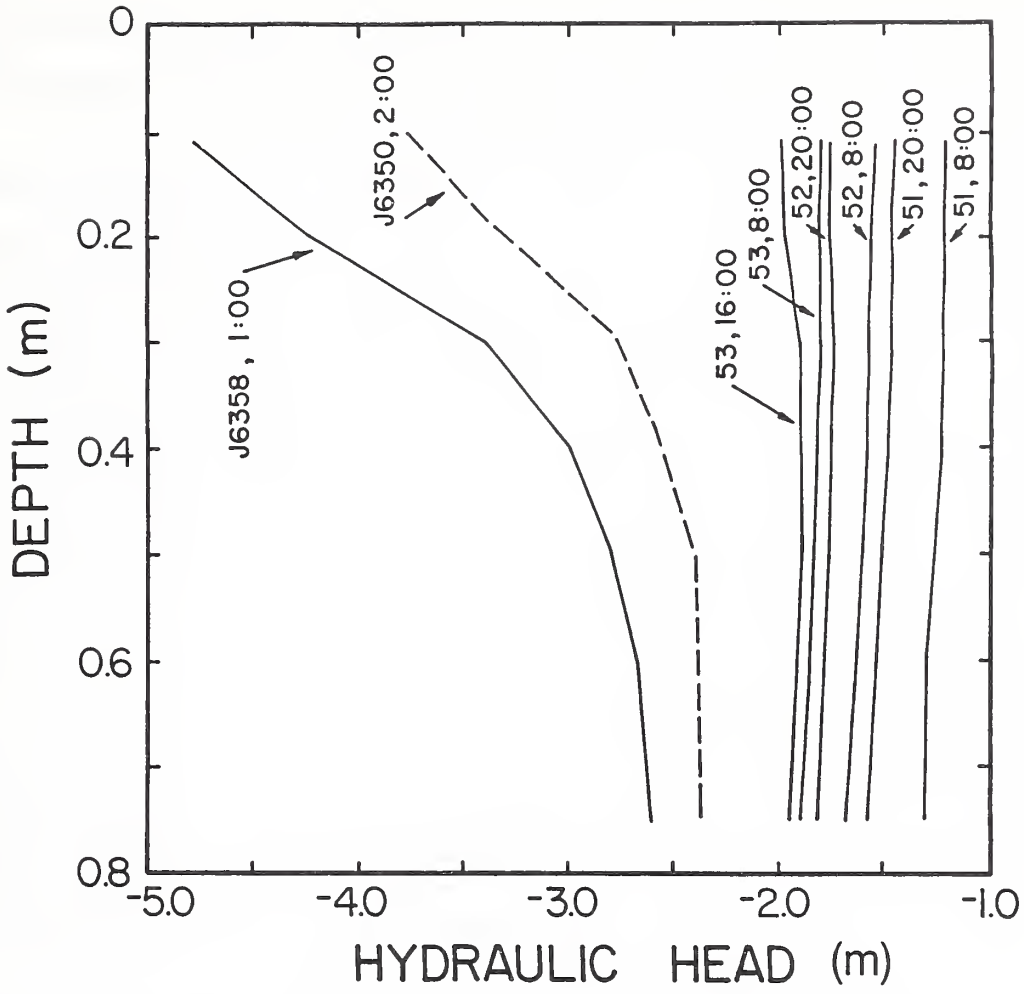

Fig. 4.6. Hydraulic head distributions in column C-8 during the second irrigation cycle of growth period XXIII.

The 171.4-mm irrigations on column D increased in the bottom part of the column by about 0.08 m^3 m^{-3} (Fig. 4.4c). The irrigation water proper must have occupied initially about 0.60 m, while subsequent redistribution must have moved the original water still deeper into the column. The water contents in column D-12 showed unusually large and frequent variations over relatively short distances near the soil surface. This is probably due to the extreme drying at the end of the 12-day irrigation intervals, causing lasting changes in soil packing. The decrease in θ towards the soil surface, attributed earlier to pore space occupied by root crowns (Chapter 2), is also evident from Figures 4.4a and b. The hydraulic heads in Figure 4.5c show that the irrigation water was applied in two stages. Again, steady

values of h_h were not reached anywhere. The soil above 0.50 m before application of the first amount of water was too dry for the tensiometers to function properly. It appears likely that the hydraulic gradient was reversed in the entire column.

Columns A-6 and E-6 behaved similarly to column B-4, the more so because these end columns exhibited higher *ET*-values, thus causing them to dry out further at the end of the irrigation intervals. As a consequence, the higher amounts of irrigation wetted these columns to only slightly larger depths than column B-4. Column E-6 was more saline at its bottom than column B-4 (Fig. 4.3) because of higher *ET*-rates and the resulting lower leaching fractions. The lower salinities in the top part of column E-6 are consistent with the larger amounts of water applied per irrigation, which caused the salts to move deeper into the column than was the case with column B-4.

4.4. *Initial Phase of Non-Daily Irrigation*

All columns became very dry and most of them very saline during growth period XV because of the 10% reduction in irrigation rates, the change to 16-hour light periods, fertilization, and the installation of new lights. Changes in water contents and salinities that resulted from the irrigation schedule initiated at the start of growth period XVI will be used to illustrate characteristic features of salt and water transport under various irrigation frequencies. Figure 4.7 shows water content distributions in column E-6 on a number of days during this growth period. Irrigations were applied on J6174 (one day later than the schedule called for), J6179, J6185, and J6191, starting at around 9:00 a.m. and lasting for about 8 hours. The wetting front reached the bottom of the column with the third irrigation. Between irrigations the top of the column dried out appreciably and was not much wetter on J6197 than on J6172. Salinity pulses do not travel as fast as wetting fronts. This already was explored separately using other data (*Dirksen*, 1980). Figure 4.8 shows osmotic head profiles corresponding to the θ-distributions of Figure 4.7. Osmotic heads on J6174 were very low in the entire column due to previous under-irrigations. The first three irrigations were able to displace the salt to below 0.60 m depth, but the fourth irrigation had little

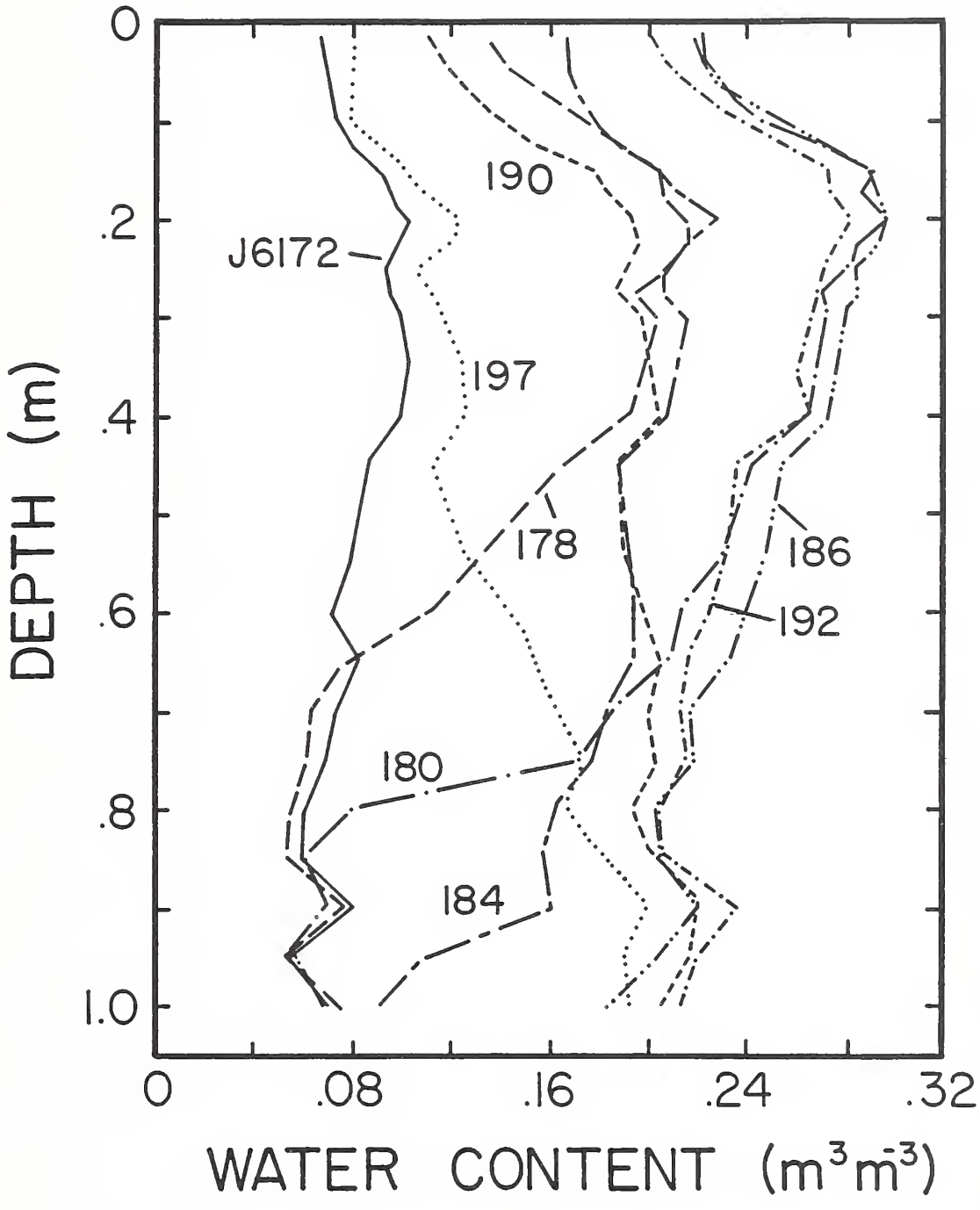

Fig. 4.7. Water content distributions in column E-6 during growth period XVI.

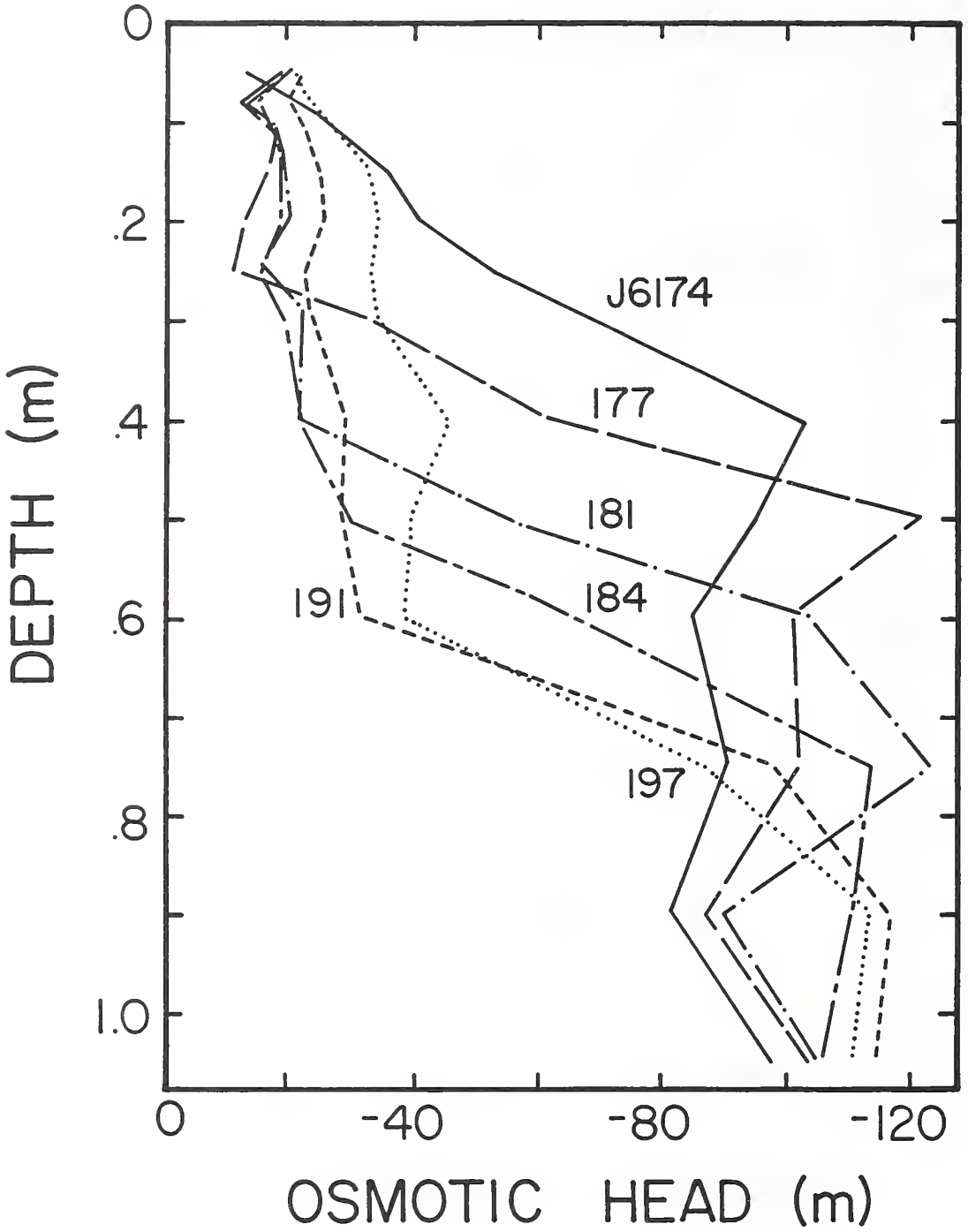

Fig. 4.8. Osmotic head distributions in column E-6 during growth period XVI.

effect below that depth. The osmotic heads below 0.75 m were even lower on J6197 than on J6174. Figure 4.2b shows that the osmotic head of the drainage water of column E-6 did not reach a temporary maximum until growth period XIX; this maximum was still very low.

Table 4.2 lists total heads (h_t, see Eq. 1.1) as a function of depth, z, for column E-6 on J6192, one day after the last irrigation, and on J6197. Pressure heads, h_p, corresponding with the observed water contents in Figure 4.7, were obtained from the soil water retention curve (Fig. 2.7). Some redistribution probably took place on J6192 and the following days. This could account for the bump in the rate of change of the water content (RCWC, Eq. 1.6) between 0.50 and 0.60 m as averaged over the hours of light for that day and shown in Figure 4.9a. Redistribution would make the actual root water uptake, λ, larger in that zone and make it more proportional to the h_t-distribution in Table 4.2. On J6197, the column had dried out to the point where all water movement had stopped, making the RCWC-curve equal to the λ-distribution. The maximum uptake occurred at 0.50 m (Fig. 4.9a), while the total head was still low at 0.60 m (Table 4.2). This discrepancy was probably due to spatial variability of the salinity. The salinity sensors measured only one

Table 4.2. Soil water contents and pressure, osmotic, and total heads in column E-6 on J6192 and J6197.

	J6192				J6197			
Depth	θ	h_p	h_o	h_t	θ	h_p	h_o	h_t
m	m^3m^{-3}	m	m	m	m^3m^{-3}	m	m	m
0.20	0.28	-1.5	-24.6	-26.3	0.115	-9.5	-33.5	-43.2
0.30	0.27	-1.6	-23.4	-25.3	0.117	-9.0	-33.9	-43.2
0.40	0.26	-1.6	-28.5	-30.5	0.125	-7.0	-44.5	-51.9
0.50	0.24	-1.6	-27.3	-29.4	0.120	-8.0	-38.2	-46.7
0.60	0.23	-1.9	-30.8	-33.3	0.144	-4.5	-37.8	-42.9
0.75	0.22	-2.0	-95.9	-98.7	0.170	-3.0	-84.6	-88.4
0.90	0.23	-1.9	-114.3	-117.1	0.200	-2.3	-110.8	-114.0

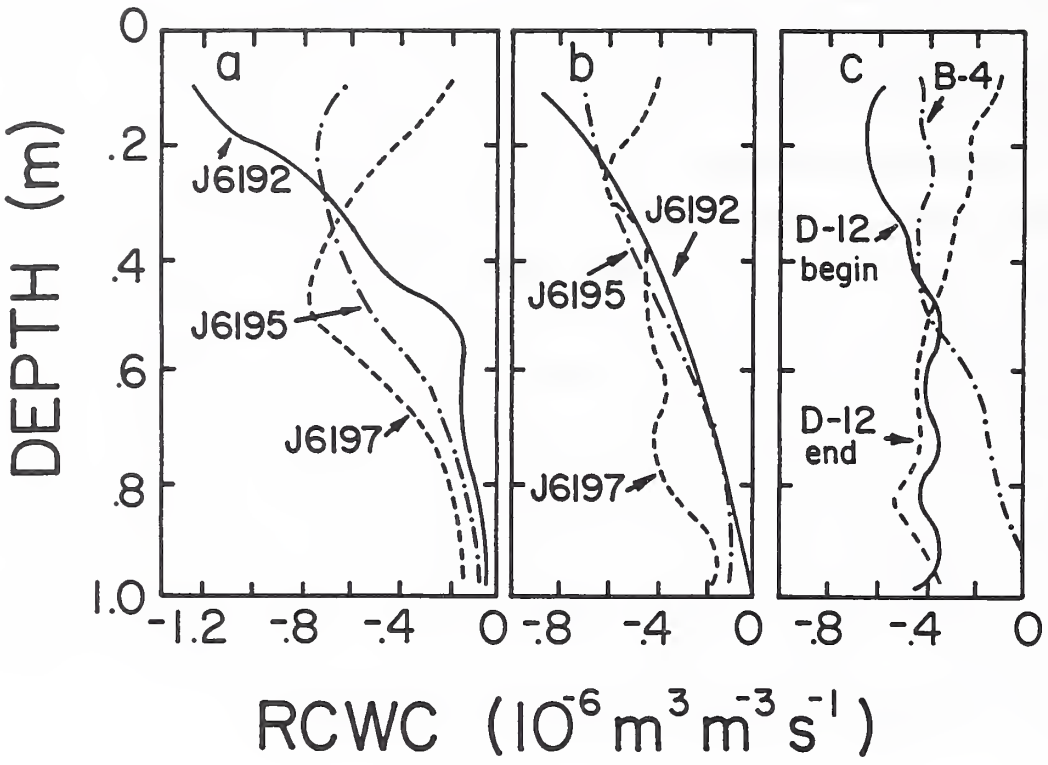

Fig. 4.9. Distributions of RCWC (rate of change of water content) in columns E-6 (a), A-6 (b) and B-4 (c) during growth period XVI. The RCWC-distributions in column D-12 at the beginning and end of the second irrigation interval are also indicated (c).

point while each water content was based on the average of three gamma measurements per depth across the column. The column was much drier on J6197 (Fig. 4.7) and the water uptake rate increased with depth in the top part of column E-6. Whereas the total heads at 0.20-0.30 m and 0.50-0.60 m were about the same, water uptake was much smaller at the shallow depth. This indicates that the low water contents in the top part of the column had an effect on root uptake over and above that of the pressure head. This could be due to increased soil resistance or to an increase in contact resistance at the soil-root interface (see Chapter 5). Figure 4.9b shows similar RCWC-data for column A-6. In the absence of salts, water uptake gradually decreased with depth throughout most of the 6-day interval. Because water contents in the top part had become small on J6197, relatively much water was taken up in the bottom part of the column.

Column D-12 was also quite saline on J6174, but Figure 4.10 shows that nearly all salts were leached out in two irrigations. The variation in osmotic head between J6191 and J6197 was typical for column D-12 during the rest of the experiments. Figure 4.2b shows that the osmotic head of the drainage water increased to a relatively stable value of about -43 m during growth periods XVII through XIX. Thus, the excess salinity was removed in little more than one growth period. The shape of the osmotic head profile in column D-12 remained essentially the same for the rest of the experimental period (Fig. 4.3), but the drainage water became more saline with time (Fig. 4.2b). Figure 4.9c shows average values of RCWC in column D-12 for the daylight hours of one day at the beginning and one day at the end of the second 12-day irrigation interval of growth period XVI. The earlier curve definitely was affected by water flow, especially in the lower half of the column. For the later curve, all water flow had stopped and the curve reflects true root water uptake. Because of low salinities, roots could take up water in the lower part of the column towards the end of the interval after the top part had dried out. For comparison, Figure 4.9c also shows the RCWC-curve for column B-4 as averaged over J6193 and J6197, the last days of the last two irrigation intervals. Root water uptake in the bottom part of this column was less than indicated by the curve because drainage during the last day occurred mainly from this bottom part.

4.5. *Final Stress Period*

The columns were not irrigated at the regular end (24th day) of growth period XXIV, and the alfalfa was cut 4 days late; by then the crop on most columns was severely wilting. The data obtained at that time give additional information on water uptake patterns under non-uniform conditions. Figure 4.11 shows the water content distributions at the end of the stress period. Differences between the curves are caused by differences in salinity. Osmotic head profiles on J7017, just prior to the stress period, were already presented in Figure 4.3. Columns A-6 and D-12 dried out the most. Of these, column D-12 was wetter in the top part because of a higher irrigation water salinity. Column A-6 was wetter at the bottom because of a higher salinity there caused by the low leaching fraction at which this

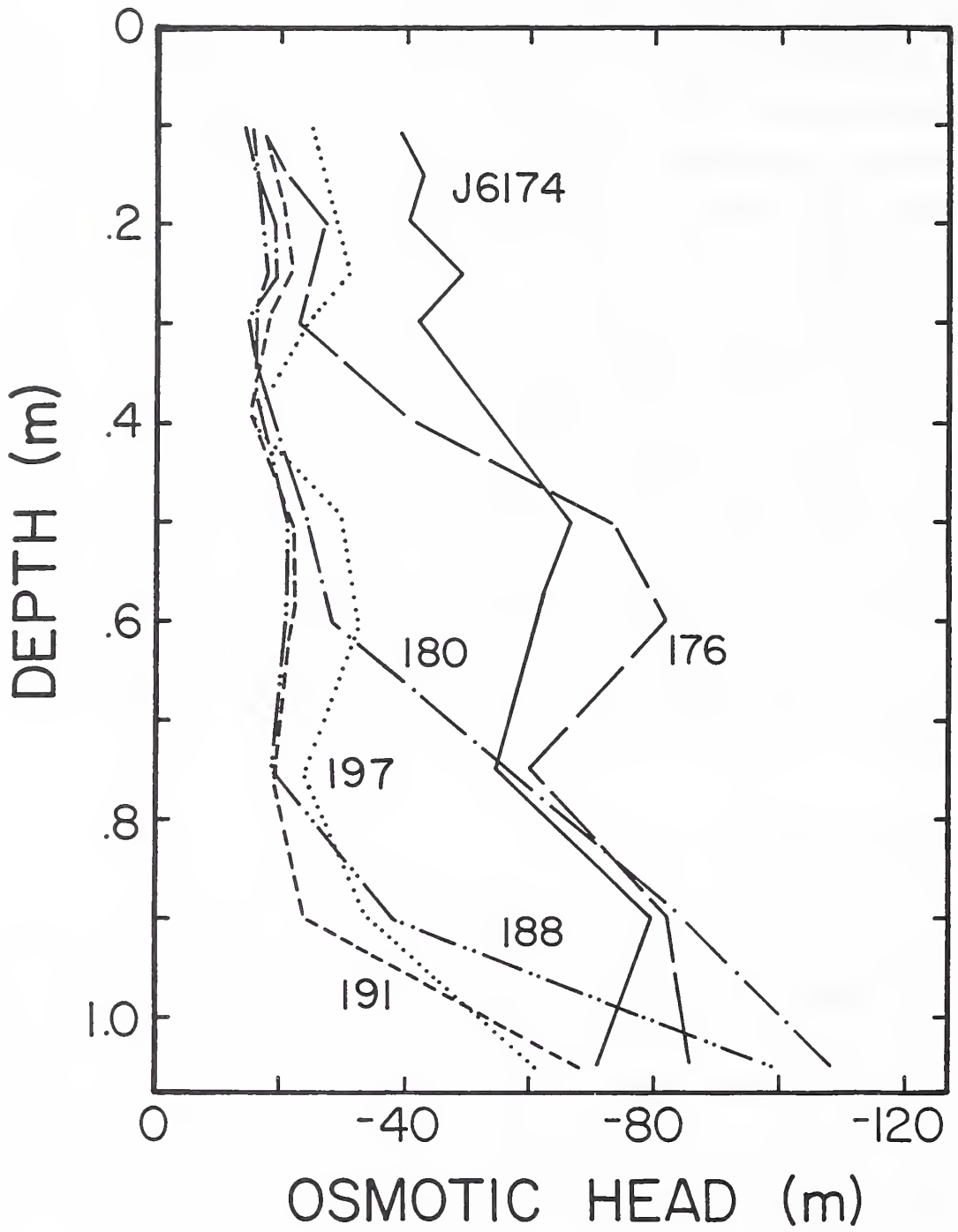

Fig. 4.10. Osmotic head distributions in column D-12 during growth period XVI.

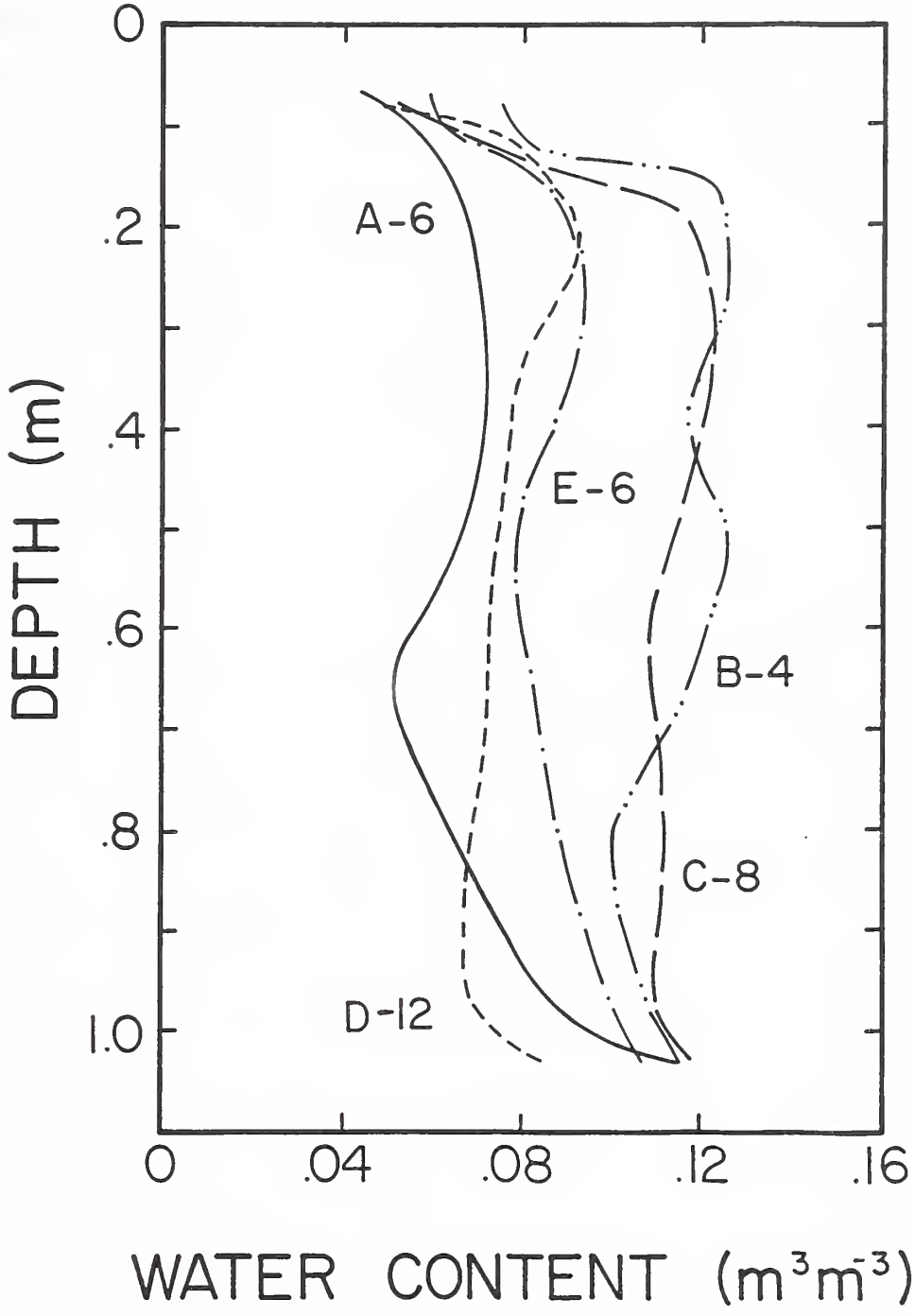

Fig. 4.11. Water content distributions in five columns at end of the stress period after growth period XXIV.

column was operated. Salts in the irrigation tap water had accumulated there over a long period of time. The osmotic head of the drainage water on J7017 was about -89 m. Columns B-4 and C-8 had about equal and much higher water contents than columns A-6 and D-12, while column E-6 had intermediate water contents at the end of the stress period.

Figure 4.12 on pages 90 and 91 shows how the final water contents in Figure 4.11 were reached over the last eight days, from J7020 to J7027. RCWC for each column was averaged over the light hours of four consecutive two-day periods. The first two periods covered the last four days before the regular harvesting date on J7024; the last two periods covered the next four days. Because of some redistribution following the irrigation on the evening before the first period, the first RCWC-curve for column B-4 is omitted. Redistribution in the other columns was negligible compared to water uptake. Column A-6 exhibited a very pronounced change in water uptake distribution. More than 70% of the uptake during the first period occurred above a depth of 0.55 m; thereafter most uptake took place below 0.55 m (Fig. 4.12a).

Table 4.3, which lists the daily amounts of *ET* during the final stress period, shows that column A-6 started with the largest daily *ET* (20 mm) and finished with the lowest (4.5 mm). On J7027, its soil was the driest and the alfalfa was wilting severely; its plants had the lowest (measurable) leaf water potentials and the highest percentage of dry weight (Table 5.2). Column D-12 had received its last irrigation eight days prior to the start of the first period. The daily amount of *ET* at that time was already reduced to 13.5 mm and at the end it was near that of column A-6 (5 mm). Water uptake increased nearly linearly with depth during the entire eight-day period. Column B-4 was the wettest throughout; its daily *ET* was normal (16 mm) during the regular irrigation interval, but decreased sharply to about 7 mm beyond that time. Even when corrected for redistribution, most of the uptake during the first period (not shown) took place above 0.40 m depth. During the second period, about 2/3 took place above 0.50 m. Uptake during the last two periods was nearly uniform below 0.30 m, but decreased linearly to zero at the soil surface. Column E-6 and C-8 showed gradual rates of decline in *ET* and gradual shifts in water uptake distributions from the top to the bottom.

Table 4.3. Daily amounts of evapotranspiration and total leaf water heads during the last stress period.

Column:	A-6	B-4	C-8	D-12	E-6
Day		*Evapotranspiration, mm*			
J7020					
	20.0	16.0	13.0	13.5	17.0
J7021					
	16.0	16.0	12.5	12.5	13.0
J7022					
	14.0	16.0	12.5	12.0	13.0
J7023					
	10.0	16.0	12.5	10.0	12.5
J7024					
	6.5	11.0	11.5	7.5	10.5
J7025					
	5.5	10.0	10.5	6.5	9.0
J7026					
	4.5	7.0	9.5	5.0	9.0
J7027					
		Total head, m			
J7024					
	-205	-159	-147	-164	-194
J7025					
	-203	-187	-162	-197	-194
J7027					
	-265	-187	-168	-*	-196*

* Inaccurate because of wilting.

The uptake distributions and final water contents were determined largely by the pressure and osmotic head distributions that developed during the stress period. As the columns dried out, the salinity sensor readings became less reliable. Moreover, the salinity sensors were removed from column B-4 on J7017. For these reasons, osmotic heads for J7027 were calculated from the observed values on J7017 (Fig. 4.3) or J7020, and the observed changes in water content between those dates. We assumed in-situ concentration of the soil solution as a result of water uptake and no water movement. Similar to Table 4.2, the projected osmotic heads h_o were added to the pressure heads h_p, derived from observed water contents, and the gravitational heads h_g to obtain the total heads h_t in Table 4.4. This table must be interpreted with caution. The soil water retention curve is very

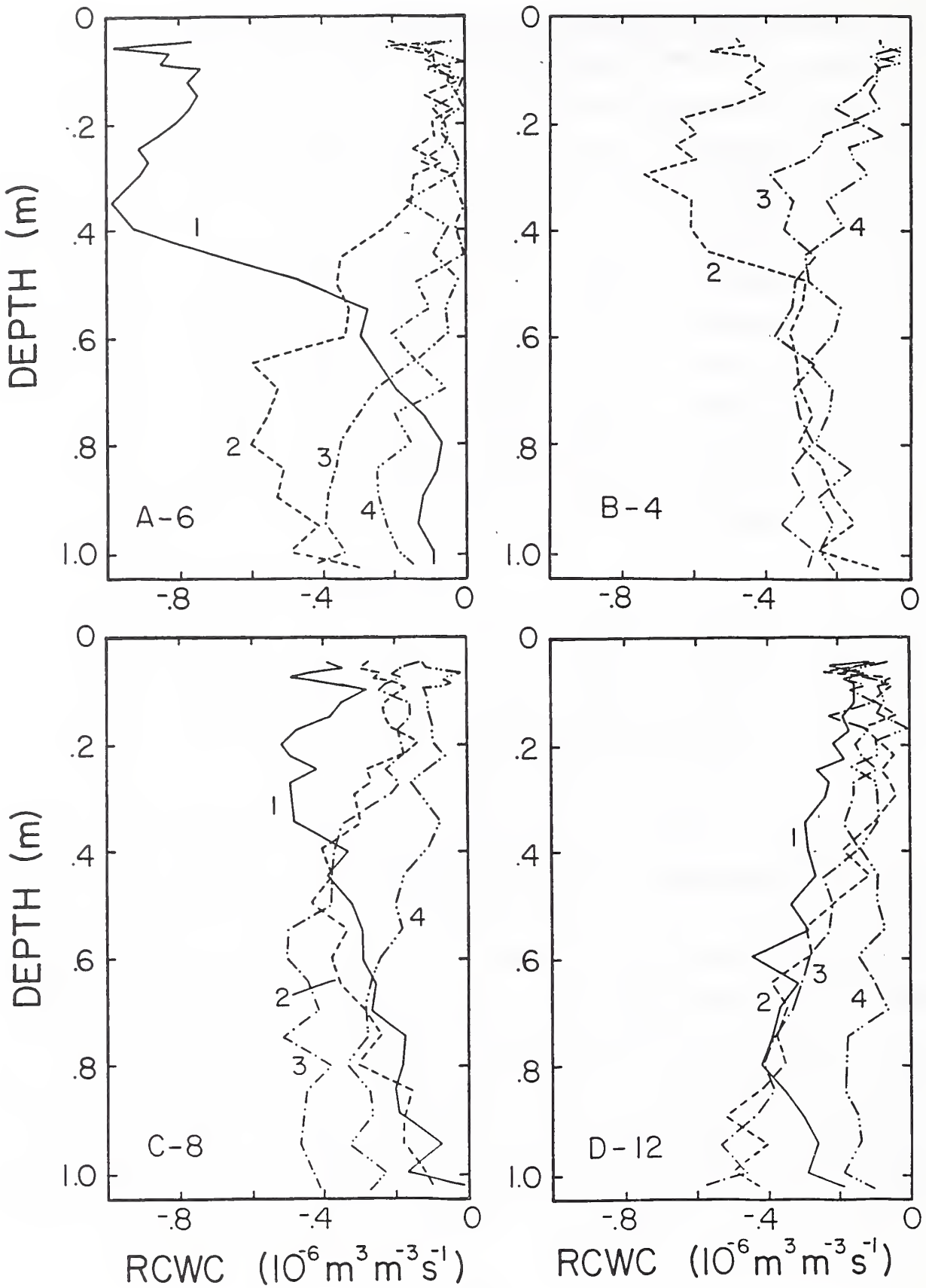
DEPTH (m)
0
.2
.4
.6
.8
1.0
-.8
-.4
0
A-6
B-4
C-8
D-12
1
2
3
4
RCWC (10⁻⁶ m³ m⁻³ s⁻¹)

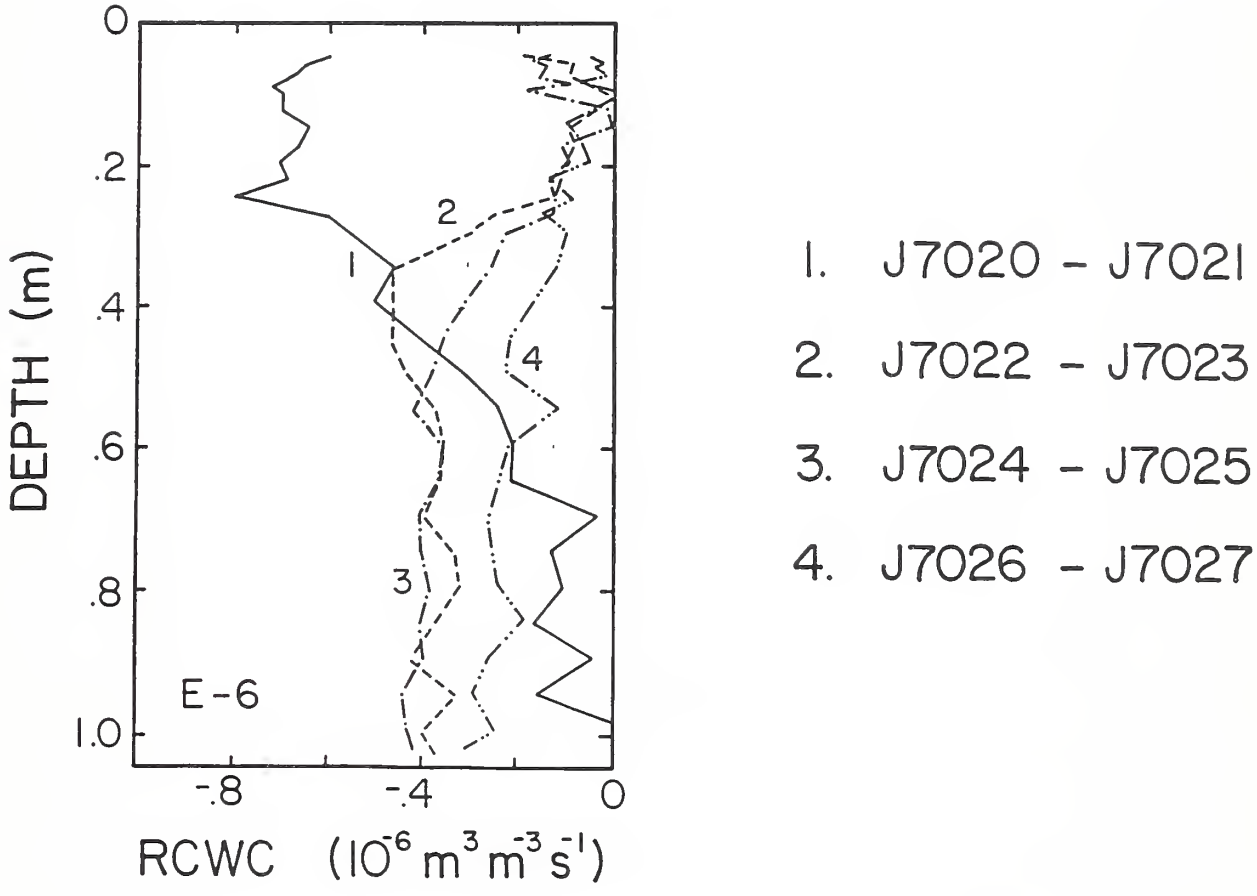

Fig. 4.12. Distributions of the average RCWC (rate of change of water content) during the last four consecutive two-day stress periods of growth period XXIV.

Table 4.4. Soil water pressure, osmotic, and total heads on J7027.

Column:	A-6			B-4			C-8			D-12			E-6		
Depth m	h_p m	h_o m	h_t m	h_p m	h_o m	h_t m	h_p m	h_o m	h_t m	h_p m	h_o m	h_t m	h_p m	h_o m	h_t m
0.15	-180	-3	-183	-13	-69	-82	-35	-27	-62	-56	-24	-80	-42	-34	-76
0.20	-130	-4	-134	-9	-82	-91	-7	-32	-39	-60	-26	-86	-29	-36	-65
0.25	-110	-5	-115	-8	-92	-100	-7	-32	-39	-66	-41	-107	-27	-65	-92
0.30	-100	-6	-106	-8	-106	-114	-7	-42	-49	-75	-32	-105	-25	-90	-115
0.40	-80	-10	-90	-8	-91	-99	-8	-61	-69	-80	-23	-103	-35	-130	-165
0.50	-110	-20	-131	-7	-98	-106	-9	-63	-73	-63	-60	-124	-43	-142	-186
0.60	-200	-25	-226	-7	-93	-101	-10	-79	-90	-66	-58	-125	-45	-130	-176
0.75	-240	-33	-274	-9	-81	-91	-10	-83	-94	-80	-61	-142	-35	-131	-167
0.90	-70	-50	-121	-9	-86	-96	-10	-81	-92	-66	-89	-156	-25	-127	-153
1.00	-30	-90	-121	-7	-108	-116	-9	-94	-104	-40	-124	-165	-15	-118	-134

steep for the low water contents observed in columns A-6 and D-12; in addition, the scatter in these water contents was large. As was noted earlier, we observed a large variability in salinity. The observed osmotic head profiles were not very smooth and any errors in calculating h_t were magnified by the extrapolation procedure. Therefore, the errors in the total heads of Table 4.4 may be large.

The h_t-values were the highest in column C-8 where they decreased with depth. This column was still relatively wet, causing h_p to be high. The main negative contribution to h_t was made by h_o. The next highest values of h_t were observed in column B-4, and h_o again provided the largest negative contribution to h_t. The total head was more or less constant with depth in this column. B-4 is the only column where h_t was approximately uniform on J7027, in agreement with predictions by *Wadleigh et al.* (1947). In column D-12, h_t decreased nearly linearly with depth, reaching a value of about -180 m at the bottom. This is surprising because water uptake during the last two days of the stress period was the highest in the bottom part (Fig. 4.12d). The total potential in column E-6 first decreased with depth until 0.50 m and then increased again towards the bottom. Finally, column A-6 had very low pressure heads near the surface and at the 0.60-0.75 m depth zone, corresponding with a total head of less than -250 m at the latter depths.

4.6. *Conclusions*

All columns in this study received the same amount of water and in equal amounts per irrigation per column, but the amounts differed among the columns in proportion to the irrigation interval. The lower the amount per irrigation, the less deep the salts moved with each irrigation, and the faster salinity increased with depth in the top part of the columns. For a constant leaching fraction and a constant salinity of the irrigation water, a high rate of increase of salinity near the top must coincide with a low rate of increase in the bottom. This is because the salinity of the drainage water, in the absence of salt precipitation, is determined by the leaching fraction. Thus, under these restrictions, the average salinity of the root zone increases with increasing irrigation frequency. Although the leaching fractions

were not the same in our experiments, the qualitative relationship between average salinity and irrigation frequency was still prevalent. In addition, the amounts of drainage and the amounts of salt discharged with it, decreased with increasing frequency, making the differences in average salinity between high and low frequency irrigation even larger. This was true only for frequencies up to once in four days since the behavior under that frequency was in many respects similar to that under daily irrigation.

The high average salinities with high frequency irrigation are usually associated with high average water contents and pressure potentials. As a result, root water uptake under frequent irrigation tends to be rather steady and takes place mainly at shallow depths. This, in turn, reinforces the steep increase in salinity near the surface. Because of the shallow water uptake under frequent irrigation, the uptake-weighted mean salinity (to be discussed in Chapter 5) will be smaller than the average salinity. The longer the irrigation intervals, the lower the salinities are in the lower half of the root zone, and the lower the pressure potentials become towards the end of the irrigation intervals. The rate of root water uptake under low frequency irrigation initially decreases gradually with depth, probably in proportion to the root density. However, as water is being depleted in the upper part of the rootzone, water uptake can shift downward because of the low salinity. Yields obtained in these experiments (see also Chapter 5) indicate that the low pressure heads with the 12-day intervals are more detrimental to plant yield than the low osmotic potentials with the 4-day intervals. However, this may have been caused in part also by a decreased *ET* as a result of increased soil-root interface resistances at low water contents.

The water and salt transport data for Column E-6 during growth period XVI, represented by the water content and osmotic head distributions in Fig. 4.7 and 4.8, respectively, were simulated quite successfully with the model HYSWASOR (*Dirksen, et al.*, 1993).

5. PLANT ASPECTS

The preceding three chapters focused on the experimental details (Chapter 2), and on water and salt transport processes in the soil under daily irrigation (Chapter 3) and non-daily irrigation (Chapter 4). This last chapter concentrates on such plant aspects as alfalfa yields, transpiration ratio's, root length and root weight distributions, and leaf water potentials. The evaporative demand was reasonably constant throughout the two-year period; the total leaf water potentials for the same size canopy should then be a measure of how well the plants integrate the various non-uniform soil water potential distributions. Based on this reasoning and because of a lack of experimental methods to measure root water potentials in situ, leaf water potentials will be correlated with soil water potentials using various techniques of spatial averaging. A maximum root conductivity will be derived also.

In this study, water potentials have been expressed in head units (energy per unit weight of solution). The total head h_t is given by Eq. (1.1), i.e.,

$$h_t = h_p + h_o + h_g \tag{5.1}$$

where the subscripts p, o, and g refer, respectively, to the pressure, osmotic, and gravitational components of the total head. To prevent confusion, we will distinguish between the components of the water potential in the soil, leaves and roots by adding an additional subscript: s, l and r, respectively.

Cells of plant leaves are surrounded by semi-permeable membranes, and thus the driving force for bulk flow in and out of these cells is determined by the gradient of the total leaf water potential, h_{tl}. This variable can be measured with psychrometers and pressure chambers. When cell walls are destroyed, for example by dipping them in liquid nitrogen, h_{pl} becomes zero. Since h_g remains the same, h_{tl} measured with psychrometers is then also equal to h_{ol} of the original cell vacuole, provided that dilution with water originally outside the vacuoles is negligible. The difference between h_{tl} before and after destroying the cell wall equals the turgor of the vacuoles in their original state (h_{pl}).

5.1. *Experimental*

Alfalfa was grown at a density of 230 plants per m^2 in laboratory soil columns for more than two years. During this time, various distributions of the soil water pressure head, h_{ps}, and osmotic head, h_{os}, were established by varying either the amount and osmotic head h_o of the irrigation water, or the frequency of application. During the daily irrigation phase, leaf water potentials were measured only between days J5239 (Julian date 239 of 1975) and J5246. These measurements were made on excised leaf discs with thermocouple-psychrometers (*Hoffman et al.*, 1969).

After total heads h_l were measured, the leaf discs were immersed momentarily in liquid nitrogen to break down the cell walls and to measure also the osmotic heads h_{ol}. The difference between h_l and h_{ol} was assumed to be equal to the turgor pressure head. Each set of measurements was made on approximately six replicate leaf discs. The observed large variations between replicate measurements appeared to be due to random experimental errors rather than actual variations in leaf water potentials. We therefore started to measure h_l with a pressure chamber (Plant Water Status Console, Model 3005, Soilmoisture Equipment Co., Santa Barbara, CA). Unfortunately, h_{ol} can not be measured with this instrument. The six replicate measurements of h_l with the pressure chamber generally showed little variations. Each measurement was made on the common stem of an end cluster of alfalfa leaves that was exposed to direct light. The cluster was wrapped immediately in moist paper tissue and placed in the pressure chamber. The protruding end of the stem was kept as short as practically possible. The measurements were made during the last few days of each growth period, starting on J6090. The psychrometer measurements were discontinued on J6109 when it became apparent that the quality of these data was considerably less than that obtained with the pressure chamber.

Column F was sampled on J6014 after having been under daily irrigation for 9 growth periods. The method of soil sampling used to determine root lengths was described in Part 2. The samples were kept in a preservative liquid before and after the soil was washed away until root lengths could be determined by the line-intercept technique

(*Newman*, 1966). The roots were cut into short segments and spread uniformly in an acrylic plastic container with a line-grid etched on its flat bottom. This container was then placed on an overhead projector which showed the grid pattern and the root segments on a large screen; this method facilitated the counting procedure considerably. The number of intercepts was counted along a limited number of randomly chosen horizontal and vertical grid lines. Root lengths were converted to a volumetric basis using the weight of the original soil samples and the bulk densities of the soil cores. Columns B, D and E were sampled around J7175 in essentially the same way as column F before. The washed-out root samples were simply centrifuged and weighed rather than used to determine root lengths with the more time-consuming line-intercept technique. The root samples for each depth interval of column F were also weighed. Further experimental details are given in Chapter 2.

5.2. *Yields and Transpiration Ratios*

Table 5.1 gives yields of green and dry weight and percentages of dry matter of harvests I through IX during daily irrigation; Table 5.2 gives similar values for harvests XVI to XXIV during non-daily irrigation. Growth periods II to IX varied between 20 and 33 days. The low yield of harvests V and VI coincide with a general reduction in the percentage dry matter. This may have been due to a decrease in illuminance as a result of high temperatures of the lights. Green weight yields were not reduced as much. Column B consistently produced the lowest yield, caused either by the low illuminance received by this column, or more likely, by the high salinity of the irrigation water. This water had an osmotic head h_o of -22.0 m which was well below the salinity threshold of -16 m for the initial yield decline of alfalfa (*Maas and Hoffman*, 1977). Column B did not have the highest average nor the maximum soil salinity. This is consistent with the conclusion reached by *Bernstein and Francois* (1973) that plants respond more to the lowest salinity in a soil profile (that of the irrigation water) than to the highest salinity. Having the highest leaching fraction, L, column B was also the wettest. However, oxygen probes indicated that

Table 5.1. Green and dry weights in kg, and percent dry matter for harvests I-IX at indicated Julian dates.

Julian Date	Growth Period	Column A	B	C	D	E	F
		0.1201	0.1003	0.1050	0.1426	0.1345	0.1229
J5174	I	0.0218	0.0170	0.0187	0.0256	0.0227	0.0225
		18.1	17.0	17.8	18.0	16.9	18.3
		0.1633	0.0947	0.1148	0.1820	0.1431	0.1700
J5204	II	0.0296	0.0171	0.0199	0.0307	0.0241	0.0289
		18.2	18.1	17.4	16.9	16.8	17.0
		0.1919	0.1128	0.1156	0.1959	0.1595	0.1595
J5227	III	0.0307	0.0184	0.0174	0.0297	0.0268	0.0251
		16.0	16.3	15.3	15.2	16.9	14.7
		0.1599	0.1097	0.1666	0.2496	0.1502	0.2012
J5252	IV	0.0255	0.0192	0.0286	0.0388	0.0254	0.0331
		15.9	16.6	17.1	15.6	16.9	16.4
		0.1542	0.1192	0.1619	0.2168	0.1757	0.1843
J5272	V	0.0214	0.0175	0.0227	0.0303	0.0255	0.0266
		13.9	14.6	14.0	14.0	14.5	14.4
		0.1438	0.1238	0.1555	0.1851	0.1833	0.1577
J5297	VI	0.0298	0.0178	0.0231	0.0273	0.0278	0.0247
		14.5	14.4	14.9	14.8	15.2	15.7
		0.0987	0.1355	0.1787	0.1998	0.1713	0.1697
J5321	VII	0.0155	0.0225	0.0299	0.0335	0.0296	0.0313
		15.7	16.6	16.7	16.8	17.3	18.5
		0.1750	0.1703	0.2133	0.2650	0.2219	0.2086
J5346	VIII	0.0259	0.0276	0.0335	0.0443	0.0352	0.0351
		14.8	16.2	15.7	16.7	15.9	16.8
		0.1535	0.1177	0.1380	0.1848	0.1765	0.1596
J6014	IX	0.0238	0.0178	0.0223	0.0306	0.0305	0.0294
		15.5	15.2	16.2	16.6	17.3	18.5

Table 5.2. Green and dry weights in kg, and percent dry matter for harvests XVI - XXIV at indicated Julian dates.

Julian Date	Growth Period	Column A-6	B-4	C-8	D-12	E-6
		0.1963	0.1839	0.1627	0.2193	0.2317
J6197	XVI	0.0307	0.0287	0.0230	0.0316	0.0370
		15.6	15.7	14.1	14.4	16.0
		0.2794	0.2151	0.1974	0.2042	0.2424
J6221	XVII	0.0405	0.0331	0.0275	0.0287	0.0377
		14.5	15.4	13.9	14.1	15.6
		0.2833	0.2187	0.1793	0.2013	0.2351
J6245	XVIII	0.0469	0.0359	0.0273	0.0310	0.0399
		16.6	16.4	15.2	15.4	17.0
		0.2841	0.2240	0.1846	0.2058	0.2304
J6269	XIX	0.0466	0.0367	0.0279	0.0314	0.0407
		16.4	16.4	15.1	15.3	17.7
		0.2836	0.2261	0.1847	0.1932	0.2358
J6293	XX	0.0441	0.0351	0.0272	0.0287	0.0395
		15.7	15.5	14.7	14.8	16.8
		0.2707	0.2161	0.1789	0.1830	0.2098
J6317	XXI	0.0423	0.0342	0.0268	0.0281	0.0360
		15.6	15.8	15.0	15.4	17.2
		0.2200	0.1917	0.1969	0.1836	0.1856*
J6341	XXII	0.0384	0.0311	0.0301	0.0308	0.0257*
		17.5	16.2	15.3	16.8	13.8*
		0.2303	0.1823	0.1473	0.1669	0.1893
J6365	XXIII	0.0358	0.0284	0.0218	0.0261	0.0283
		15.5	15.6	14.8	15.7	14.9
		0.1343	0.1762	0.1460	0.1282	0.1481
J7027	XXIV	0.0385	0.0354	0.0272	0.0282	0.0317
		28.6	20.1	18.6	22.2	21.4

*Affected by plastic cover.

the O_2 concentration in column B was about 12%, a value generally considered to be more than adequate for normal root functioning. Column A yielded well until J5272; after that date it was at one time severely infested with thrip. Later, one plant died in this column, the only plant during the entire study period. Both before and after their salinization on J5172 (the start of growth period VI) yields per unit surface area for columns D and F were nearly identical. During the first five growth periods, column E yielded 19.6% less than columns D or F. Because column E was located between D and F and always received essentially the same illuminance, this difference is a good measure of the yield reduction caused by the higher salinity in column E. The salinization of columns D and F decreased the yields of the sixth growth period somewhat, but the eighth harvest yielded more than before. During growth periods VI through IX, the yields of column E also increased such that they were only about 10% less than those of columns D and F. Thus, mature alfalfa plants apparently were able to adjust better to saline conditions than younger plants.

Growth periods XVI to XXIV under non-daily irrigation (Table 5.2) all lasted 24 days. It is not clear why column C-8 consistently yielded the least. Harvest XVI of column A-6 was very poor because of severe wilting during the previous growth period. The dry weight percentage of this harvest was 36.6%, the highest value recorded in this study. Whereas harvest XVII of column A-6 was already higher in dry matter than for the other columns, it was not until growth period XVIII that column A-6 had fully recovered from wilting. After harvest XVI, the order in dry matter yields was A-6 > E-6 > B-4 > D-12 > C-8. The only exception was column E-6 after harvest XXI. In an attempt to measure the soil hydraulic conductivity after the roots were established and the column was salinized, a plastic cover was placed over this column to prevent evapotranspiration during the first 12 days of growth period XXII. Unfortunately, this effort was not successful because of problems with the tensiometer system (see Chapter 4). The plastic cover not only reduced ET to zero and increased drainage during the 12-day period (see Fig. 4.2a), but it also badly damaged the canopy due to molds and fungi that developed in the 100 percent relative humidity. As a result, harvests XXII and XXIII of column E-6 were low, which caused the period of low ET and high drainage to prolong further.

Table 5.3. Transpiration ratios (in kg water per kg dry matter) for the indicated growth periods.

Growth Period	Column A	B	C	D	E	F
IV	761	907	770	638	637	591
V	703	694	600	557	500	526
VI	819	832	742	-	623	-
I-IX	770	860	780	-	640	-
XVI-XXIV	563	611	703	650	605	-

Table 5.3 compares the transpiration ratio (the inverse of the water use efficiency) of the various treatments during growth periods IV, V, and VI. Column B was the least efficient during period IV, needing 907 kg water to produce 1 kg dry matter. The transpiration ratio during period V fell to 694 kg kg^{-1}, but rose again to 832 kg kg^{-1} during growth period VI. All other columns showed the same trend. Because growth periods IV and VI lasted longer (25 days) than period V (20 days), these numbers suggest that during the last five days either the plants transpired without producing much additional dry weight, or that most of the photosynthates were translocated to the roots. Alfalfa usually grew 0.60 m or more in 20 days, but the plants did not grow much more thereafter. The highest efficiency was obtained by column E during period V: 500 kg water per kg dry matter. Water use efficiency was not calculated for columns D and F during period VI because of their irregular salinization process.

Table 5.3 lists also average transpiration ratio's for the nine daily irrigation cycles, covering growth periods I - IX, and for the nine non-daily irrigation cycles, covering growth periods XVI - XXIV. Transpiration ratios for the non-saline column A were much lower during the 6-day irrigation phase than during daily irrigation. This indicates that, in the absence of salinity, the higher pressure heads during daily irrigation may have induced the plants to take up water without leading to a higher dry matter production (luxury consumption). Thus, frequent irrigation with high quality water at moderate to high leaching fractions may be undesirable from the point of view of water conservation. The

average transpiration ratio for column B was not excessive during non-daily irrigation, but was relatively high during daily irrigation. As mentioned earlier, this was most likely because the osmotic head of the daily irrigation water (-22.0 m) was below the salinity threshold value of about -16 m for the initial decline in alfalfa yield. The osmotic head of the non-daily irrigation water (-12.0 m) was still well above this threshold value. Columns C and E showed essentially the same average transpiration ratio's during the two irrigation phases, but the values were significantly different between the two columns. Low soil water salinities because of low leaching fractions and the use of irrigation water with osmotic heads above the threshold value, such as in column E, apparently improved the water use efficiency of the plants without adversely affecting yields. Column D had a somewhat higher transpiration ratio during the 12-day irrigation cycle than during daily irrigation. This also could point to some luxury water consumption during the first part of the irrigation intervals when the column was very wet and moderately saline.

The illuminance was not uniform in time, but decreased during both daily and non-daily irrigation. There were also no replicate treatments, only multiple growth periods for each of the treatments. Therefore, the conclusions reached here about the effects of salinity distributions and irrigation frequencies on yields and transpiration ratios can only be tentative.

5.3. *Root Measurements*

Figure 5.1 shows root length distributions along four vertical planes of column F on J6014. The highest root densities occurred at about 0.10 m depth, with a maximum of 13 x 10^4 m m^{-3}. Below 0.35 m, root lengths were fairly uniform at about 3 x 10^4 m m^{-3}. From about 0.55 to 0.75 m depth, the root density increased monotonically across the column towards the end of the model, similarly as for the observed salinity distributions (Fig. 2.13).

Figure 5.2 gives root weight distributions in kg m^{-3} for columns B, D, E, and F. Column F was sampled 527 days earlier than the others and had far less root weights than the other three columns, indicating that there was still significant root growth after the first 250 days. The large peak at 0.20 m depth in column E is the result of sub-surface

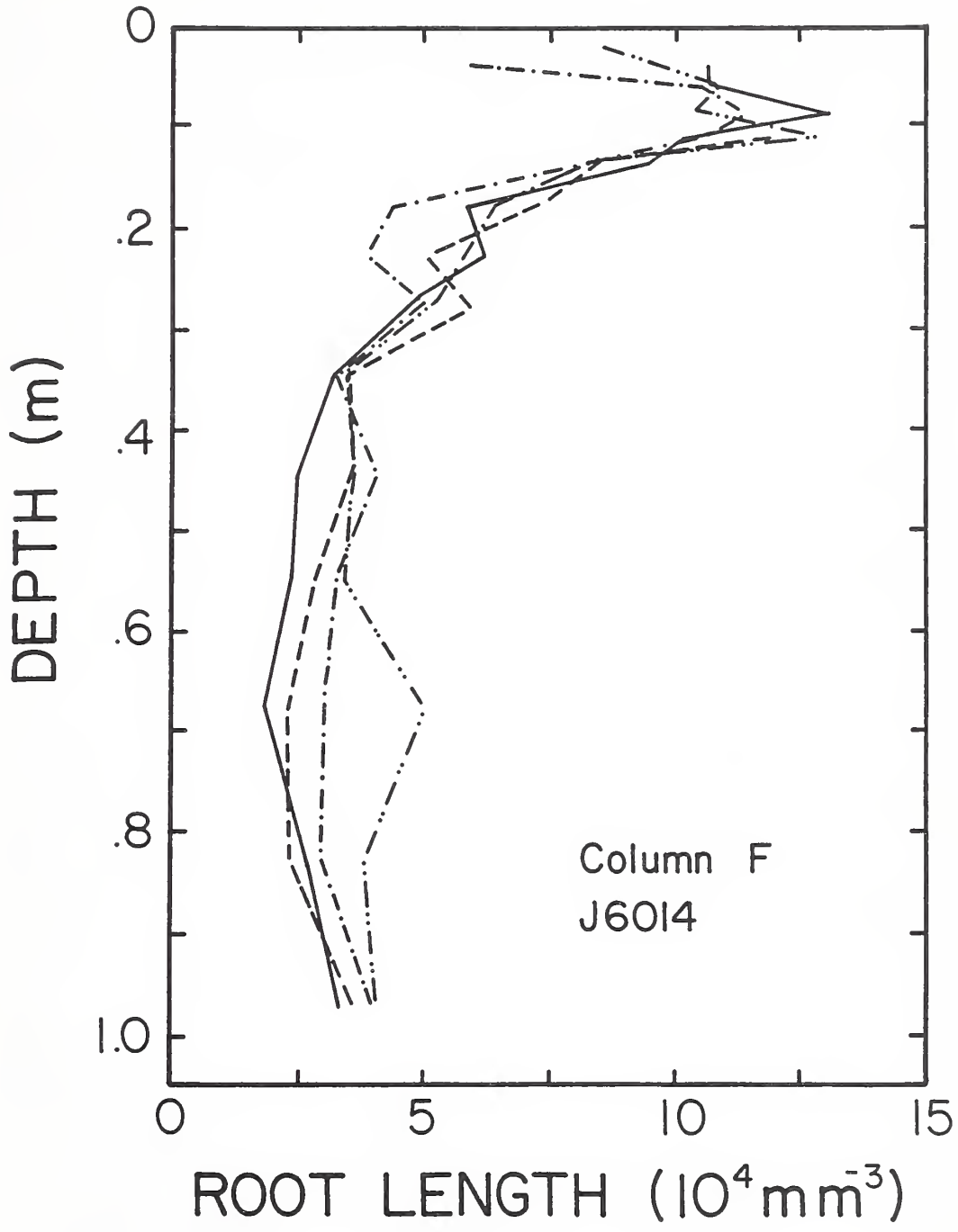

Fig. 5.1 Root length distributions in four vertical sections of column F on J6014.

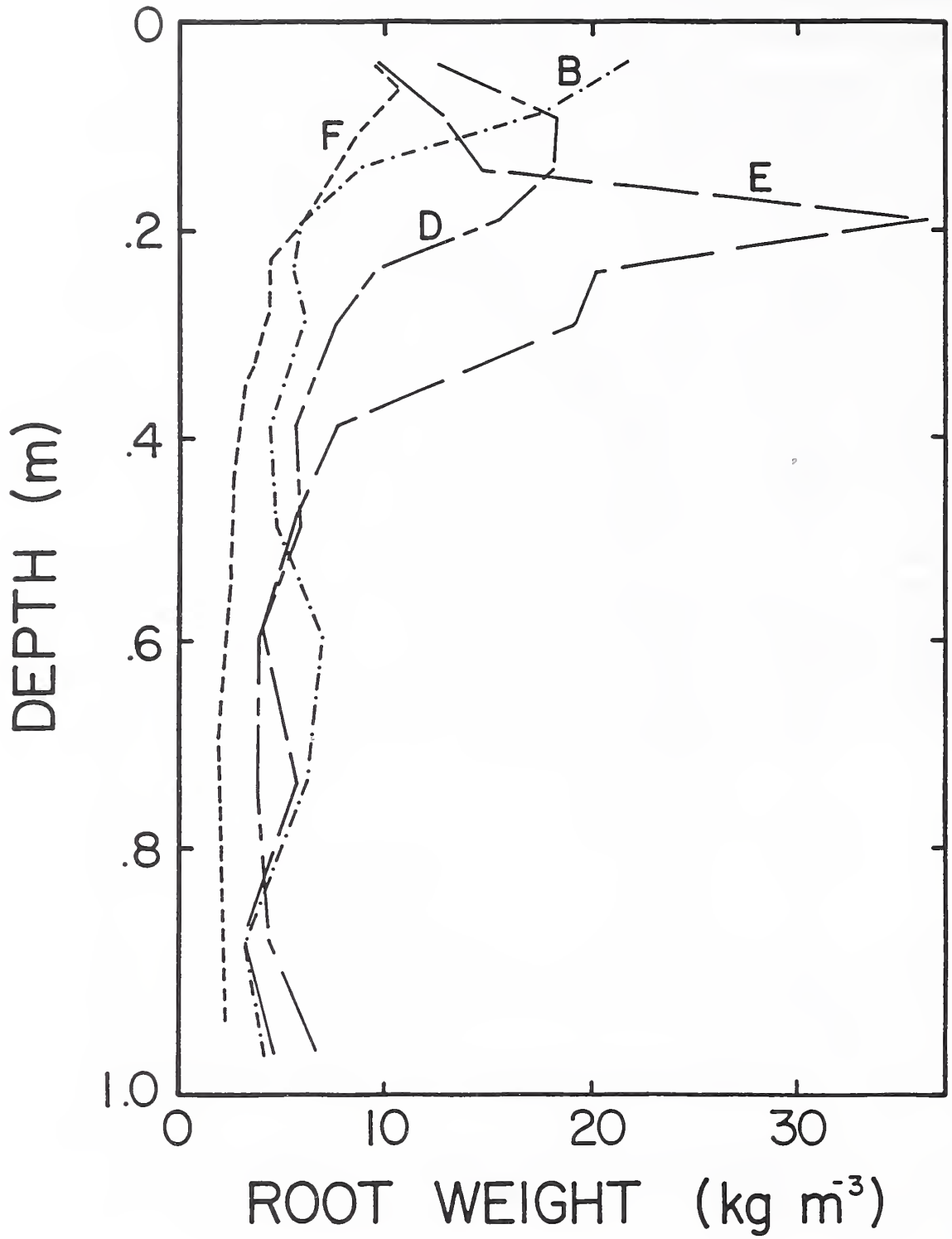

Fig. 5.2. Root weight distributions in columns B, D, E, and F at the end of the experiments.

irrigation at that depth during the last five months prior to sampling.

Figure 5.3 shows root lengths per unit weight of root for column F derived f rom the data in Figures 5.1 and 5.2. The solid line was eye-fitted to the data . The soil already contained some dead root material before packing. No corrections for these dead roots were made, but they must have been about 1 x 10^4 m m^{-3} (*S. M. Merrill*, personal communication). We tried to use the staining method of *Ward et al.* (1978) to distinguish between dead and living roots, but this method did not work well for the alfalfa roots. The living white roots stained the most. The percentage of dead roots was most likely the largest in the samples of the older roots (Fig. 5.2). If needed a reasonable estimate of the root

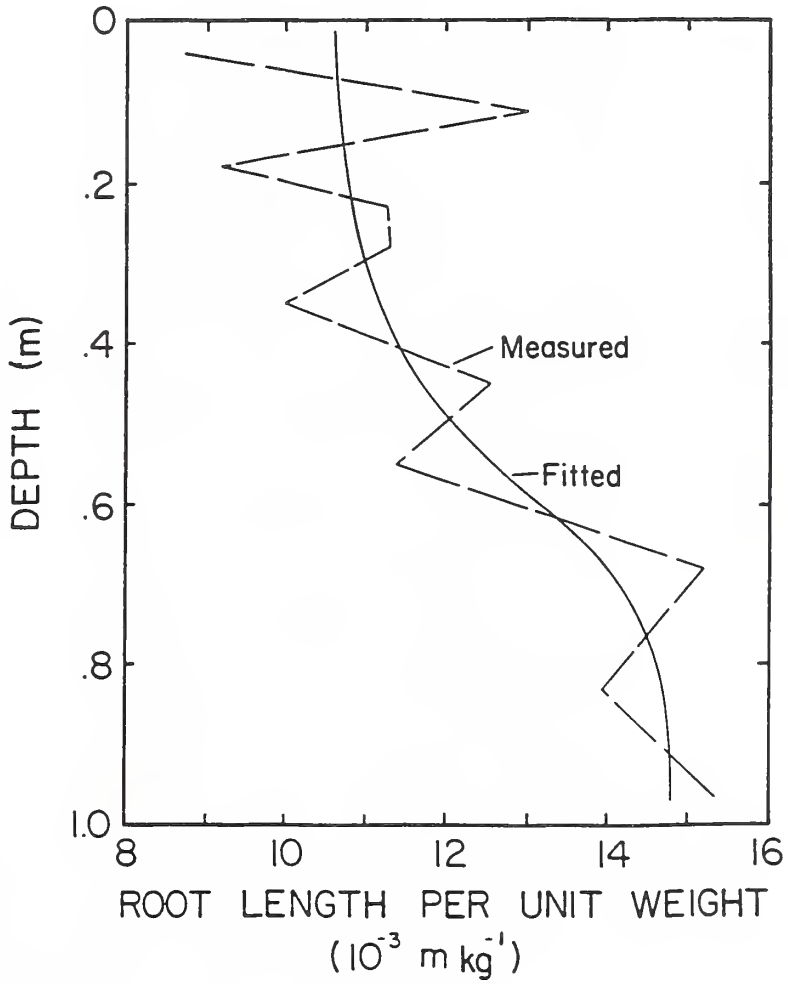

Fig. 5.3 Distributions of root length per unit weight of root for column F. The solid line was visually fitted to the measured curve.

length density distribution of columns B, D, and E probably could be obtained by combining the data in Figures 5.2 and 5.3.

We intended to follow root distributions by observing them through the glass walls of the columns, but this was only successful in the beginning. Alfalfa roots apparently behave quite differently than those of annual crops (see *Taylor and Klepper*, 1975). We failed to observe a rapid appearance or disappearance of roots. Once alfalfa roots were established, they remained intact for a long period of time, even through relatively dry periods, although they did discolor with time. Moreover, when the soil dried out and shrank away from the glass wall, the roots often grew preferentially in the gap between glass and soil. Few roots were visible at those places where the soil stuck to the glass.

Figure 5.4 shows a photograph of the root system of column A on a nail board after most of the soil was washed away. The thick root crowns referred to earlier are clearly visible. Tap roots extend all the way to the bottom of the column. There was a relative abundance of fine roots at 0.55 m depth around the ceramic tubes through which this column was irrigated for some time. Another picture of the same root system is shown in *Dirksen and Raats* (1985). These pictures and the root distribution of column E in Figure 5.2 show that, irrespective of depth, roots proliferated the most near irrigation points where the pressure and osmotic soil water potentials were the most favorable.

5.4. *Effect of Soil-Water Potentials on Leaf Water Potentials*

Figure 5.5 shows total heads (h_l) and osmotic heads (h_{ol}) of leaf water as measured with psychrometers from J5239 to J5246 for columns A through E. Each point is the average of about six replicate measurements. They are plotted against the average osmotic head ($\bar{h}_{os}$) of the soil columns at the time of measurement. The solid lines were drawn by sight. The difference between the two lines, generally assumed to be the turgor head h_{pl}, is shown also. The turgor head decreases with decreasing $\bar{h}_{os}$, first slowly to about $\bar{h}_{os}$ = -50 m, and then rapidly beyond that value. The extrapolated value of $\bar{h}_{os}$ for zero turgor head (wilting) is -62 m, but this value can only be a rough estimate because of limited data.

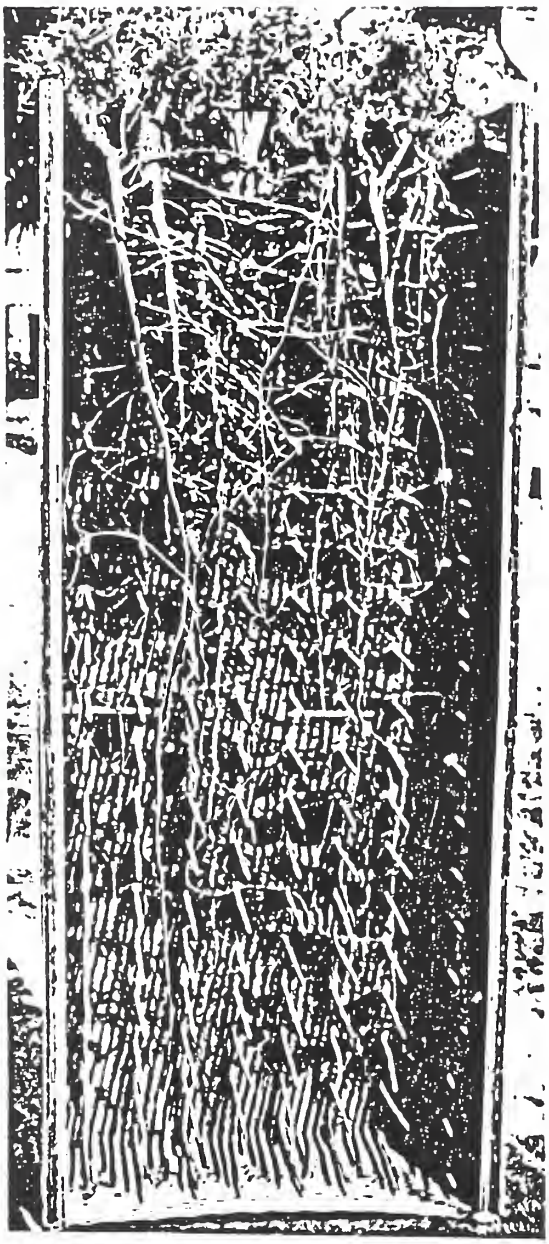

Fig. 5.4. Root system of alfalfa in column A.

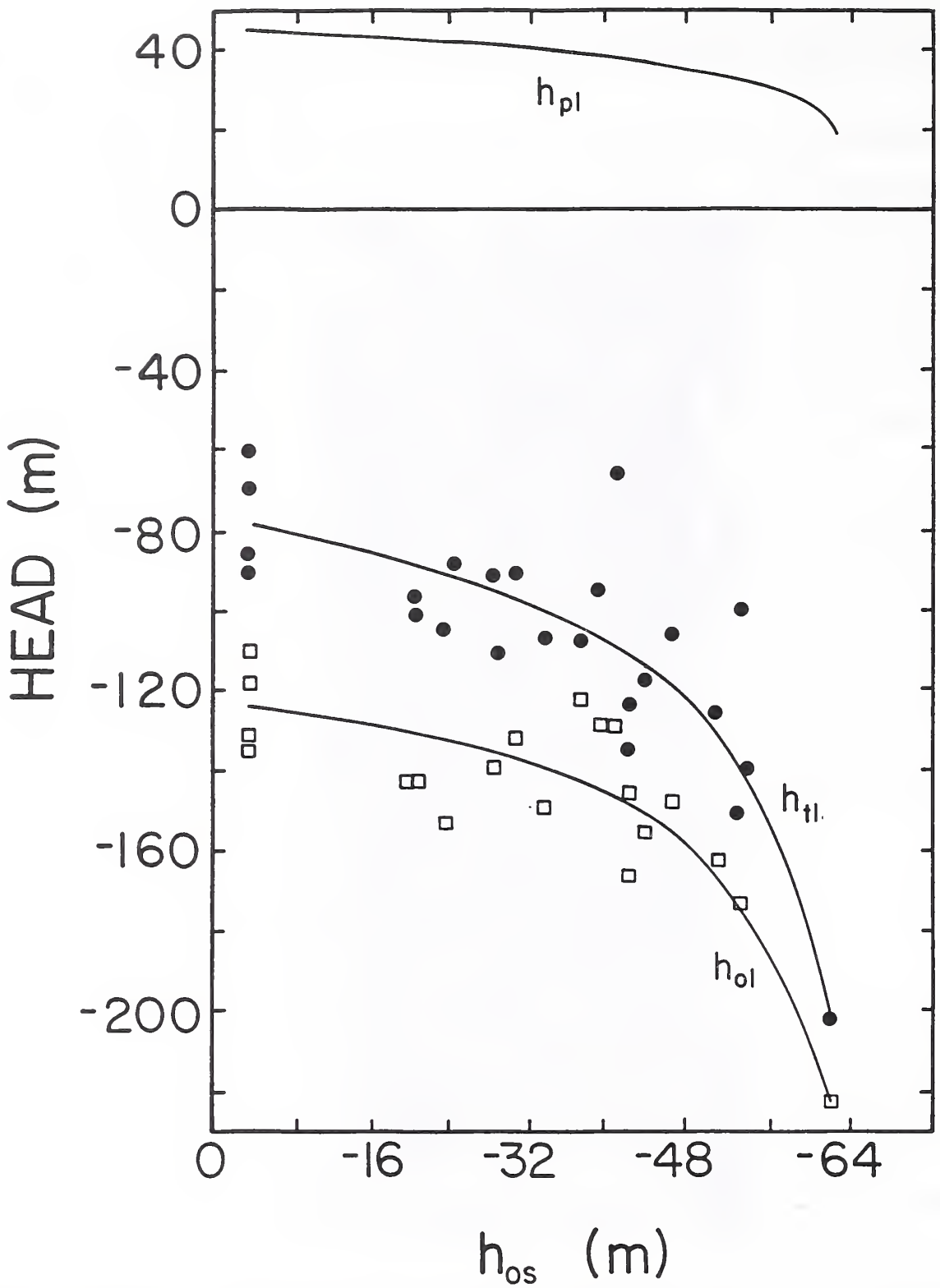

Fig. 5.5 Average leaf water potential, derived from psychrometer measurements between J5239 and J5246, as a function of the average soil-water osmotic head.

The measurements for Figure 5.5 were taken after different light periods; some measurements were taken also in the dark. Table 5.4 shows leaf water potentials for columns D and E that were taken between J6194 and J6196. The elapsed time periods since the lights were switched on or off are indicated also. The data show a decrease in total head with time after the lights were turned on and an increase after the lights were turned off. h_{tl}, during darkness, recovered about 40 and 45 m for columns D and E, respectively. Other data showed similar or somewhat lower recovery values. The one set of htl-measurements made with the pressure chamber agreed quite well with the psychrometer data.

Leaf water potentials depend not only on the osmotic head, h_{os}, of the soil solution, but also on the soil water pressure head, h_{ps}, and the evaporative demand. The "micro-meteorological" conditions in the laboratory, except for the illuminance, were more or less constant throughout the experimental period; however, the actual evapotranspiration, *ET*, varied in the course of each growth period because of changing canopy size. Table 3.1 shows

Table 5.4. Total, osmotic, and turgor heads of leaf water in columns D-12 and E-6 from J6194 until J6196.

Julian Day	Lights hr		Column D-12 h_{tl} m	D-12 h_{ol} m	D-12 h_{pl} m	Column E-6 h_{tl} m	E-6 h_{ol} m	E-6 h_{pl} m
J6194	0.5	ON	-69	-106	37	-66	-103	37
J6914	4.0	ON	-75	-124	49	-99	-150	51
J6195	9.0	ON	-91	-139	48	-96	-140	44
J6195	2.0	OFF	-60	-108	48	-74	-120	46
J6195	7.0	OFF	-60	-116	56	-83	-139	56
J6195	12.5	OFF	-49	-119	70	-50	-103	53
J6196	5.5	OFF	-51*			-74*		
J6196	12.0	OFF	-63	-122	59	-52	-100	48

*Pressure chamber data.

variations in *ET* with time for growth periods IV, V, and VI. Because all h_u data were obtained during the last few days before the alfalfa was cut, the effect of evaporative demand on h_u in Figure 5.5 is nearly eliminated. However, the effects of varying h_{ps}, and hence θ_s, on h_u are still included. These last effects will be treated separately in the next section. The water contents varied between 0.24 and 0.06 $m^3\ m^{-3}$, corresponding with pressure heads of -1.8 and -200 m. The lower water contents generally, but not consistently, coincided with the lower osmotic heads. As for the data in Table 5.4, the average osmotic head, $\bar{h}_{os}$, in column D was about -29 m and the average water content, $\bar{\theta}_s$, about 0.135 $m^3\ m^{-3}$, corresponding with an average $\bar{h}_{ps}$ of about -5.5 m. Similar values for column E were about -52 m, 0.16 $m^3\ m^{-3}$, and -3.5 m, respectively.

5.5. *Effect of Soil Water Contents on Leaf Water Potentials*

The effect of soil water content on leaf water heads, separate from the direct pressure head effect, separate from the direct pressure head effects, can be derived from the pressure chamber data for column A. This column had no salt other than fertilizers added to the applied tap water (h_o = -2.3 m). Most of the column was relatively salt free, although the drainage water was very saline towards the end of the experiments as a result of consistently high evapotranspiration rates and low leaching fractions. Figure 5.6 shows values of h_u for column A plotted against the average soil water content ($\bar{\theta}_s$). Below $\bar{\theta}_s \simeq$ 0.12 $m^3\ m^{-3}$, h_u decreased rapidly with decreasing $\bar{\theta}_s$. The relationship between h_{ps} and $\bar{\theta}_s$ in Figure 5.6 defines the soil water retention curve (see also Fig. 2.6 of Chapter 2), and shows a similar steep increase. The difference between h_{ps} and h_u as a function $\bar{\theta}_s$ is plotted in the top part of Figure 5.6. Because the salinity in column A was low (the h_{os} values were close to zero), and because the gravitational head h_{gs} is small as compared to h_u, we can equate h_{ps} - h_u with h_{ls} - h_u. Thus, the total head difference between the soil and the leaves increased with decreasing average water content, first slowly to about $\bar{\theta}_s$ = 0.11 $m^3\ m^{-3}$, and then rapidly to about $\bar{\theta}_s$ = 0.07 $m^3\ m^{-3}$. This change in head difference represents an effect of water content over and above the immediate effect of a changing pressure head. This

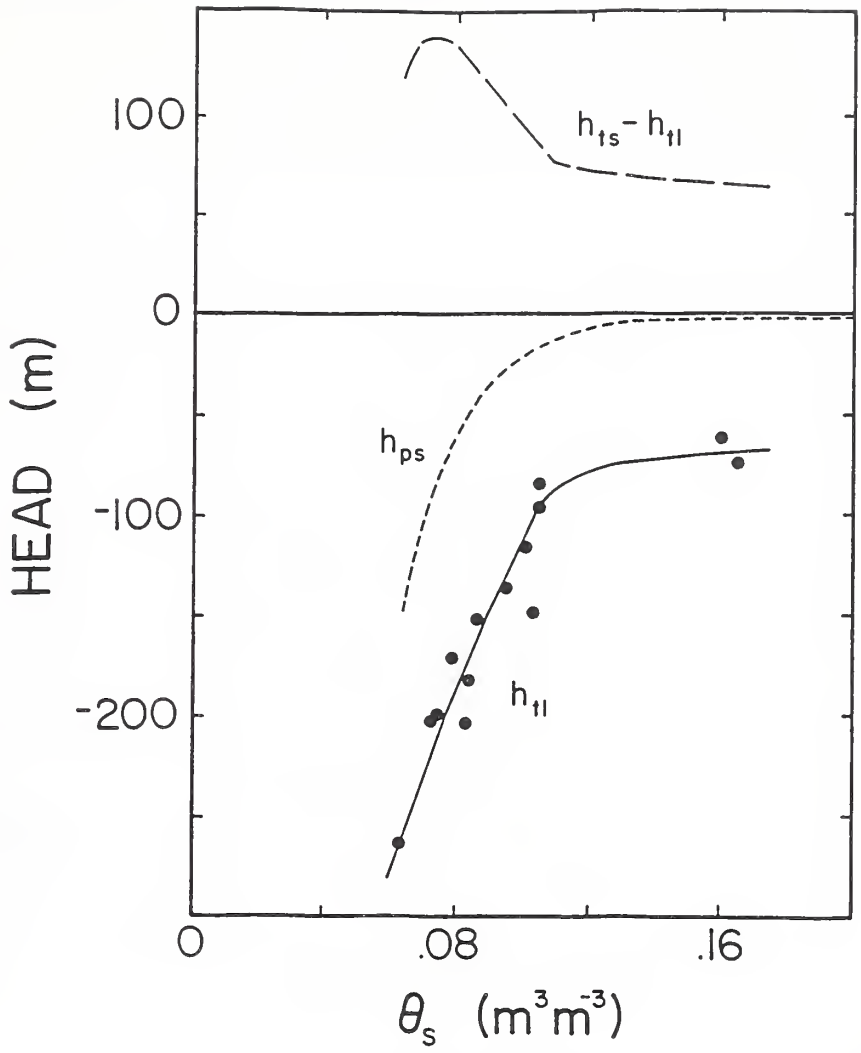

Fig 5.6. Total leaf-water head, soil-water pressure head, and their difference, as a function of the average soil water content in nonsalinized column A.

was to be expected because the hydraulic resistance of the soil increases as it dries out. However, the steep increase in h_{ts} - h_{tl} with lower water contents could also be the result of flux-dependent plant resistances (*Weatherley*, 1976), or because of contact resistances at the soil root interface (*Herkelrath et al.*, 1977). The latter authors suggested that contact resistances increase inversely proportional to the water content. Since the transpiration flux density q decreases when the soil dries out, a linear increase in h_{ts} - h_{tl} corresponds to a more than linear increase in total resistance, R. The maximum value of about 140 m at $\overline{\theta}_s$

= 0.07 m^3 m^{-3}, and the decrease of h_{ts} - h_{tl} below that water content, was based on only one set of h_{tl}-measurements.

5.6. *Maximum Root Conductivity*

The highest local rates of water uptake, λ, measured in the non-saline column A at various times and depths are plotted in Figure 5.7 as a function of the measured local water content. Obviously, there can be many low local rates of root water uptake for a given water content, but there must be some upper limit. Figure 5.7 indicates a linear relationship between the maximum rate of uptake, λ_{max}, and the local water content. Extrapolation of this line suggests that uptake ceased altogether at $\theta \simeq 0.055$ m^3 m^{-3}, a value which agrees well with other data (e.g., see Fig. 4.11). Figure 5.7 also indicates the depths in the profile where the maximum rates were observed. The maximum rate decreased with increasing depth, which at least partly must be due to the lower root length density deeper in the column, but partly also may reflect some axial resistance in the root system.

The potential difference h_{ts} - h_{tl} in Figure 5.6 and the maximum rates of water uptake λ_{max} in Figure 5.7 are both functions of water content. They can be combined with the measured root length densities, L_r, at the appropriate depths as shown in Figure 5.1 to calculate a maximum root conductivity, $C_{r,max}$, according to:

$$C_{r,\max} = \frac{\lambda_{max}}{L_r(h_{ts} - h_{tl})} \tag{5.2}$$

where $C_{r,max}$ is measured in (m^3 water) (m head)$^{-1}$ (m root)$^{-1}$ s^{-1}. The results in Table 5.5 show a linear relationship between $C_{r,max}$ and θ, similar to that found by *Taylor and Klepper* (1975). In fact, if one assumes that their diurnally fluctuating *ET* can be represented by 8 hours (28,800 s) of steady average *ET*, then the data in Table 5.5 virtually coincide with the upper limit of the data in Figure 5.6 of Taylor and Klepper. The last column of Table 5.5 shows values of $(\theta_{sat}/\theta)C_{r,max}$ which corrects the influence of the soil-water content on the apparent root conductivity according to the model of *Herkelrath et al.* (1977). The much smaller variation in these values than in $C_{r,max}$ could be considered to support this model.

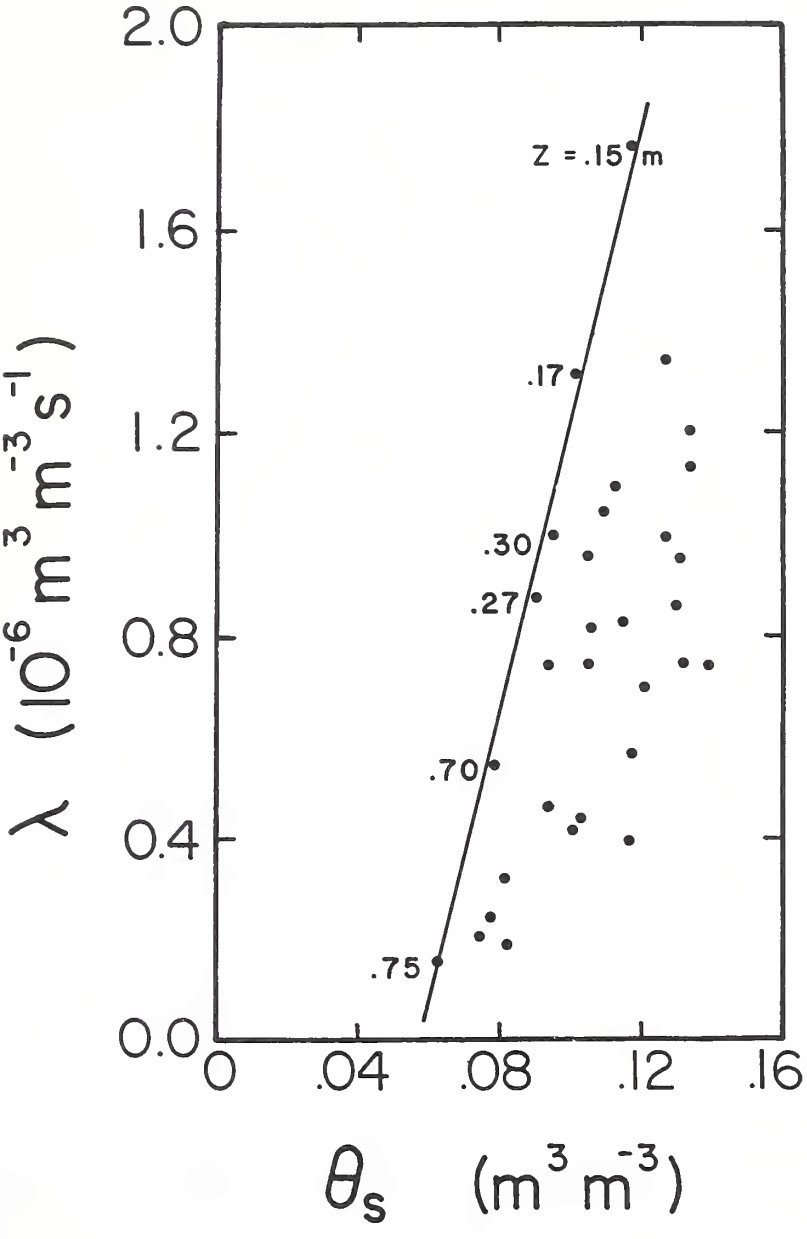

Fig 5.7. Highest local rates of root water uptake versus soil water content. The solid line was eye-fitted to the data with the maximum uptake rates.

Table 5.5. Calculated maximum root conductivities $C_{r,max}$ as a function of water content (see also Eq. 5.2).

θ	z	λ_{max}	L_r	h_{ts}-h_{tl}	$C_{r,max}$	$\theta_{sat}C_{r,max}/\theta$
$m^3\ m^{-3}$	m	$m^3m^{-3}s^{-1}$	$m\ m^{-3}$	m	$m^3m^{-1}m^{-1}s^{-1}$	$m^3m^{-1}m^{-1}s^{-1}$
.118	.15	1.78×10^{-6}	8.0 x 104	75	3.0×10^{-13}	8.9×10^{-3}
.102	.17	1.33×10^{-6}	6.5 x 104	90	2.3×10^{-13}	7.9×10^{-3}
.092	.30	1.00×10^{-6}	4.2 x 104	115	2.1×10^{-13}	8.0×10^{-3}
.087	.27	$.27 \times 10^{-6}$	5.0 x 104	115	1.5×10^{-13}	6.0×10^{-3}
.076	.70	$.70 \times 10^{-6}$	3.0 x 104	140	1.3×10^{-13}	6.0×10^{-3}
.062	.75	$.75 \times 10^{-6}$	3.0 x 104	100	$.56 \times 10^{-13}$	3.2×10^{-3}

5.7. *Uptake-Weighted Mean Salinity*

Total heads of leaf water htl obtained with the pressure chamber during non-daily irrigation did not correlate well with either the average water content $\bar{\theta}_s$ or the average osmotic head $\bar{h}_{os}$ of various sub-layers of the soil columns. For example, Figure 5.8 gives a plot of h_{tl} versus $\bar{h}_{os}$ for the middle third depth interval of the soil columns. One could reason that this correlation should be better than those for the upper and lower thirds of the columns. The $\bar{h}_{os}$-values of the upper third normally were dominated by the constant and rather high $\bar{h}_o$-values of the irrigation water, whereas the $\bar{h}_{os}$ values of the lower third often were too low for significant water uptake. The salinity of the middle third could be an indication of how much energy is required for the plant to take up water in addition to that what is more easily available in the top zone; this energy requirement should be reflected in the observed leaf water potentials. Yet, there is no clear relationship visible in Figure 5.8. Figure 5.9 shows per column reasonably good correlations between h_{tl} and $\bar{h}_{os}$ as averaged over an entire column, but for all columns together the correlation is not good. Because of varying experimental treatments, $\bar{h}_{os}$ differed appreciably between columns. For each column, however, $\bar{h}_{os}$ was quite insensitive to changes in the osmotic and pressure head distributions that caused large variations in h_{tl}.

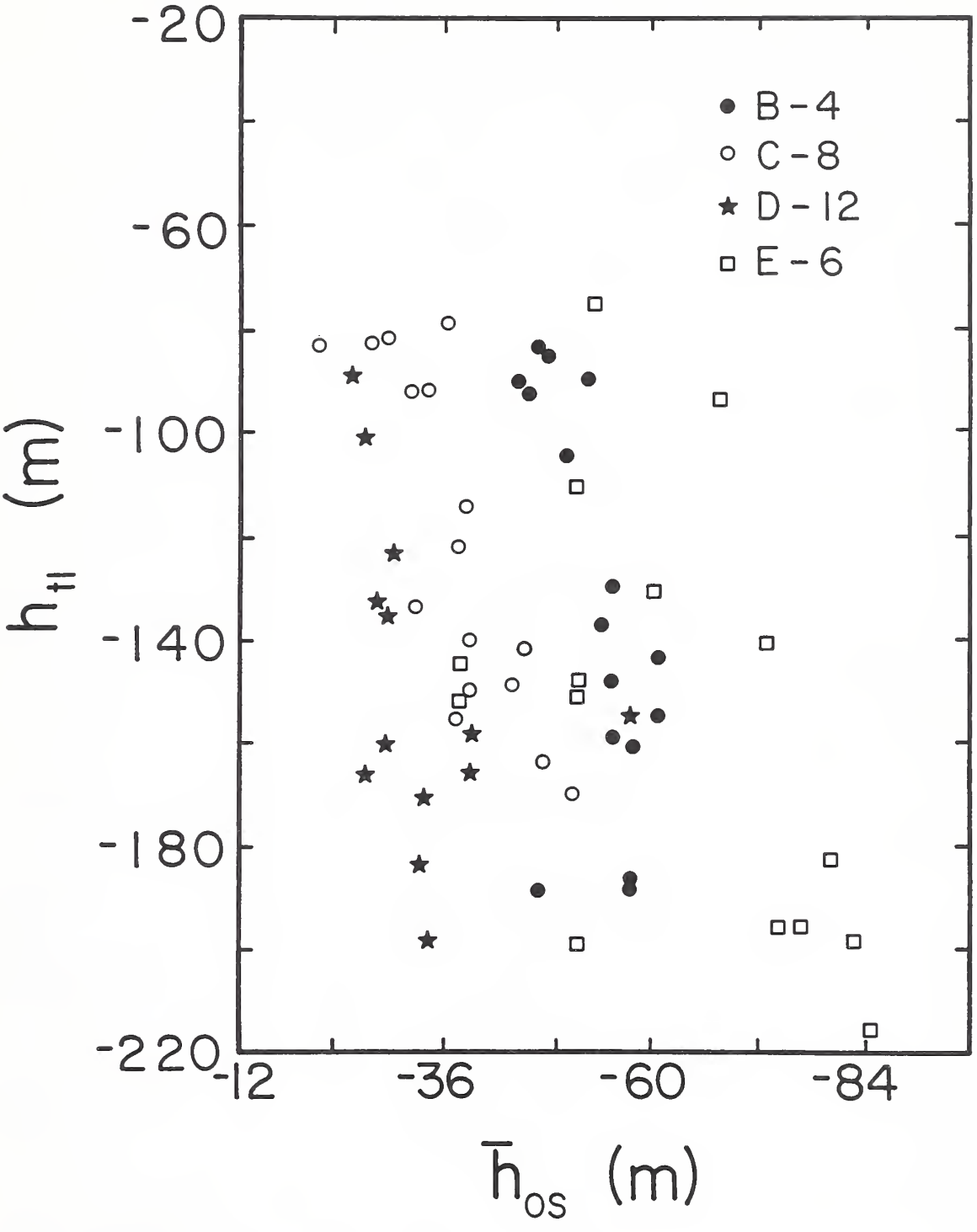

Fig 5.8. Total leaf water head versus average soil-water osmotic head of the middle third depth intervals of four soil columns.

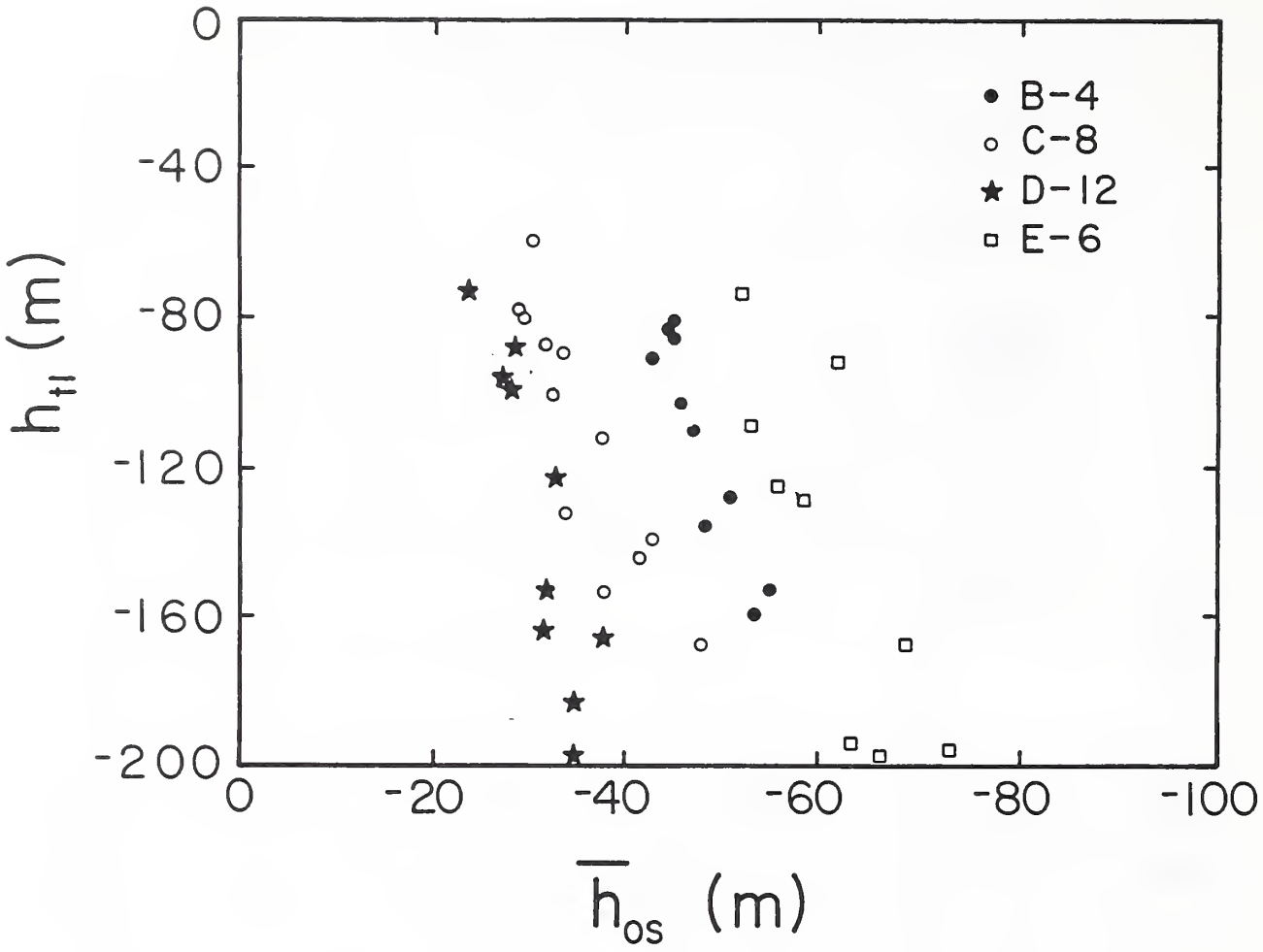

Fig 5.9. Total leaf water head versus the average soil water osmotic head of entire columns. The curves were eye-fitted to the observed data points per column.

It has been suggested (e.g., *Bernstein and Francois*, 1973; *Raats*, 1974; *Ingvalson et al.*, 1976) that plants minimize the uptake-weighted mean salinity of the root zone. The equivalent uptake-weighted mean osmotic head $\tilde{h}_{os}$ can be defined by

$$\tilde{h}_{os} = \frac{\int_0^{\infty} \lambda(z)\, h_{os}(z)\, dz}{\int_0^{\infty} \lambda(z)\, dz} \tag{5.3}$$

where $\lambda(z)$ is the rate of water uptake per unit volume at depth z, and $h_{os}(z)$ is the osmotic head of the soil solution at depth z. Figure 5.10 shows the same h_{tl}-values as in Figure 5.9,

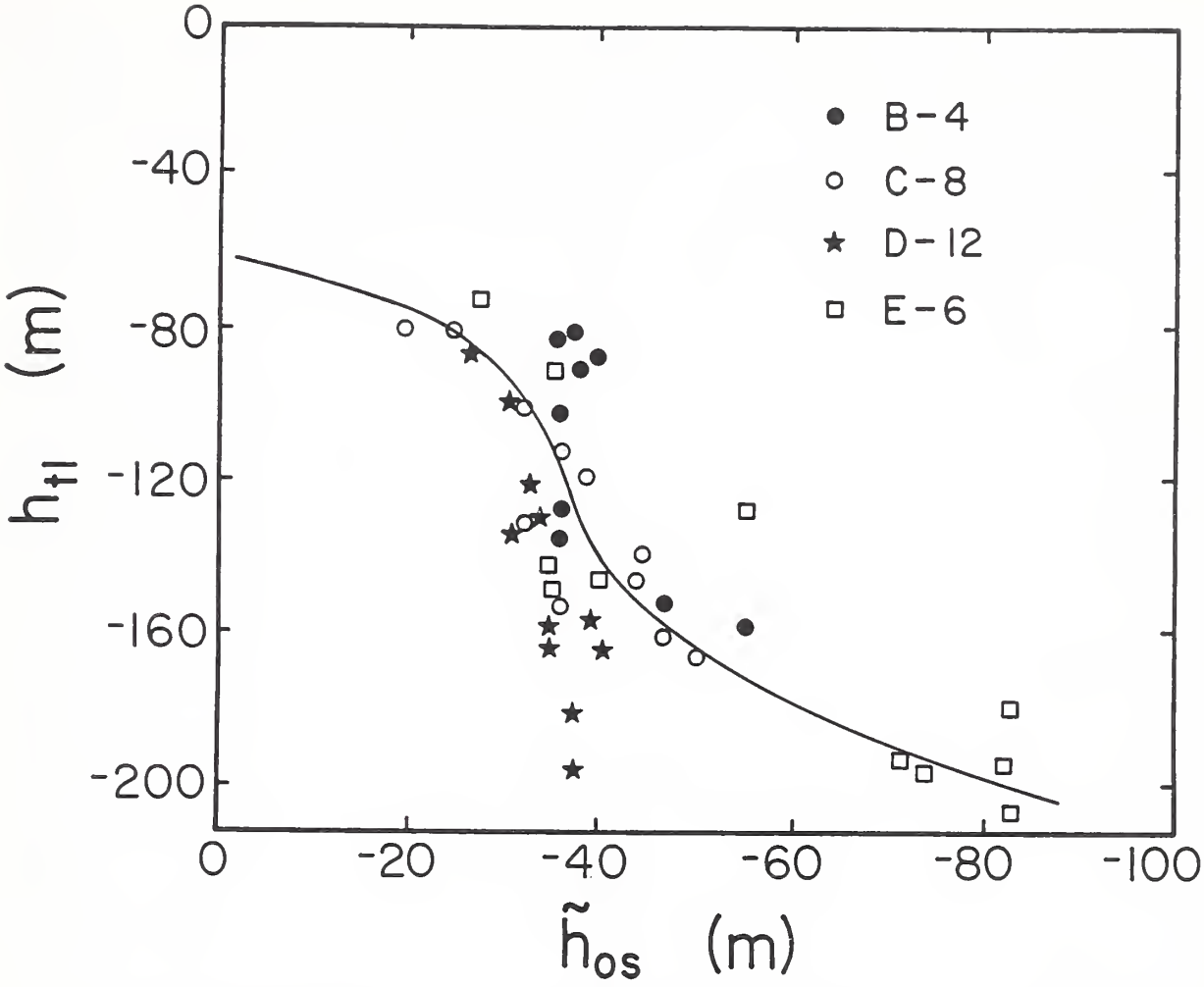

Fig 5.10 Total leaf water head versus uptake-weighted mean osmotic head of soil water.

but now plotted against $\tilde{h}_{os}$-values calculated with Eq. (5.3) from measured rates of change of the water content (RCWC) and h_{os}-distributions. Except for some data for column B-4, the RCWC-values should provide good approximations for the actual λ-values, because all data used were obtained towards the end of the last irrigation interval of each growth period when the hydraulic fluxes in the soil were negligible (see Chapter 3). The data in Figure 5.10 coalesce nicely. This is remarkable because $\tilde{h}_{os}$ was very sensitive to errors in the measured rates of change of water content, whereas the values of $\bar{h}_{os}$ in Figure 5.9 are independent of such errors. Moreover, $\tilde{h}_{os}$ varied considerably over relatively short periods of time, while $\bar{h}_{os}$ varied only slowly in time. This is also illustrated by the range in the values of $\bar{h}_{os}$ and $\tilde{h}_{os}$ in Figures 5.9 and 5.10, respectively. For column E, $\bar{h}_{os}$ varied from

about -50 to -70 m, whereas $\tilde{h}_{as}$ varied from about -27 to -82 m. The solid curve in Figure 5.10 was fitted visually to the data points. The value of -70 m at the ordinate was taken from Figure 5.6. This value also reflects observations that during light periods h_{tl} was seldom higher than -70 m, even at relatively high values of h_{ps} and h_{as}. The other end of the curve indicates that at low values of h_{ts}, h_{tl} apparently was limited to values seldom becoming less than -200 m, probably due to stomata closure.

The higher values of $\tilde{h}_{tl}$ for column D-12, the lower values for column B4, and all values for columns C-8 and E-6 (except one) fit the curve in Figure 5.10. The lowest h_{tl}-values of column D-12 do not fit the curve, because of the relatively low salinity in that column. Even when this soil column dried out to the point that the plants started wilting ($h_{tl} \leq$ -200 m), the calculated values of $\tilde{h}_{as}$ still were not lower than -40 m. Under those extremely dry conditions the salinity sensors were not functioning properly because of poor contact with the soil and because of the very low hydraulic conductivity. Hence, for the lowest values of h_{tl} of column D-12, the actual values of $\tilde{h}_{as}$ most likely were located closer to the curve than indicated in Figure 5.10. Similarly, the highest values of $\tilde{h}_{as}$ for column B-4 were too low to fit the curve. The salinity in this column increased rapidly with depth (see Fig. 4.3) and kept $\tilde{h}_{as}$ relatively low. However, there was always enough water in this most-frequently irrigated column to keep h_{ps} and h_{tl} relatively high (see also Table 4.4).

The reasoning above suggests that h_{tl} should correlate better with the uptake-weighted mean total head ($\tilde{h}_{ts}$) in the soil, rather than with $\tilde{h}_{as}$. Similar to Eq. (5.3), $\tilde{h}_{ts}$ can be defined as:

$$\tilde{h}_{ts} = \frac{\int_0^{\infty} \lambda(z)\, h_{ts}(z)\, dz}{\int_0^{\infty} \lambda(z)\, dz} \tag{5.4}$$

Figure 5.11 shows the same h_{tl}-values as in the previous figures, now plotted against $\tilde{h}_{ts}$ calculated with Eq. (5.4) from measured values of RCWC, h_{as} and h_{ps}. The low values of h_{tl} for column D-12, and the high values of h_{tl} for column B-4 indeed fall much closer to the new curve than is shown in Figure 5.10. Most absolute values of h_{ps} were generally small

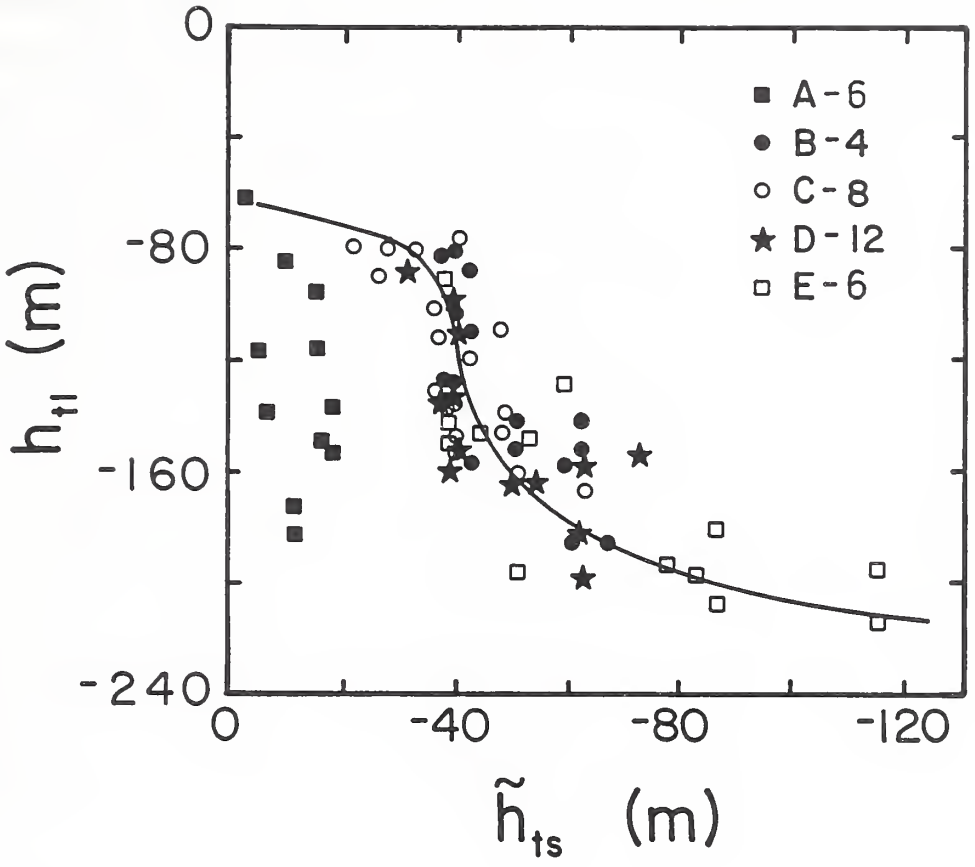

Fig. 5.11. Total leaf water head versus uptake-weighted mean total head of soil water.

compared to those of h_{os}, so that the curve in Figure 5.11 deviates little from the curve in Figure 5.10. The h_{ps}-values for the non-saline column A-6 were the lowest while the h_{os}-values, as expected, were the highest. The corresponding values of h_{ts} are shown also in Figure 5.11. They all fall far below the curve for the saline columns. Thus, h_{os} has a much smaller effect on h_{tl} than h_{ps}. This points again to an extra resistance associated with low water contents, not only because of lower hydraulic conductivities in the soil but possibly also at the soil-root interface. The saline columns generally remained too wet (Fig. 4.11) for this effect to become noticeable.

Of course, one should not expect a perfect correlation between $\tilde{h}_{os}$ or $\tilde{h}_{ts}$ and h_{tl}. The energy that must be expended for evapotranspiration, which is reflected in the value of h_{tl},

depends not only on the prevailing soil water salinity and pressure distribution, but also on the magnitudes and locations of the hydraulic resistances in the transpiration stream, and thus on the root distribution. If plants took up the same amount of water against the same values of h_{os} and h_{ts}, but at different locations in the root zone, h_u would be different depending on the distribution of the resistances in each pathway. On the other hand, if plants could take up all the water they need with equal ease at any single depth without restriction by the root distribution, minimizing $\tilde{h}_{os}$ would mean that the salinity always would tend to be uniform throughout the root zone. Any water of lower salinity, for example irrigation, would be taken up first, until its salinity had reached the same values as anywhere else in the root zone. This situation is approached in the bottom of the root zone under frequent irrigation. Based on these considerations, and on a comparison of Figs. 5.8 to 5.11, we feel that in the intermediate ranges of salinity and water content, alfalfa plants in this study took up water according to distributions that kept the uptake-weighted mean total head as high as possible. Because the pressure heads in the saline columns generally were high compared to the osmotic heads, essentially the same conclusion follows for the uptake-weighted mean salinity. The analysis in this section is also presented in *Dirksen* (1985).

5.7. *Conclusions*

Alfalfa plant aspects, discussed in this last Chapter, include yields, transpiration ratio's, root distributions, leaf water potentials, hydraulic resistances, and various weighted average osmotic and total heads of the soil solution. During daily irrigation, column E had the lowest leaching fraction and the highest salinity (h_o = -75 m) in the lower part of the column. Yields for this column were about 20% less than those for the non-saline columns. Transpiration ratios of column E during three consecutive growth periods varied between 500 and 638 kg water per kg dry matter produced. The average value for the nine growth periods of daily irrigation was about 640 kg kg^{-1}. Column E had appreciably higher yields than column B which was irrigated at a high leaching fraction ($L \sim 0.5$) and with water of h_o = -22.0 m. This osmotic head value is well below the threshold value for initial yield

reduction of alfalfa. Column B had by far the highest transpiration ratio's; the maximum value calculated was 907 kg kg^{-1}, while the average for the nine growth period was about 860 kg kg^{-1}. Late salinization (columns D and F) caused less yield reduction than early salinization (column E).

During non-daily irrigation, the 6-day saline irrigation treatment (column E-6) generated 13% less yield than the 6-day non-saline irrigation treatment (column A-6). These two columns were located at each end of the model and had higher yields than the middle three columns. Column B-4 yielded about 10% more than column D-12 and about 20% more than column C-8. It was not clear why column C-8 yielded the least throughout the non-daily irrigation phase. Its average transpiration ratio was the highest of all columns: 703 kg kg^{-1}. Column A-6 had the lowest transpiration ratio during non-daily irrigation: 563 kg kg^{-1}, a value that is appreciably lower than the average of 770 kg kg^{-1} during daily irrigation. This may indicate that high frequency irrigation with high quality water at moderate to high leaching fractions can lead to luxury consumption of water, a situation that is undesirable from a water conservation point of view.

Root densities were rather high throughout the columns and in most cases were relatively uniform below 0.35 m depth. Roots proliferated near irrigation points, irrespective of depth. Root observations through the glass walls apparently were not very reliable. There was some preferential growth along the glass windows, whereas inactive roots in dry soil discolored, but did not disappear. Except during the initial growth stages there were enough roots everywhere in the soil columns for high rates of water uptake to occur at locations where the osmotic and pressure heads were most favorable.

Leaf water potentials obtained with thermocouple psychrometers exhibited large standard variations, whereas those obtained with a pressure chamber were all very consistent. Total heads during evapotranspiration under no-stress conditions varied from about -70 m to -100 m; they decreased to values approaching -200 m under stress conditions. The lowest leaf water total head of -265 m was measured during wilting in the non-saline column. The turgor head, which could be derived only from psychrometer data, varied from about 50 m for non-saline conditions to zero at a projected average soil water osmotic head of -62 m. The recovery in leaf water total head during the night was about 45 m.

For the non-saline column, total leaf water heads decreased, whereas the total head difference between soil water and leaf water increased rapidly with decreasing average soil water contents below 0.12 $m^3 m^{-3}$. These changes, which could not be explained by changes in soil water pressure heads, and appear to be due to an increase in soil resistance and possibly also in the contact resistance at the soil-root interface with decreasing soil water content. The maximum root conductivity in the non-saline columns increased linearly with soil water content to a value of about 3×10^{-13} m^3 (m root)$^{-1}$ (m head)$^{-1}$ s^{-1} at θ = 0.12 m^3 m^{-3}. No root uptake was observed below θ = 0.055 m^3 m^{-3}.

For lack of experimental methods to measure root water potentials in situ, it was assumed that leaf water potentials were a measure of how the plants integrated various non-uniform soil water potential distributions. Since leaf water potentials always were measured on full canopies and under essentially constant evaporative demands, they could be correlated with variously averaged soil water potentials. Only the uptake-weighted mean osmotic and total heads gave good correlations for all columns combined. This was interpreted as indicating that the plants attempt to minimize these quantities. The 10% higher yields for column B-4 as compared to column D-12 were in spite of the fact that the uptake weighted mean osmotic heads of column B-4 were lower than those of column D-12. Apparently, the lower osmotic heads in column B-4 were more than compensated for by the generally higher pressure heads in this column. Only under extremely dry conditions did the pressure head drop to a level that was significant with respect to the osmotic head.

6. REFERENCES

Austin, R. S. and S. L. Rawlins. 1977. Optoelectronic level detector for mercury manometers. *Agric. Eng.*, 58:29-30.

Bernstein, L. and L. E. Francois. 1973. Leaching requirement studies: Sensitivity of alfalfa to salinity of irrigation and drainage waters. *Soil Sci. Soc. Am. Proc.*, 37:931-943.

Bower, C. A., G. Ogata, and J. M. Tucker. 1969. Rootzone salt profiles and alfalfa growth as influenced by irrigation water salinity. *Agron. J.*, 61:783-785.

Bingham, F. T., and M. J. Garber. 1970. Zonal salination of the root-system with NaCl and boron in relation to growth and water uptake of corn plants. *Soil Sci. Soc. Am. Proc.*, 34:122-126.

Dirksen, C. 1979. Flux-controlled sorptivity measurements to determine soil hydraulic property functions. *Soil Sci. Soc. Am. J.*, 43:827-834.

Dirksen, C. 1980. The relative speed of wetting and salinity fronts under high-frequency irrigation of alfalfa with saline water. *Int. Symp. Salt-Affected Soils*, Karnal, India, Feb. 1980, pp. 243-250.

Dirksen, C. 1985. Relationship between root uptake-weighted mean soil water salinity and total leaf water potentials of alfalfa. *Irrig. Sci.*, 6: 39-50.

Dirksen, C. 1987. Water and salt transport in daily irrigated root zone. *Neth. J. Agric. Sci.*, 35:395-406.

Dirksen, C. 1991. Unsaturated hydraulic conductivity. In: K. A. Smith and C. E. Mullins (eds.), *Soil Analysis, Physical Methods*. Marcel Dekker, Inc., New York, NY, pp. 209-269.

Dirksen, C. and M. J. Huber. 1978. Soil water flow model with two-dimensional automatic gamma ray attenuation scanner. *Water Resour. Res.*, 14:611614.

Dirksen, C., J. B. Kool, P. Koorevaar, and M. Th. van Genuchten. 1993. HYSWASOR - Simulation model of hysteretic water and solute transport in the root zone. In: D. Russo and G. Dagan (eds.), *Water Flow and Solute Transport in Soils.* Springer Verlag, New York, NY, pp. 99-122.

Dirksen, C., and P. A. C. Raats. 1985. Water uptake and release by alfalfa roots. *Agron. J.*, 77:621-626.

Eching, S. O., J. W. Hopmans, and O. Wendroth. 1994. Unsaturated hydraulic conductivity from transient multistep outflow and soil water pressure data. *Soil Sci. Soc. Am. J.*, 58:687-695.

Herkelrath, W. N., E. E. Miller, and W. R. Gardner. 1977. Water uptake by plants, II. The root contact model. *Soil Sci. Soc. Am. J.*, 41:1039-1043.

Hoffman, G. J., W. N. Herkelrath, and R. S. Austin. 1969. Simultaneous cycling of Peltier thermocouple psychrometers for rapid water potential measurements. *Agron. J.*, 61:597-601.

Hoffman, G. J., and M. Th. van Genuchten. 1983. Soil properties and efficient water use: Water management for salinity control. In: H. M. Taylor, W.R., Jordan, and T. R. Sinclair (eds.), *Limitations to Efficient Water Use in Crop Production*. Am. Soc. Agron., Madison, WI, pp. 73-85.

Ingvalson, R. D., J. D. Rhoades, and A. L. Page. 1976. Correlation of alfalfa yield with various indices of salinity. *Soil Sci.*, 122:145-153.

Itai, C. and Y. Vaadia. 1971. Cytokinin activity in water-stressed shoots. *Plant Physiol.*, 47:87-90.

Kool, J. B., J. C. Parker, and M. Th. van Genuchten. 1987. Parameter estimation for unsaturated flow and transport models - A review. *J. Hydrol.* 91:255-293.

Koorevaar, P. G. Menelik, and C. Dirksen. 1983. *Elements of Soil Physics*. Elsevier, Amsterdam, The Netherlands, 228 p.

Lunin, J. and M. H. Gallatin. 1965. Zonal salinization of the root system in relation to plant growth. *Soil Sci. Soc. Am. Proc.*, 29:608-612.

Maas, E. V. and G. J. Hoffman. 1977. Crop salt tolerance - current assessment. *J. Irrig. and Drainage Div.*, ASCE, 103(IR2):115-134.

Newman, E. I. 1966. A Method of estimating the total length of root in a sample. *J. Appl. Ecol.*, 3:139-145.

Raats, P. A. C. 1974. Movement of water and salts under high frequency irrigation. Proc.,

2nd Int. Drip Irrigation Congress, San Diego, CA., July, 1974. pp. 222-227.

Shalhevet, J. and L. Bernstein. 1968. Effects of vertically heterogeneous soil salinity on plant growth and water uptake. *Soil Sci.*, 106:85-93.

Taylor, H. M. and B. Klepper. 1975. Water uptake by cotton root systems: An examination of assumptions in the single root model. *Soil Sci.*, 120:57-67.

van Genuchten, M. Th. 1980. A closed-form equation for predicting the hydraulic conductivity of unsaturated soils. *Soil Sci. Soc. Am. J.* 44:892-898.

Wadleigh, C. H., H. G. Gauch, and D. G. Strong. 1947. Root penetration and moisture extraction in saline soil by crop plants. *Soil Sci.* 63:341-345.

Ward, K. J., B. Klepper, R. W. Rickman and R. R. Allmaras. 1978. Quantitative estimation of living wheat-root lengths in soil cores. *Agron. J.* 70:675-677.

Watson, K. K. 1966. An instantaneous profile method for determining the hydraulic conductivity of unsaturated porous materials. *Water Resour. Res.*, 2:709-715.

Weatherly, P. E. 1976. Introduction: Water movement through plants. *Phil. Trans. Royal Soc.*, London, B, 273:435-444.